

AD-A011 406

MEASUREMENT OF SEA SCATTER AND BUOY
TRACKS AT LONG RANGES BY HIGH-RESOLUTION
OTH-B RADAR

W. F. Marshall, et al

Stanford Research Institute

Prepared for:

National Science Foundation

January 1975

DISTRIBUTED BY:

NTIS

National Technical Information Service
U. S. DEPARTMENT OF COMMERCE

**Best
Available
Copy**

189117

Technical Report 1

May 1975

ADA011406

**MEASUREMENT OF SEA SCATTER
AND BUOY TRACKS AT LONG RANGES
BY HIGH-RESOLUTION OTH-B RADAR**

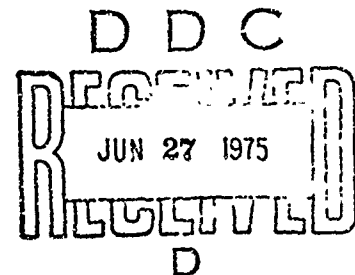
By. W. F. MARSHALL J. R. BARNUM

Prepared for:

OFFICE OF NAVAL RESEARCH
OCEAN SCIENCE AND TECHNOLOGY DIVISION (CODE 481)
ARLINGTON, VIRGINIA 22217

CONTRACT N00014-74-C-0138 (NR 083-320)

Approved for public release, distribution unlimited.



Sponsored by

THE OFFICE OF NAVAL RESEARCH
AND THE
NATIONAL SCIENCE FOUNDATION



STANFORD RESEARCH INSTITUTE
Menlo Park, California 94025 • U.S.A.

19

Copy No.

NATIONAL SCIENCE FOUNDATION
WASHINGTON, D.C. 20540

UNCLASSIFIED

SECURITY CLASSIFICATION OF THIS PAGE (When Data Entered)

REPORT DOCUMENTATION PAGE		READ INSTRUCTIONS BEFORE COMPLETING FORM	
1 REPORT NUMBER	2 GOVT ACCESSION NO	3 RECIPIENT'S CATALOG NUMBER	
4. TITLE (and Subtitle) MEASUREMENT OF SEA SCATTER AND BUOY TRACKS AT LONG RANGES BY HIGH-RESOLUTION OTH-B RADAR		5. TYPE OF REPORT & PERIOD COVERED Technical Report 1 December 1973 through 30 September 1974	
7 AUTHOR(s) W. F. Marshall and J. R. Barnum		6. PERFORMING ORG. REPORT NUMBER Technical Report 1, Project 3071-1	
9. PERFORMING ORGANIZATION NAME AND ADDRESS Stanford Research Institute 333 Ravenswood Avenue Menlo Park, California 94025		8 CONTRACT OR GRANT NUMBER(s) N00014-74-C-0138	
11. CONTROLLING OFFICE NAME AND ADDRESS Office of Naval Research (Code 481) Arlington, Virginia 22217		10. PROGRAM ELEMENT, PROJECT, TASK AREA & WORK UNIT NUMBERS NR 083-320	
14 MONITORING AGENCY NAME & ADDRESS (if diff. from Controlling Office)		12 REPORT DATE January 1975	13 NO OF PAGES
		15. SECURITY CLASS. (of this report) Unclassified	
		15a. DECLASSIFICATION/DOWNGRADING SCHEDULE	
16. DISTRIBUTION STATEMENT (of this report) Approved for public release; distribution unlimited.			
17 DISTRIBUTION STATEMENT (of the abstract entered in Block 20, if different from report)			
18 SUPPLEMENTARY NOTES			
19. KEY WORDS (Continue on reverse side if necessary and identify by block number)			
Ocean surveillance		Sea backscatter	
Buoy tracking		OTH radar	
Ship tracking		HF radar	
Wind monitoring		Radar displays	
20 ABSTRACT (Continue on reverse side if necessary and identify by block number)			
<p>A land-based over-the horizon backscatter (OTH-B) high-frequency (HF) radar located in California has been used for remote-monitoring operations in the Pacific Ocean north of Hawaii in support of the North Pacific Experiment (NORPAX). The radar has (1) detected and accurately tracked drifting buoys, each carrying a low-power HF repeater, (2) provided accurate position</p>			

D D C
 RECEIVED
 JUN 27 1975
 RECEIVED
 D

DD FORM 1473

EDITION OF 1 NOV 65 IS OBSOLETE

UNCLASSIFIED

SECURITY CLASSIFICATION OF THIS PAGE (When Data Entered)

UNCLASSIFIED

SECURITY CLASSIFICATION OF THIS PAGE (When Data Entered)

12 KEY WORDS (Continued)

20 ABSTRACT (Continued)

data on two research vessels, and (3) recorded sea backscatter data for subsequent correlation of Doppler spectra with measurements of wind direction, wind speed, and wave height.

A drifting buoy was detected and tracked over a 4-month period at ranges of 2300 to 3100 km. New radar data-processing and display systems were developed to ensure high position accuracy and correct buoy and ship identification. The radar position of the R.V. Flip was confirmed with a mean accuracy of 15 nmi at a 3100-km range.

Three types of sea backscatter Doppler spectra were recorded for correlation with oceanic winds and waves. (1) backscatter from wide areas of the ocean, to develop techniques for mapping wind fields, (2) backscatter from limited areas near the R.V. Flip, for correlation with local measurements of wind and sea conditions, and (3) long-term coherent samples of backscatter for high-resolution off-line processing.

These correlation studies are now in progress at Scripps Institution of Oceanography and Stanford University, with participation by Stanford Research Institute.

DD FORM 1473 (BACK)
1 JAN 73

EDITION OF 1 NOV 65 IS OBSOLETE

11

UNCLASSIFIED

SECURITY CLASSIFICATION OF THIS PAGE (When Data Entered)

CONTENTS

LIST OF ILLUSTRATIONS	v
LIST OF TABLES.	ix
ACKNOWLEDGMENTS	xi
I INTRODUCTION	1
II SUMMARY AND CONCLUSIONS.	3
A. Buoy and Ship Tracking	3
B. Sea Backscatter Measurements	5
C. Future Work.	7
III BUOY-TRACKING EXPERIMENT	9
A. Principles of Over-the-Horizon Radar	9
B. Buoy Tracking at OTH Ranges.	9
C. NORFAX Repeaters	12
D. NORFAX Buoy- and Ship-Tracking System.	13
E. Tracking Results	16
F. Propagation Conditions	45
G. Recommendations for Future Operations.	50
IV SEA BACKSCATTER MEASUREMENTS	55
A. Continuous Sampling for High Doppler Resolution.	55
B. Wide-Area Mapping of the Ocean Surface	60
C. Isolated Recordings Near R.V. Flip and R.V. Washington .	71

APPENDICES

A	WARF OVERVIEW	73
B	REPEATER ELECTRONICS.	83
C	RECEIVING AND DATA-PROCESSING SYSTEMS	91
D	OFF-LINE PROCESSING FOR BUOY AND SHIP POSITIONS	109
E	VIRTUAL-HEIGHT MEASUREMENT.	123
	REFERENCES	129
	DISTRIBUTION LIST.	131

ILLUSTRATIONS

1	Over-the-Horizon Radar	10
2	Track of a Repeater Installed in a Buoy as Observed by the WARF Radar Between 3 May and 9 August 1973.	11
3	Launch Positions and Times for NORPAX Buoys.	18
4	Detection Record of Buoy B, 29 January 1974.	19
5	Detection Record of Buoy C, 29 January 1974.	20
6	Detection Record of Buoy E, 29 January 1974.	21
7	Detection Record of Buoy F, 29 January 1974.	22
8	Detection Record of Buoy C on the Last Day it Was Observed, 27 February 1974	24
9	Detection Record of Buoy E on the Last Day it Was Observed, 31 May 1974.	26
10	Example of False Detection of Buoy D. The upper- and lower-sideband frequencies are unequally shifted,.	28
11	Display Format for Video-Receiver Buoy-Tracking Scheme . . .	29
12	Facsimile Record of Video Receiver Showing Buoys C and E on 9 February 1974	31
13	Detection Record of Flip, 29 January 1974.	34
14	Detection Record of R.V. Washington, 8 February 1974	35
15	Initial Positions of Buoys on 29 January 1974 From WARF Data.	36
16	Track of Buoy C as Observed from the Los Banos WARF Site, 29 January to 27 February 1974	39
17	Track of Buoy E as Observed from the Los Banos WARF Site, 29 January to 31 May 1974.	40
18	Radar and Satellite Positions of Flip, 29 January to 8 February 1974.	42
19	Relative Positions of R.V. Washington and R.V. Flip on Three Days of Simultaneous Detections.	44

20	Backscatter Ionogram of Target Area on 1 February 1974 . .	47
21	Backscatter Ionogram Showing Heavy E-Layer Blanketing and Direct Scatter, 23 May 1974.	48
22	3D Display of a Buoy-E Detection with Multimodes	51
23	Off-Line Sea-Clutter Spectrum Showing Effects of Multimode Propagation.	59
24	Off-Line Sea-Clutter Spectrum Under Good Ionospheric Conditions	61
25	Map Coverage Area, NORPAX-POLE Experiment, 30 January to 13 February 1974.	63
26	Sea Backscatter Spectra During a Storm Showing Winds Blowing Away from the Radar.	65
27	Sea Backscatter Data for a Cross-Wind Condition.	66
28	Sea Backscatter Data for Winds Blowing Toward the Radar.	67
29	Map Coverage Area, NORPAX, Beginning 4 March 1974.	70
30	Log of Sea Clutter Parameters as Recorded by the WARF Radar.	72
A-1	The WARF Radar System.	76
A-2	Receiving Array at Los Banos WARF Site	77
A-3	The WARF 18-Element Eastward-Looking Transmitting Array Located Near Lost Hills, California.	78
A-4	The 18-Element Westward-Looking Transmitting Array Located Near Lost Hills, California.	79
A-5	Present and Proposed Coverage of WARF.	80
B-1	Block Diagram of NORPAX Buoy Repeater.	86
B-2	Photograph of a NORPAX Buoy Being Launched from the R.V. Washington	88
C-1	NORPAX Frequency-Conversion Diagram.	94
C-2	NORPAX Buoy-Tracking Receiving and Data-Processing System	95
C-3	Sample Processor Record Showing Buoy Detection in Range Cell G. Numbered Items are Described in the Text. .	96
C-4	Sample TTY Log of Operating Parameters for NORPAX Data File.	102

C-5	Sample TTY Log Showing all Data on Detections	103
C-6	Buoy Detection Record in 3D Format.	105
C-7	Flip Repeater Detection in 3D Format.	105
D-1	Buoy and Ship Detection Log and Position Data from Post-Processor, 29 January 1974	114
D-2	Latitude and Longitude Plot for Buoy E, 29 January 1974	116
D-3	Averaged Positions for Buoys and R.V. Flip on 29 January 1974	117
D-4	Relative Positions of Buoys with Respect to R.V. Flip on 29 January 1974.	117
D-5	Detection List for Buoy E on 11 April 1974.	118
D-6	Latitude and Longitude Plot for Buoy E, 11 April 1974	119
D-7(a)	VCO Plot for Buoy E, 11 April 1974.	120
D-7(b)	Averaged Position Data for Buoy E, 11 April 1974. . . .	120
E-1	Geometry for Ionospheric Propagation.	126
E-2	Vertical Ionograms on 17 May 1974 Showing Change of More than 50 km in Virtual Height.	128

TABLES

1	Reported Launch Times and Positions for NORPAX Buoys. . . .	17
2	NORFAX Buoy Positions from Tracking Data.	37
3	Positions of R.V. Flip from Satellite and WARF Data	41
4	Relative Positions of R.V. Flip from Satellite and WARF Data	42
5	Positions of R.V. Washington from WARF Data	43
6	Data Log for High-Resolution Backscatter in the Vicinity of R.V. Flip	57
7	Coordinates of Map Corners for Wide-Area Mapping of the Pacific Ocean.	64
C-1	NORPAX Buoy Frequencies and Local-Oscillator Injection Frequencies	93

Preceding page blank

ACKNOWLEDGMENTS

We wish to acknowledge the contributions of a number of SRI staff members in this research effort. William Preuss and the late Len Schlageter contributed significantly in the operation of the radar system and in data collection. Douglas Westover provided the basic programming for the radar system and reduction of the sea-scatter data. Dorothy McKinney developed the programming for the reduction of buoy and ship positions. Gloria Kojala assisted with organizing the data output.

Our colleagues outside SRI during the buoy-tracking effort were Mr. G. McNally at Scripps Institution of Oceanography and Dr. A. D. Kirwan at Texas A & M. The sea-scatter effort was conducted with the cooperation of Dr. R. H. Stewart at Scripps and Dr. A. M. Peterson and his associates at Stanford University.

We are also grateful for the continued financial support by the Office of Naval Research and National Science Foundation in the NORPAX program.

Preceding page blank

I INTRODUCTION

The North Pacific Experiment (NORPAX) is a long-term research effort to study the variability of the upper layer of the central North Pacific ocean and the overlying atmosphere, with time scales of months to years and space scales to 1000 km or more. The effort is sponsored by the U.S. Navy, Office of Naval Research, and the National Science Foundation. Stanford Research Institute has participated jointly with the Scripps Institution of Oceanography and Stanford University to provide a capability for remote sensing of ocean parameters using a unique OTH radar facility located in Los Banos, California.

The first-generation experiments under NORPAX are concerned with gathering data required to plan later experiments and to test techniques for carrying them out. A large-scale experiment was undertaken during January and February 1974 in a region north of Hawaii near 35° N, 155° W. This experiment was named POLE, because the horizontal sampling spanned little more than a point on the NORPAX scale. Other participants provided radio-scatter measurements from the ocean surface, and local sensing of sea-surface temperature, surface-wave direction and height, and wind direction and velocity.

The remote sensing by the Wide Aperture Research Facility (WARF) designed and operated by SRI^{1-*} provided four types of data: (1) the positions of drifting buoys by tracking HF repeaters housed in the buoys, (2) the positions of two research vessels in the POLE test area each

* References are listed at the end of the report.

operating an HF repeater, (3) the Doppler spectra of radio signals back-scattered from small areas of the sea near the local sensors to provide data on wind direction and speed, and (4) surface-wind maps of large sections of the ocean. Recording these four types of data by WARF required a different operating technique for each type, and the effort was divided accordingly. An overview of WARF is given in Appendix A.

The repeater tracking efforts required monitoring a signal received by the repeater from the WARF radar transmitter at Lost Hills, California and retransmitted to the receiving facility at Los Banos. The signal parameters were selected to provide positive identification of six different buoys and two ships, and at the same time to avoid any interference from signals reflected from the ocean surface. The other two types of data were obtained using signals scattered directly from the ocean surface. The measurement of the Doppler spectra of these ocean backscatter signals required similar techniques that differed largely in the integration times used for recording the data. The effort was therefore divided into two tasks: Tracking of repeaters in buoys and ships, and sea backscatter measurements. This report describes these efforts and the results obtained by SRI.

In addition to the description of the final buoy tracks and the data recorded for sea-scatter analysis, a summary of hardware and software development is included herein. Many innovations in radar processing for buoy echoes were developed in the project. The long-term effects of the ionosphere on the radar propagation to 3000-km ranges are described here, in order to facilitate future operation. Most importantly, the 1974 project yielded results that will be useful for an improved design of buoy repeaters and better operating procedures in future experiments and sea-scatter recording.

II SUMMARY AND CONCLUSIONS

A. Buoy and Ship Tracking

The feasibility of tracking a low-powered repeater installed in a drifting buoy was demonstrated over a four-month period by SRI using the WARF facility. An accuracy of about 15 nmi was achieved in a similar test against a repeater on the R.V. Flip, where the position of this ship was accurately determined by independent means. The echoes received from the Flip were comparatively few in number, owing to the limited time during which its repeater was operated. Based on previous radar tracking accuracies, it is probable that buoy position accuracy was better than 10 nmi, since the buoy echoes were usually received and position-averaged over relatively long time intervals.

Novel buoy repeaters were built to SRI specifications by Barry Research Corporation. These repeaters were similar to the one that SRI had previously tracked and are based on an earlier design by A. C. Phillips of SRI. The NORPAX buoy repeaters were improved with regard to (1) smaller antenna design for less wind capture, (2) a new clock design that controlled on/off periods, and (3) a new modulation format that improved radar detection and echo sorting. A capability for measuring ocean temperature was provided in the repeater electronics; however, an appropriate temperature sensor (thermistor) was not incorporated in the buoy design. A total of six repeaters were deployed on buoys. Portable SRI repeaters were installed on two ships, the R.V. Flip and the R.V. Washington.

A new radar detection and processing system was designed and built especially for the NORPAX buoy-tracking project. This system enabled

rapid switching of radar parameters between any two preset buoy radar locations and buoy modulation formats. The WARF five-receiver radar processor was adapted to provide accurate location by means of echo comparison on adjacent radar azimuths, and buoy identification. New software for post-processing was developed to automatically sort buoy and ship echoes and to calculate smoothed radar position estimates. New radar search and display techniques were developed for the purpose of buoy location given large initial uncertainty in position.

Four of the six deployed buoys were detected on 29 January 1974, the first day after launch. One each of the drogued (Buoy A) and undrogued (Buoy D) buoys were not detected. It is fairly certain that the latter two buoys initially malfunctioned (they either sank, or the electronics did not work).

Two of the four remaining buoys (Buoys C and E) were tracked following the second day; both were the drogued type. Only one of these (Buoy E) produced a radar echo of the originally specified magnitude ($RCS = 10^5 \text{ m}^2$). Buoy E was tracked until 31 May. Buoy C operated at a magnitude some 10 dB below design, then ceased to function after 27 February. The fate of the two buoys that were never detected after the second day (Buoys B and F) is uncertain. It is probable that they either sank, ceased to repeat, or headed approximately northwest at a speed greater than 0.5 knot, thus escaping radar coverage. The last possibility, although contrary to the original expectations of oceanographers, is now considered to be the most likely.

It had been hoped that two buoys could be located and returned to the R.V. Washington for examination after the POLE experiment, but with only two still in operation this was not considered advisable. It would have been particularly valuable to recover a buoy that ceased to function in order to determine the cause of the failure.

The ability to illuminate by radar the area around buoy positions was found to vary diurnally and seasonally in the predicted manner. Adequate illumination would have been possible almost every day, even into the summer months, had the operation been totally flexible. However, buoy antenna design ultimately limited operation to the 15-to-25-MHz range, and the buoy repeaters were on between 1700Z and 2300Z. Thus, the operation was restricted to the use of a single hop via the daytime F layer. Since the buoys were launched about 250 nmi further away than originally anticipated, we found that although illumination was often good during the first part of the experiment, the illumination during the last part of the experiment was often totally inadequate. The implementation of a lower repeater cutoff frequency and nighttime "on" periods would have solved these problems.

Because of the limited time available to complete installation of the repeaters in the buoys, it was not feasible to conduct controlled preliminary tests prior to the POLE experiment. It is very important that future tests include a test period during which buoys are tethered and operated over a period of at least two weeks to check overall performance. Moreover, once buoys are deployed, no probable direction of buoy movement should be assumed. It is clear that successful multiple-buoy tracking, to even greater ranges and for longer periods, could be conducted in the future by means of OTH radar.

B. Sea Backscatter Measurements

Three types of recordings of long-range radio scatter from the sea were obtained during the NORPAX period. These were: (1) continuous samples near the R.V. Flip repeater for attainment of high Doppler resolution, hence measurement of second-order scatter components, (2) wide-area maps of the ocean surface for generation of wind-field maps, and

(3) isolated recordings near the R.V. Flip and the R.V. Washington for increased calibration of the scatter by means of repeater echoes.

Type-1 data were recorded only during the POLE experiment. These data were processed off-line; hence, Doppler-spectrum perturbations caused by the ionosphere could not be detected during recording. Also, in order to simultaneously detect the Flip repeater, these data were usually recorded at the same time of day. After all files of data were sampled, on all tapes, it was found that most of the data possessed scatter via multiple-mode propagation. This type of propagation yields combined spectra where Doppler components from each mode are shifted unequally by the ionosphere. No attempt has been made in this report to resolve the ambiguity. However, we are now exploring means to recover the significant Bragg scattered Doppler components based on their known relative frequency spacings. It is possible that recordings at other times of day should have been attempted; however, the Flip repeater operation was relatively fixed near late afternoon. It is also possible that two-hop propagation, at frequencies below repeater cutoff, would have been more suitable. It is certain that a radar antenna that permits vertical beam steering would greatly reduce ionospheric perturbation of the spectrum of sea backscatter from these ranges. Alternatively, data should be recorded at closer ranges or over longer time intervals in order to realize optimum propagation.

Type-2 data were recorded at various times during the periods 30 January to 13 February, and 4 March to 30 April 1974. A preliminary survey of the data was made by our Stanford colleagues in order to determine how much of the data was supported by good propagation. This analysis is not considered to be complete, nor have any of the data sets been reduced to wind-field maps. The samples recorded during a storm in March were, however, used to derive estimates of ocean surface-wind speeds at several spots.

Type-3 data were also used to derive ocean surface winds near the POLE experiment, where in-situ measurements of winds were made available.

C. Future Work

Current and future research with high-resolution OTH radar in NORPAX will concentrate on the improvement of our ability to infer ocean winds from Doppler-processed sea backscatter. It is now known that wind direction can be inferred fairly accurately, but improved measurements of wind speed are needed. Hence, most of our effort will be devoted to the interpretation of higher-order sea-scatter spectra for derivation of wind speed and (hopefully) significant wave height.

The effort will require the recording of new sea backscatter data. These data will be recorded at various times of day and at several different radar ranges in order to avoid the problems of last year. Ground truth will come from ships of opportunity, usually U.S. Navy ships, that traverse the newly expanded WARF coverage area. Most data recording will be conducted using extended sampling, as in the recording of Type-1 data above; however efforts are now underway to provide real-time Doppler processing and display while such data are being recorded. Effects of propagation on the scatter will thus be known. Analysis of the data will determine the resolution limit of second-order scattering components and the effect of spatial resolution and incoherent integration on these limits. This work will again be conducted in cooperation with Scripps and Stanford University.

III BUOY-TRACKING EXPERIMENT

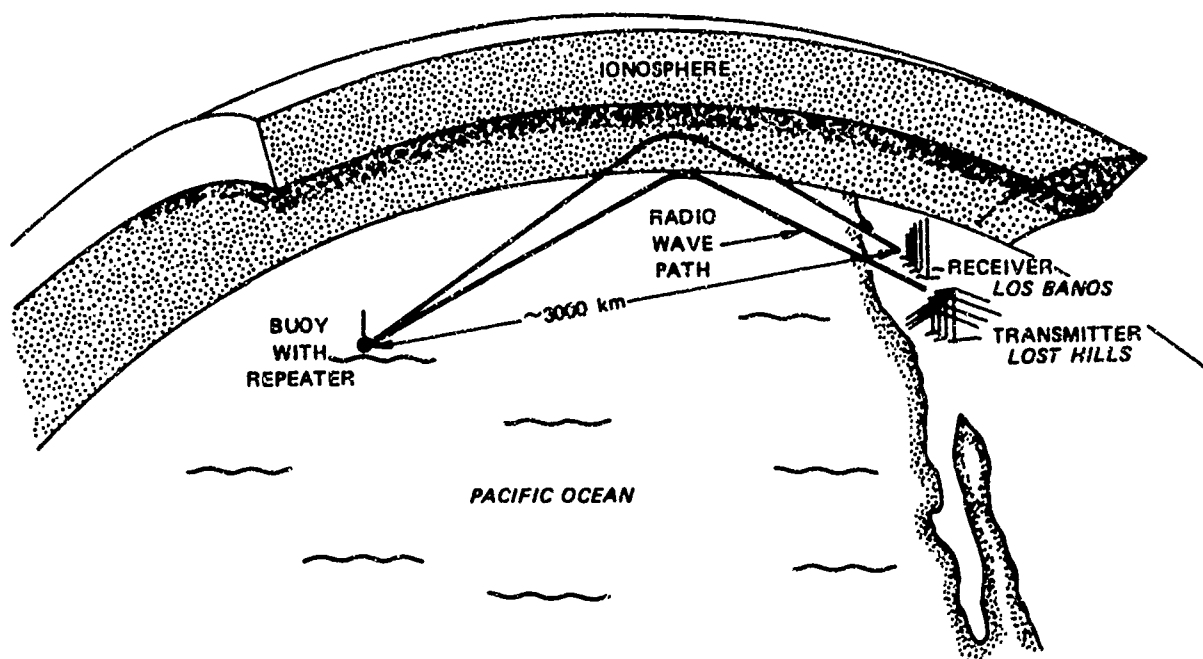
A. Principles of Over-the-Horizon Radar

Over-the-horizon (OTH) radar was developed to provide a capability for detecting targets at long ranges using ionospherically propagated HF radio waves. Most radar systems are limited to line-of-sight ranges because the frequencies used are too high to be reflected from ionospheric layers. At HF frequencies, however, propagation is possible to about 4000 km using a single-hop mode from the F-layer of the ionosphere and to much greater ranges with multiple hops and other modes. Energy reflected from a discrete target or from the earth or sea surface is backscattered over a similar ionospheric path to a receiver that is often separated from the transmitter site to minimize direct signal transmission. A typical backscatter radar (OTH-B) is shown in Figure 1. Details of the WARF system used in the NORPAX effort are given in Appendix A.

Since the signal reflected from a small target such as a buoy at a range of 3000 km would be too small to be detected, a compact amplifier or repeater can be used to provide a signal-to-noise ratio (SNR) at the receiver greater than 30 dB. The repeated signal is normally modulated, with the carrier suppressed, to improve the signal-to-clutter ratio (SCR) and provide buoy identification.

B. Buoy Tracking at OTH Ranges

SRI had previously tracked an HF-repeater in a drifting buoy during a period from 3 May 1973 through 9 August 1973. A map of the buoy track is shown in Figure 2. It was initially launched at a range of about 1410 km and was tracked until 8 June, by which time it had drifted



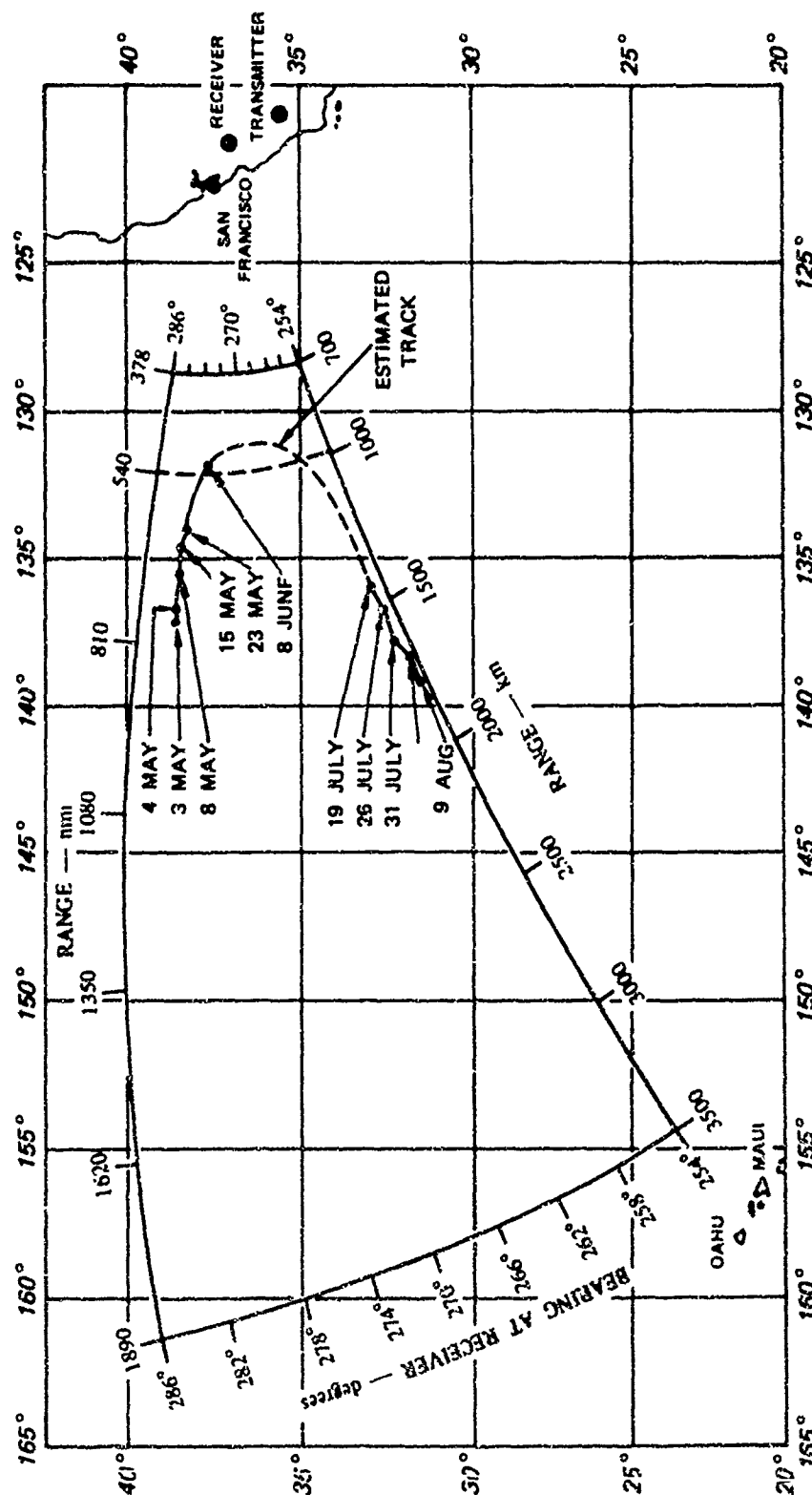
3071-1-671

FIGURE 1 OVER-THE-HORIZON RADAR

eastward to a range of about 990 km. At this range the required operating frequency was below the cutoff frequency of the repeater, and tracking efforts were discontinued. The buoy was reacquired by chance during another WARF experiment on 19 July after it had moved south and west to a range of 1400 km where the repeater operating frequency band was again satisfactory. It subsequently was tracked moving west to a range of 1800 km on 9 August.

This buoy's repeater was designed to operate at a maximum radar cross section of 10^5 m^2 on a cycle of one minute of each 5-minute period. This duty cycle plus normal fading of ionospherically propagated signals gave a data rate that was very low, yet a good tracking capability was demonstrated. The buoy repeaters for use in NORFAX had several design improvements.

By the time of the NORFAX experiment, an improved WARF processor had been developed to utilize a total of five antenna beams and to display



3071-1-472

FIGURE 2 TRACK OF A REPEATER INSTALLED IN A BUOY AS OBSERVED BY THE WARF RADAR BETWEEN 3 MAY AND 9 AUGUST 1973

all important target data on the terminal or operator console. This processor was further optimized for tracking modulated buoy repeaters.

C. NORPAX Repeaters

Details regarding the repeater hardware for buoys and ships may be found in Appendix B. The following paragraphs describe the design philosophy and details particularly pertinent to radar operation for buoy detection. The HF repeater in the buoy tracked in 1973 was completely redesigned for use with the NORPAX buoys. This was done in order to (1) increase the duty cycle, (2) move the modulation sidebands outside the Doppler spectrum of normal sea clutter, (3) provide means for buoy identification, and (4) provide the capability for a remote monitor of ocean temperature (which was instead used to monitor the repeater battery voltage).

Since the POLE experiment was a cooperative effort of a number of organizations taking data in a relatively small area of the Pacific, it was necessary to limit the operating hours of the buoy repeaters. Each repeater was a broadband amplifier reradiating any received signal in the 15-to-25-MHz band. It could therefore interfere locally with other radio transmissions in this part of the HF spectrum. Furthermore, unless very low frequencies are used (e.g., 3 to 6 MHz), good propagation conditions between the WARF facility and the target area during the winter and spring are available only for the daylight hours. Since the repeater antenna design precluded use of frequencies below 15 MHz, a period of six hours between 1700Z and 2300Z was selected for buoy repeater operation. Battery power was also conserved by restricting operating time.

A total of six buoys were deployed, three with drogues to minimize drift due to surface winds, and three without drogues. These were labeled A through F, with A, C, and E drogued, and B, D, and F not drogued.

It was expected that the drogued buoys would respond primarily to ocean currents well below the surface while the non-drogued type would be more strongly influenced by surface weather conditions. In order to identify each buoy and provide long-term tracking information, the signal transmitted by each buoy was modulated at a frequency precisely controlled by a quartz oscillator. The receiving system at Los Banos uses separate receivers for the two repeater sidebands. Since these receivers have a bandwidth of 100 Hz, and the modulation frequencies of the buoys were separated by about 120 Hz, it was not possible to receive both sidebands from more than one buoy simultaneously. To provide additional identification, the frequency separation between successive buoys was increased by 0.5 Hz so that the apparent Doppler of a spurious buoy signal as measured by the processor will differ from the Doppler of the buoy being tracked by some multiple of 0.5 Hz. An additional modulation was also used to indicate the level of the repeater batteries. For this purpose a stable voltage-controlled oscillator (VCO) provided a frequency offset in the 0-to-5-Hz range as a linear function of battery voltage. The VCO was initially set to a frequency of 3.75 Hz, and during the expected period of operation of four months it would decrease possibly 20%. The data processor was programmed to read the VCO frequency and provide a check on probable repeater life.

D. NORPAX Buoy- and Ship-Tracking System

Details regarding the receiving, recording, and display equipment are given in Appendix C. The purpose of this subsection is to outline the novel way in which individual repeaters were detected, identified, and located by sampling and processing the outputs of five HF receivers simultaneously.

1. Operational Design

The WARF receiving system for tracking the buoy repeaters at Los Banos utilized a processor designed for five-azimuth coverage of targets at OTH ranges. Because of the requirement for buoy identification it was necessary to use one receiving channel to monitor the lower sideband (LSB) of the repeater signal and compare it with a receiver channel monitoring the upper sideband (USB). If both sidebands had the same apparent time delay and Doppler offset due to the VCO frequency, it was possible to conclude that they originated at the same buoy.

It was necessary to use a third receiver channel to monitor the sea clutter in the target area and provide a reference signal against which to measure target and ionospheric Doppler frequencies. These three receiving channels (LSB, USB, and Clutter) were connected to the center (0°) azimuth beam of the WARF array through a power splitter. The two remaining receiver channels were connected to beams at $\pm 1/4^\circ$ from the main beam, and each monitored the upper-sideband signal from the repeater. Thus, azimuthal measurement accuracy was provided by three adjacent antenna beams, each covering an area roughly 60 km in range by 20 km in azimuth, and the three beams were spaced by $1/4^\circ$, or about 15 km. Four receivers were tuned for a particular buoy modulation by remote control of two synthesizers (USB and LSB) using one of six push-button switches. These switches also provided the computer with an identification of the buoy being tracked. A seventh switch was provided to connect all receivers to receive sea clutter, simultaneously, in conjunction with sea backscatter measurements made under the second task of the SRI effort under NORPAX. This mode of operation also was used to monitor the two repeaters installed on the ships participating in the POLE experiment, the R.V. Washington and R.V. Flip.

The radar operating time delay and azimuth were also controlled remotely by switches near the buoy selectors.

2. Radar Processing for Repeater Detections

The outputs of the five receiver channels were processed into 21 range cells. For the normal signal bandwidth of 50 kHz, the total range interval was 400 μ s, or 60 km, giving a range resolution of 3 km. Where a larger target window was needed, a bandwidth of 20 kHz was used, resulting in a 1-ms or 150-km range interval. The range resolution was then 7.5 km. The latter mode was used primarily for search of large areas when the target position was not known.

The signal was also spectrum-analyzed to provide an equivalent Doppler coverage of ± 2.5 Hz, with resolution of 0.078 Hz. The buoys drifted at such a slow rate (typically less than 0.3 knot) that any true Doppler frequency would have been less than about 0.02 Hz and not measurable. However, the modulation sidebands appear as frequency shifts, which the processor analyzes and records in the same fashion as a Doppler component. By initial choice of the VCO frequency (3.75 Hz) in the buoy and the local oscillator injection at the receiver, the frequency offset measured initially was ± 1.25 Hz for the USB and LSB, respectively. By the end of the test, the offset decreased to about ± 0.75 Hz, corresponding to a VCO of 3.25 Hz.

The operating procedure normally employed for buoy tracking included two data samples of 12.8 s each, which were then averaged by the processor to enhance detection sensitivity and position accuracy. Total sample and process time for this "2-map average," including plotting and listing all the data on a computer terminal, is about 51 s. It was thus convenient to take one data file per minute and allow time to change parameters between files as necessary.

Details of the data processing and an explanation of the computer-generated detections records are given in Appendix C.

3. Calibration Procedures

In order to verify that the radar and data processor were operating normally, a calibration check was run each day prior to the turn-on time of the buoys. A locally generated SFCW signal with modulation simulating each of the six buoy signals in sequence was radiated from a reference whip antenna near the center of the receiving array. The modulation included an offset corresponding to a different VCO frequency for each buoy to further check the real-time processor as well as the post-processor where VCO is calculated. The signal was received on the array and processed as a normal buoy signal. Hard-copy records showing the buoy identification and a detection confirmed that the radar was operating normally.

E. Tracking Results

1. Operation with Buoys

During the POLE experiment, data on buoy positions were passed by telephone to Scripps Institution of Oceanography on a daily basis. Radio communication with the R.V. Washington was used to coordinate operating periods for the repeaters on the Flip and the Washington and to exchange data on buoy detections and ship positions. Following the conclusion of the POLE experiment on 14 February, a preliminary summary of all buoy and ship positions obtained by the OTH radar was forwarded to Scripps. These data have since been refined, and corrected positions have been submitted to Scripps. During the continued tracking of Buoys C and E after the POLE experiment, reports of positions were telephoned

to Scripps as they were obtained each week. All final buoy and ship position estimates are included in this report.

a. Initial Results

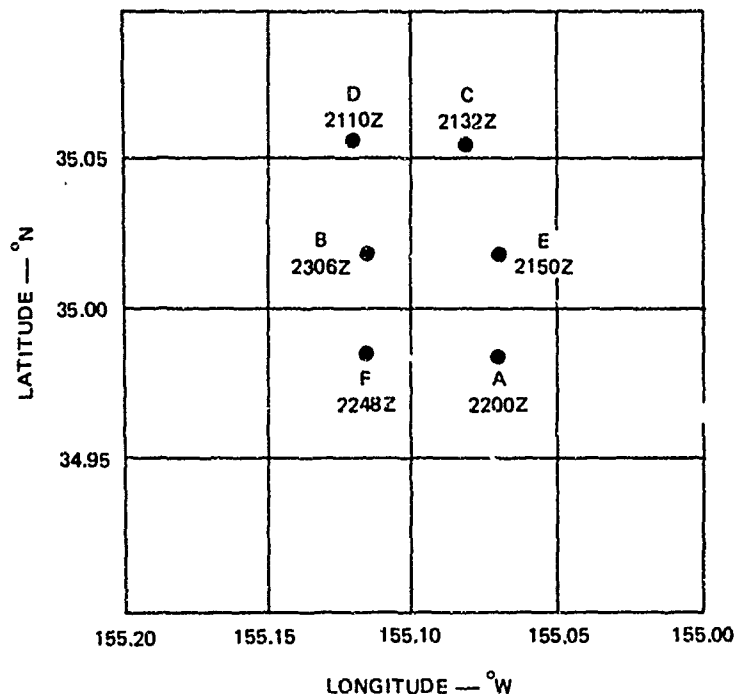
The NORPAX buoys were launched on 28 January 1974 from the R.V. Washington under the supervision of personnel from the Scripps Institution of Oceanography near 35° N, 155° W. The launch times and positions are shown in Table 1 and plotted in Figure 3.

Table 1

REPORTED LAUNCH TIMES AND POSITIONS FOR NORPAX BUOYS

Buoy ID	Launch Time (GMT)	Position	
		Latitude (° N)	Longitude (° W)
A	2200	34.983	155.070
B	2306	35.018	155.115
C	2132	35.055	155.082
D	2110	35.057	155.120
E	2150	35.018	155.070
F	2248	34.985	155.115

The buoys were designated on the SRI processor output as A, B, C, D, E, and F, corresponding to numerical identifications 1 through 6 assigned by Scripps. Buoys A, C, and E were the drogued type, and Buoys B, D, and F were not drogued. The buoys were initially spaced at about 5-km intervals with the three drogue types east of the three non-drogue types, each group along a north-south line. The repeaters were actuated at 1700Z as planned, but launching was delayed until 2100Z and the last buoy was launched after the repeaters were automatically turned off at 2300Z. No positive detections were made on the first day although

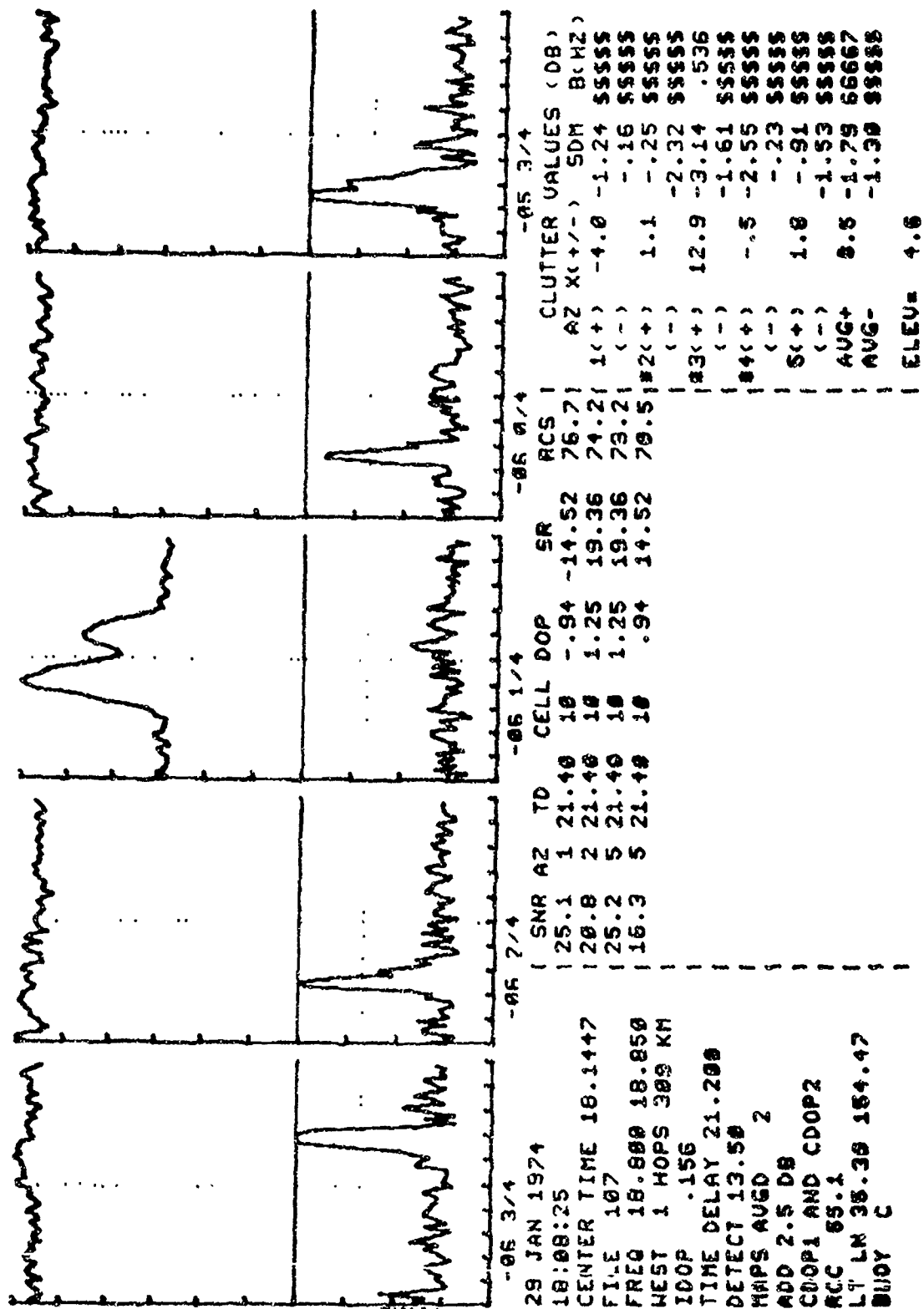


3071-1-673

FIGURE 3 LAUNCH POSITIONS AND TIMES FOR NORPAX BUOYS

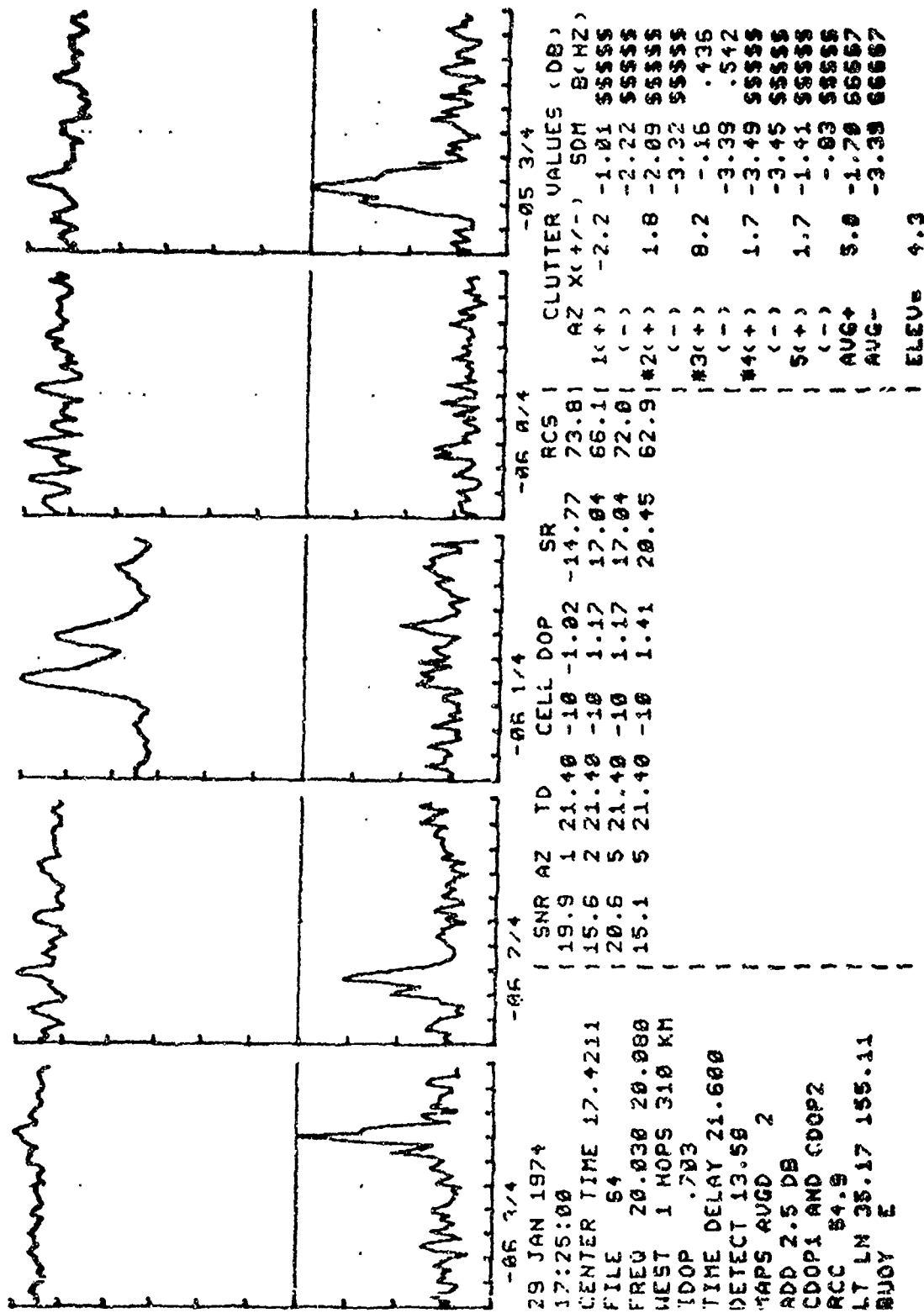
several USB signals probably originating from one or more buoys were observed. Repeaters on R.V. Flip and R.V. Washington were also operated, and positive identification of the Washington was made with 12 detections in a 20-minute period placing the ship at 35.16° N, 154.86° W. The reported ship position for that time was about 18 km west-southwest of the radar position.

On 29 January positive detections were made on Buoys B, C, E, and F. Examples of these detections are shown on the real-time records in Figures 4 through 7, respectively (note the buoy identification at the lower left of each figure). A detailed explanation of these records is given in Appendix C. No positive detection was made on Buoy A on this date or subsequently. Although apparent detections were made for Buoy D, these later proved to be false, as described below. Since a large enough area was initially searched, it has been concluded that Buoys A and D did not operate after launch.



3071-1-675

FIGURE 5 DETECTION RECORD OF BUOY C, 20 JANUARY 1974



3071-1-676

FIGURE 8 DETECTION RECORD OF BUOY E, 29 JANUARY 1974

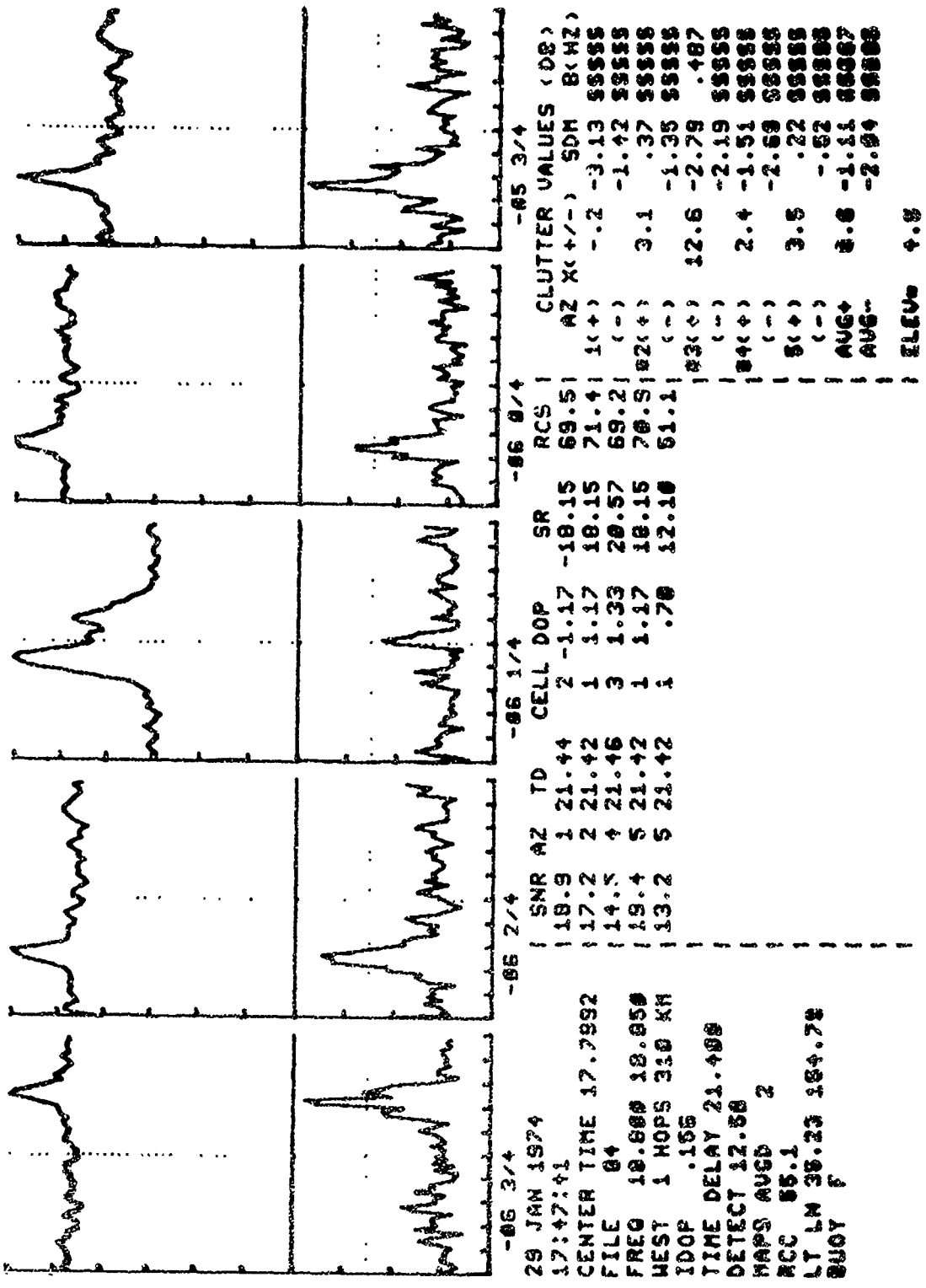


FIGURE 7 DETECTION RECORD OF BUOY F. 29 JANUARY 1974

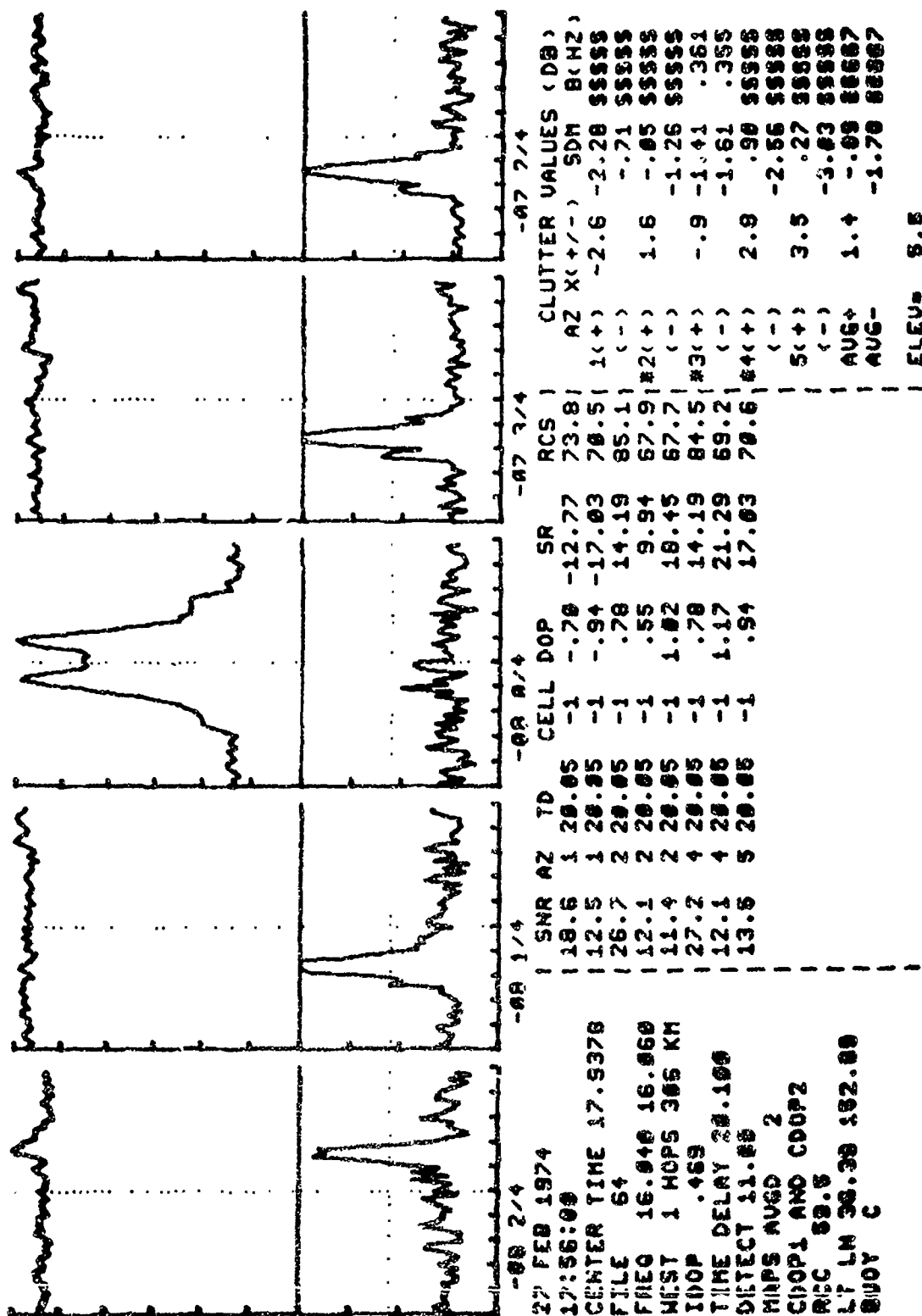
3071 1 6/7

On 30 January the entire day was devoted to recording the first set of data for the second part of our NORPAX effort with Scripps and Stanford to map the wind direction over a wide area. Judging by the strong buoy echoes on the previous day, there was no indication that some buoys might not later function or not be detected.

On 31 January, Buoy C was detected, and on 1 February and 4 February, Buoys C and E were both easily detected. Efforts to detect Buoys B and F (as well as A and D) proved futile. During this period the radar system was extensively checked using the buoy-echo simulator in order to calibrate the system. Since echoes from Buoys C and E were seen strongly, there is no doubt that the system was working normally. Despite extensive searches discussed below, no further detections of Buoys B and F were made and the specific search for these buoys was discontinued after 27 February.

b. Buoy-C History

Buoy C continued to operate strongly through most of February, but it frequently was weaker by about 10 dB than Buoy E. It was tracked through 27 February, after which no further contact was made despite extensive searches. Of 15 operating days on which buoys were tracked between 29 January and 27 February, Buoy C was detected on 14 of these days. The detection record for the last day on which it was seen, as shown in Figure 8, lists an SNR of more than 26 dB. On the next operating day, 4 March, it could not be detected and it has been concluded that it ceased to operate after 27 February. A complete history of its positions and track is given in Section III-E-3.



3071-1-678

FIGURE 8 DETECTION RECORD OF BUOY C ON THE LAST DAY IT WAS OBSERVED, 27 FEBRUARY 1974

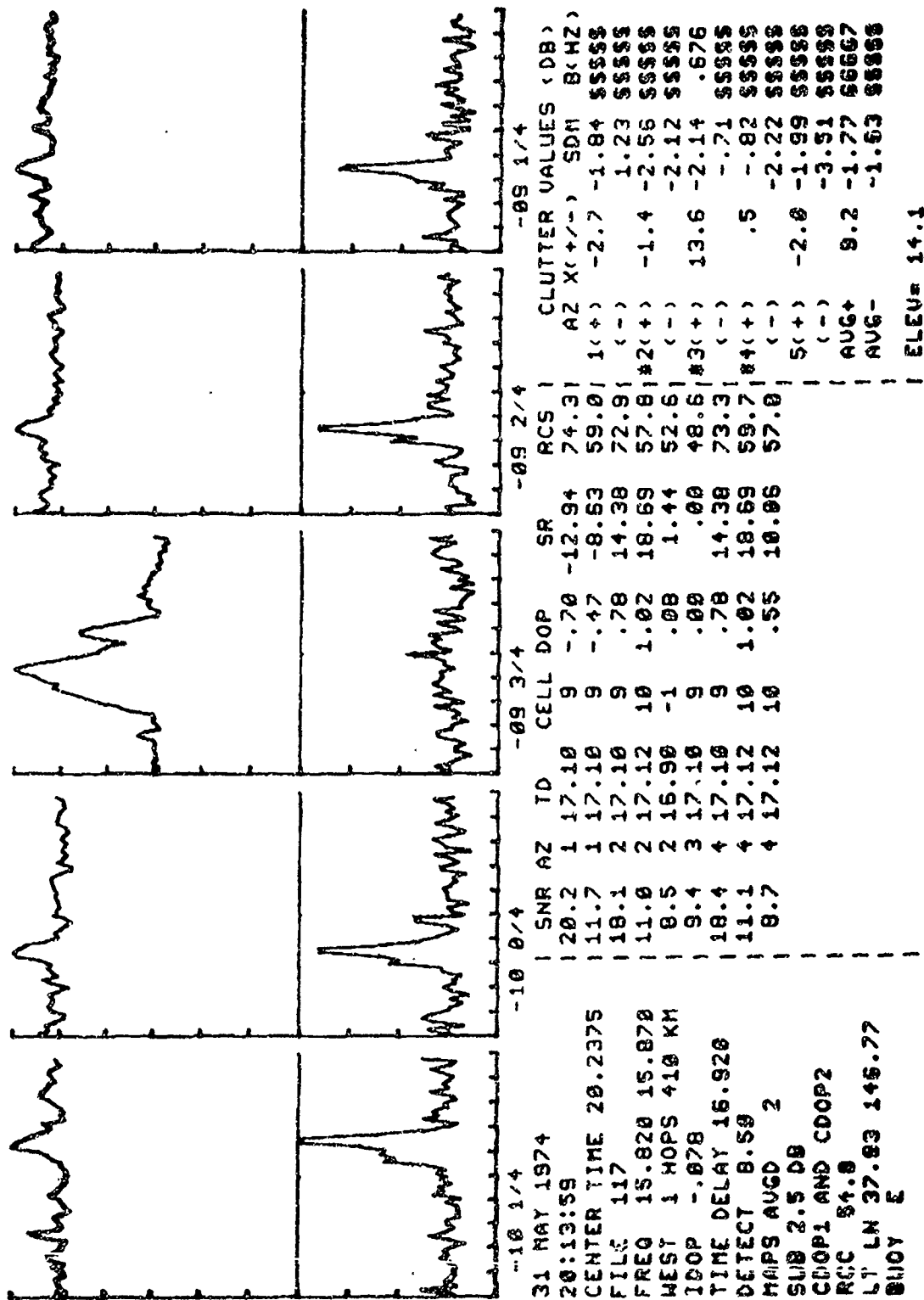
c. Buoy-E History

Buoy E was detected exceptionally well throughout the period concluding on 31 May. It was readily tracked although it appears to have broken its drogue around 8 March because it then moved rapidly eastward. It was easily located on 14 and 15 March and again on 23 March with the aid of the facsimile display, (described below) although it had drifted more than 150 km.

Daytime propagation conditions became significantly worse as summer ionospheric conditions prevailed. Heavy E-layer blanketing frequently prevented illumination of the target area during the operating hours of the buoy repeaters. Efforts to make occasional detections of Buoy E after 31 May were unsuccessful primarily because of such conditions. A record of a Buoy-E detection at the end of its tracking history is shown in Figure 9. Despite marginal propagation conditions a total of 24 detections were made on 31 May. It is likely that this buoy continued to operate beyond that date. Of 34 days devoted to buoy tracking between 29 January and 31 May, Buoy E was detected on 33 of these days.

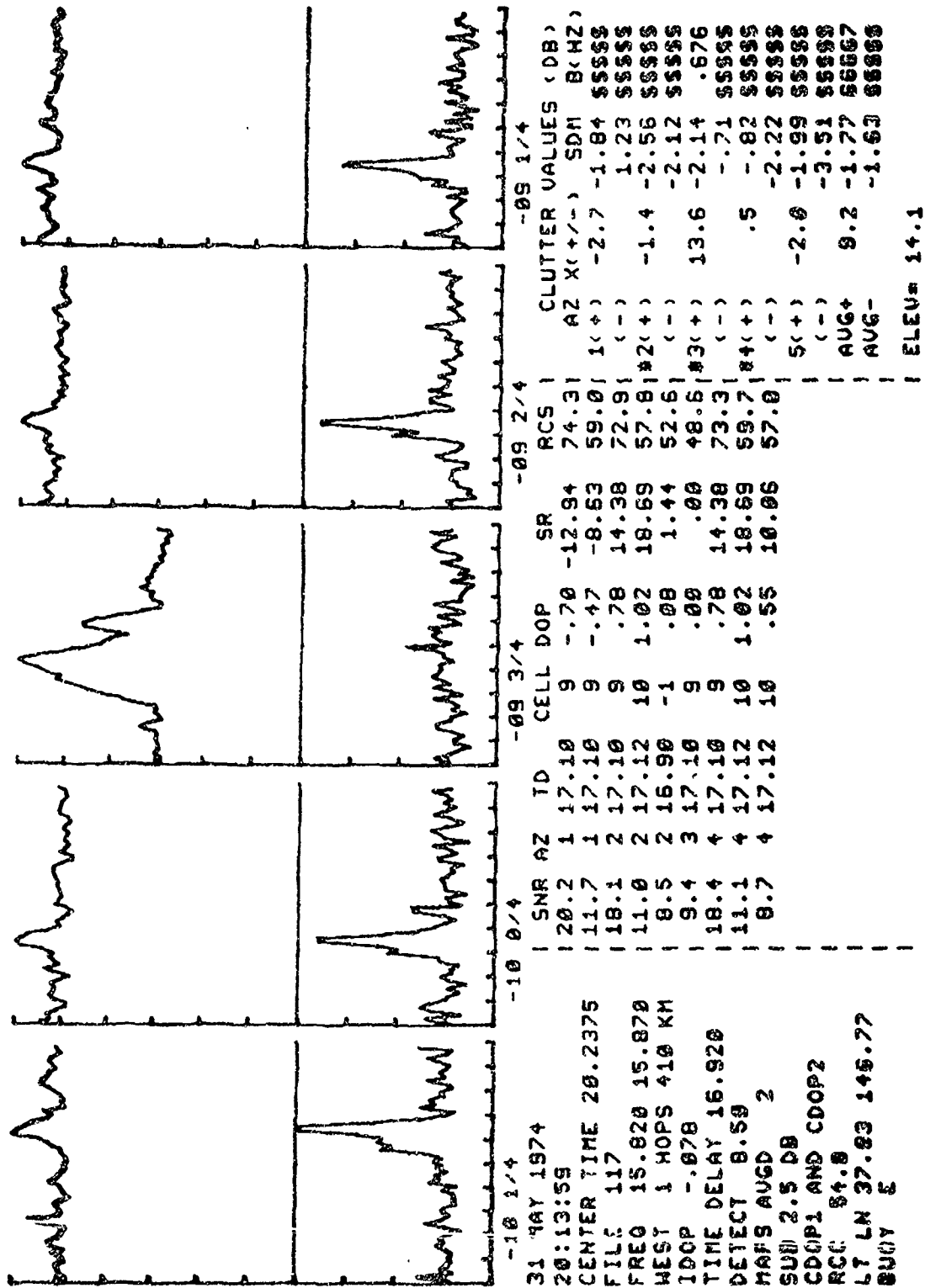
d. False Detection of Buoy D

Detection of Buoy D on 29 January was reported to Scripps, based on real-time observations and confirmed by post-processing of the data. A few similar detections were reported on 31 January, 5 February, and 12 February. However, closer examination of the data showed the apparent detections to be caused by simultaneous reception of an LSB from Buoy C and a USB from Buoy E. Such a condition can arise only if Buoys C and E are located at approximately the same time delay (range) from the radar and the search for Buoy D is being made at a time-delay difference equivalent to the 120.5-Hz separation in buoy modulation



3071-1-679

FIGURE 9 DETECTION RECORD OF BUOY E ON THE LAST DAY IT WAS OBSERVED, 31 MAY 1974



3071-1-679

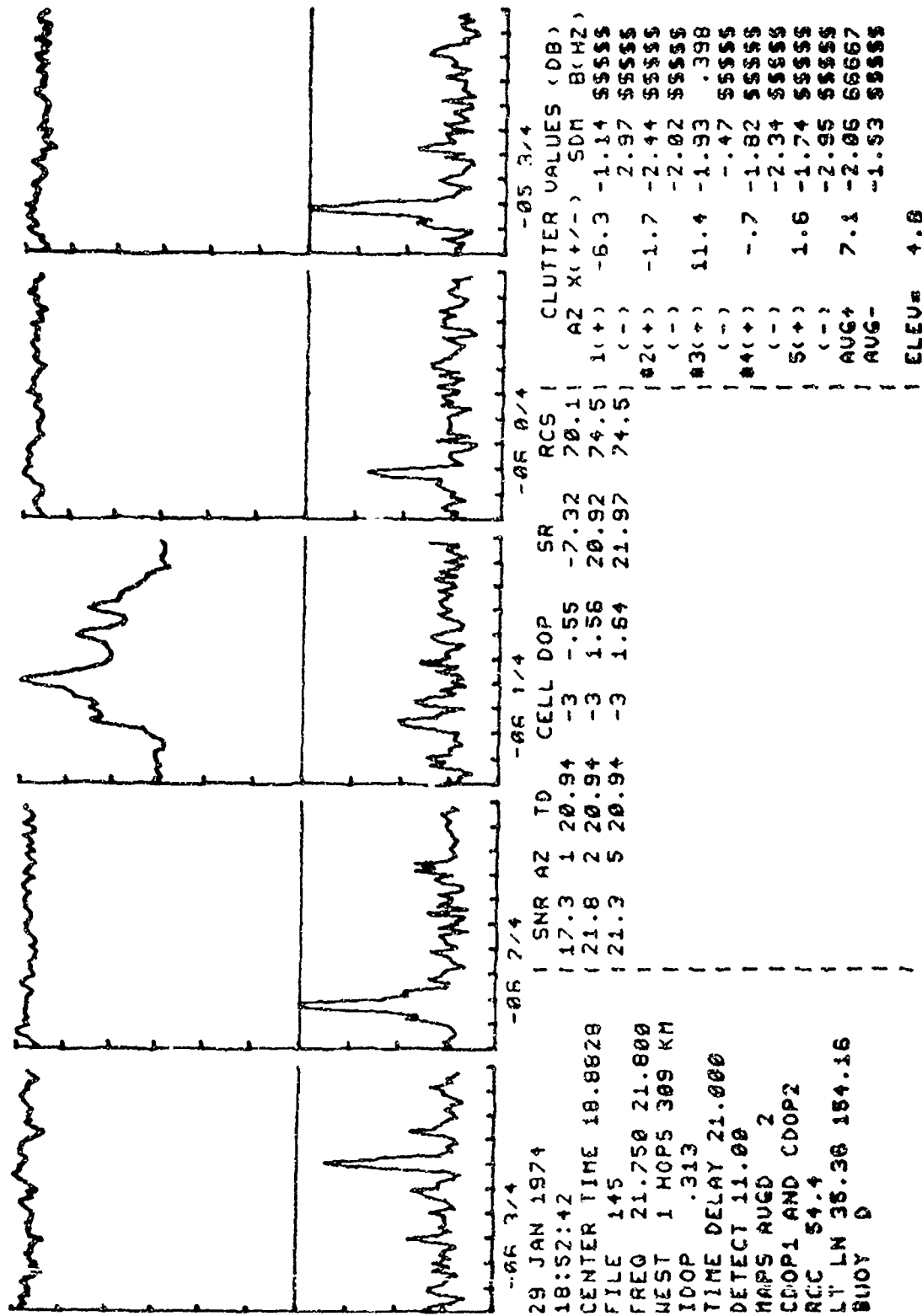
FIGURE 9 DETECTION RECORD OF BUOY E ON THE LAST DAY IT WAS OBSERVED, 31 MAY 1974

frequencies. With a 50-kHz SFCW waveform, 120 Hz is equivalent to a 0.48-ms time delay. An example of such a detection made on 29 January is shown in Figure 10 where the apparent range to Buoy D was 20.94 ms. The apparent range to Buoys C and E at nearly the same time was 21.42 ms, a difference of 0.48 ms. All apparent detections of Buoy D were similar and were proven to be spurious. It was therefore concluded that no valid detections were made and that this buoy apparently never operated.

e. Searches for Buoys B and F

Buoys B and F were not detected on 31 January or 1 February, while good detections of Buoys C and E were achieved. Since both buoys were non-drogued and we had been advised that they would drift eastward, the search area was extended up to 200 km eastward from the launch point, again with no success. The entire period of 4-9 February was devoted to buoy tracking, and the search area was extended up to 300 km west, 750 km east, 200 km north, and 100 km south, with no detections of Buoys B or F. Buoys C and E were drifting mostly northward during this period and were readily tracked.

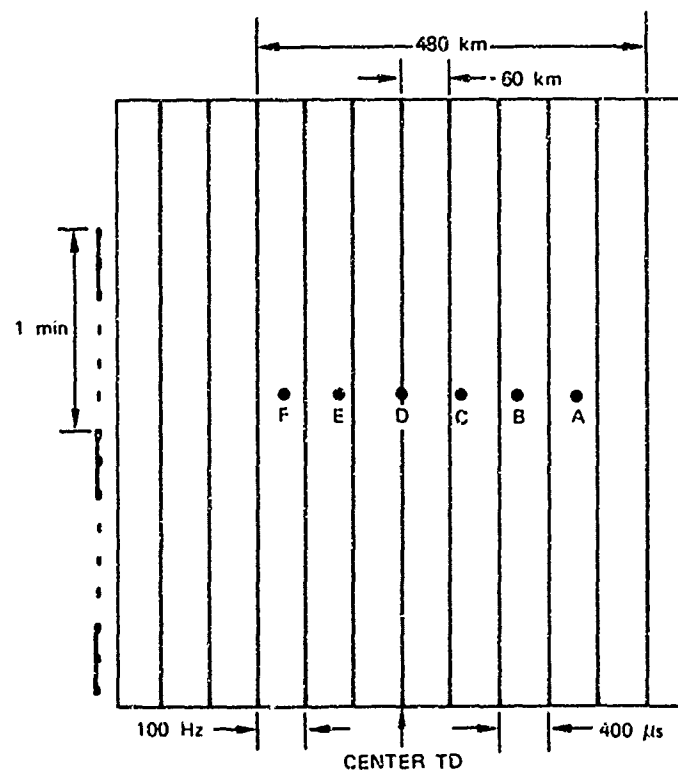
In order to provide real-time display expanded in range, a video receiver system was employed beginning on 9 February, in addition to the normal computer display. This system digitally spectrum-analyzed and displayed the receiver audio-tone output on a continuous facsimile chart. A receiver with a passband of 200 to 1400 Hz was used with a display of 0 to 1 kHz from the analyzer. The useful range that was displayed covered 800 Hz, or 480 km, with the usual 50-kHz SFCW waveform. A wider antenna beam was also used to give about 200 km azimuthal coverage. An independent SFCW generator was employed to permit setting the time delay and hence the range interval displayed without affecting the computer display. The format of the display is shown in



3071 1 680

FIGURE 10 EXAMPLE OF: FALSE DETECTION OF BUOY D

Figure 11. The receiver frequency was set to place any selected buoy at the center of the record. Other buoys at the same range would be spaced as shown. A buoy at a greater range would be displayed to the right of the position shown. Such a display provides no identification of a buoy,



3071-1-6S1

FIGURE 11 DISPLAY FORMAT FOR VIDEO-RECEIVER BUOY-TRACKING SCHEME

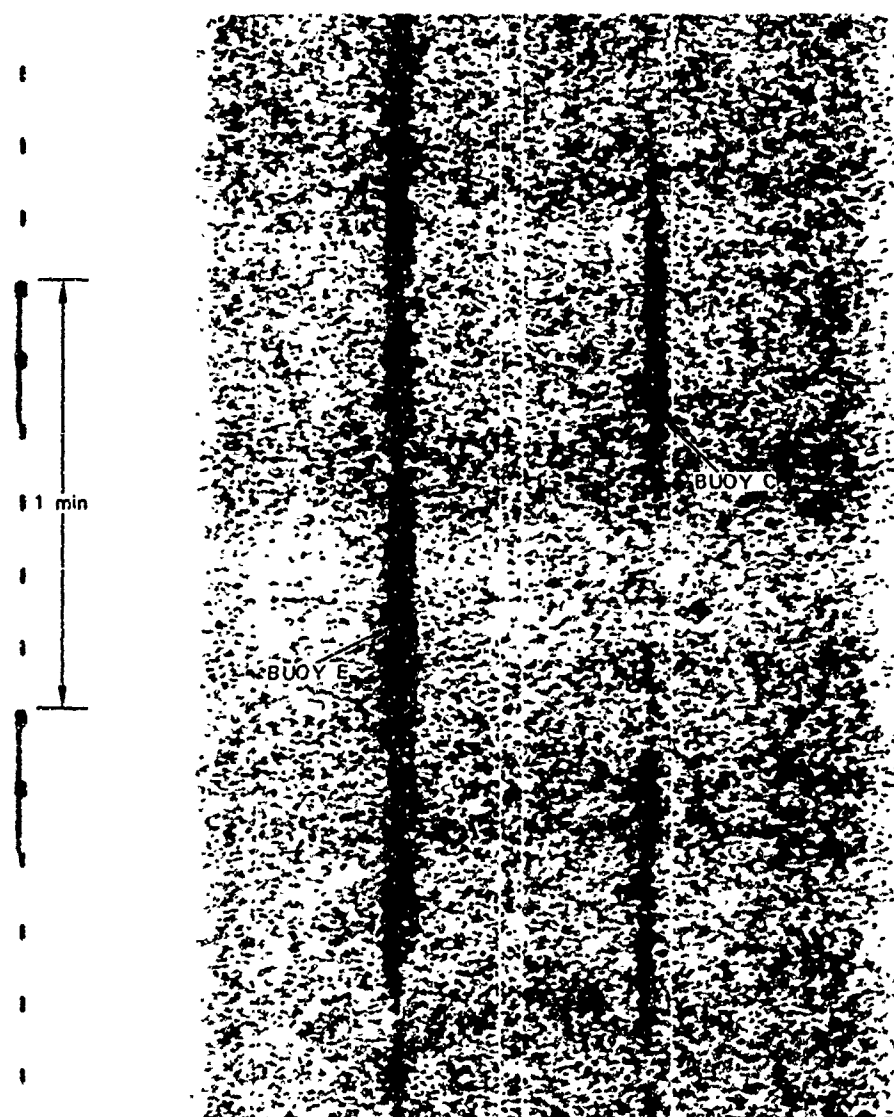
since the position on the record is a function of both the buoy modulation frequency and its range. It does show the presence of a buoy, and identification can be accomplished by the computer processor. The sensitivity of the system (i.e., the ability to detect a fading echo) was found to be only a little less than that of the computer processor, with the advantage that all buoys could be seen simultaneously over a wide ocean area. Buoys known to be operating (Buoys C and E) consistently gave very strong returns on this video recording. Range and azimuth resolution were poor, but detection of buoys was the primary goal. It was

typical that any signal producing a detection on the computer display was also visible on the facsimile record. The facsimile record also provided a continuous display of the fading of buoy signals not possible with the sampled output of the computer display. A typical record of the facsimile recorder showing Buoys C and E is shown in Figure 12 for 9 February. The figure also shows the effect of fading on the Buoy C signal. Since the processor samples for about 30 s, it could miss a detection during a fade such as the one shown; hence, several computer data samples were recorded for each buoy at every position. The facsimile display was also useful for identifying ship repeaters (discussed below).

After discussion of the search for Buoys B and F with Scripps personnel, the search on 12 February was concentrated in the quadrant northwest of the launch point and on 14 February in the northeast quadrant. On 19 and 20 February an additional receiving antenna (a single LPA) was used to look further north than was possible with the WARF array. Although system sensitivity was about 10 dB lower with this antenna, Buoys C and E were still detected, but no echoes from Buoys B or F were seen. The total area searched extended 375 km west, 800 km east, and 600 km north without success.

At this point, we concluded that one of the following had happened to Buoys B and F:

- (1) The buoys sank.
- (2) The buoys either were not operating or were repeating at a signal level considerably below the initial strength.
- (3) They traveled to the west much faster than predicted such that on 6 February they had moved over 300 km at a rate of about one knot.
- (4) They moved rapidly north such that on 4 February they had moved over 200 km at a rate of about one knot.



3071-1-682

FIGURE 12 FACSIMILE RECORD OF VIDEO RECEIVER SHOWING BUOYS C AND E
ON 9 FEBRUARY 1974

- (5) They moved approximately northwest at 0.5 knot or more, such that the early extended scans to the north and west did not encompass their tracks.
- (6) They went south.
- (7) They were picked up by some other party, either U.S. or foreign.

Both Scripps and SRI were inclined to reject Alternative 1. Item 2 is possible because Buoys A and D apparently did not operate and Buoy C operated at a level some 10 to 20 dB lower than designed. Our Scripps colleagues could not accept 3, 4, or 6, and we could not accept 7 because it would have been too risky.

This left Item 5 as most probable. Therefore during the period of 25-27 February additional searches were made north and west of the launch point for Buoys B and F, but without success. Buoy C ceased to operate after 27 February and concerted efforts to find Buoys B and F were also discontinued after that date. However, during March and April, in conjunction with the wide-area ocean-scatter mapping effort, two receiver channels were operated as buoy detectors. A total of 15 scans were made covering about 1 million square miles, over ranges of 1800 to 3600 km from the WARF radar. Although Buoy E was readily detected during this period, no echoes from Buoys B, C, or F were received.

We have concluded, therefore, that if the buoys operated as designed, they could have escaped detection if they headed approximately northwest at an unusually (and unpredicted) high speed, thus moving beyond the areas searched and not returning to the WARF coverage area.

2. Operation with Ships

Repeaters on R.V. Flip and R.V. Washington produced echoes for use in signal calibration for sea-scatter measurements and for evaluation of the OTH radar position accuracy. The design of these repeaters differed from that of the buoy repeaters, as described in Appendix B. All receivers operated to receive sea clutter and both repeater sidebands. The signals from the ship repeaters were also quite strong, and the repeater on the Flip was reduced by 10 dB on 5 February with no loss of detectability. The antenna used with the Flip repeater was also changed to provide a better radiation pattern for calibrating radar equipment on the Washington.

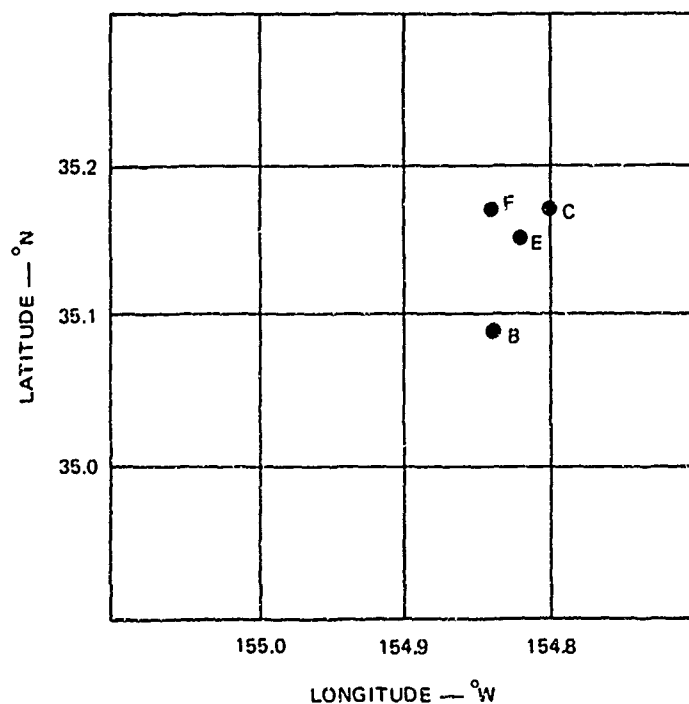
Since the two sidebands of the ship repeaters were separated in range it was necessary to select a time delay that placed both sidebands in the receiver bandwidth of 100 Hz. For the Flip, the spacing was 46 Hz, and little difficulty was found in centering the returns. For the R.V. Washington, the spacing of 86 Hz required more careful positioning of the center time delay. To avoid identification problems, operation of the repeaters was scheduled at different times where possible. Typical detection records for the Flip and the Washington are shown in Figures 13 and 14, respectively. The repeaters could also produce sidebands at odd harmonics of the modulation frequency. However, the apparent Doppler of the harmonics differed from that of the fundamental; hence identification of such spurious signals was accomplished.

3. Final Data Processing for Buoy Positions

The computer data processor used for the NORPAX buoy tracking did not provide real-time target positions since the antenna configuration used was not compatible with the software. Since additional post-experiment processing was required in any event to obtain buoy

identification, daily latitude/longitude plots, VCO measurement, mean target coordinates, and relative target positions, the main processing software was not rewritten. Instead, a comprehensive processor was devised to examine all detections made during a test, list them by buoy identification number, compute their actual coordinates, plot the latitude/longitude versus time for each buoy, measure and plot the VCO frequency versus time, and determine relative target positions. The design and use of this processor, with typical detection examples, are described in Appendix D.

The daily positions of the buoys that were obtained from the post processing records are listed in Table 2. Figure 15 shows the 29 January positions of the four buoys detected on that date and the only detections of Buoys B and F. A plot of the track of Buoy C is shown in



3071-1-685

FIGURE 15 INITIAL POSITIONS OF BUOYS ON
29 JANUARY 1974 FROM WARF DATA

Table 2

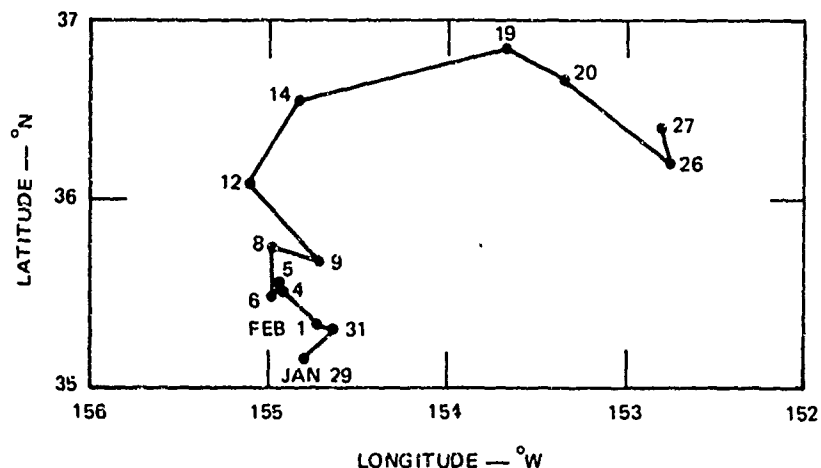
NORPAX BUOY POSITIONS FROM TRACKING DATA

Date	Buoy ID	Latitude (° N)	Longitude (° W)
29 Jan	B	35.09	154.84
	C	35.17	154.80
	E	35.15	154.82
	F	35.17	154.84
31 Jan	C	35.31	154.69
1 Feb	C	35.29	154.79
	E	35.27	154.85
4 Feb	C	35.55	154.94
	E	35.32	155.16
5 Feb	C	35.60	154.93
	E	35.31	155.20
6 Feb	C	35.43	154.98
	E	35.62	154.95
7 Feb	E	35.70	154.81
8 Feb	C	35.86	155.01
	E	35.58	154.91
9 Feb	C	35.97	154.83
	E	35.75	154.70
12 Feb	C	36.22	155.22
	E	35.77	155.14
14 Feb	C	36.60	154.79
	E	36.35	154.95
19 Feb	C	36.85	153.67
	E	36.39	154.62
20 Feb	C	36.70	153.32
	E	36.27	154.67
26 Feb	C	36.29	152.72
	E	36.51	155.52
27 Feb	C	36.42	152.79
	E	36.50	155.32

Table 2 (Concluded)

Date	Buoy ID	Latitude (° N)	Longitude (° W)
4 Mar	E	36.49	155.69
6 Mar	E	36.41	155.83
8 Mar	E	36.37	155.51
14 Mar	E	36.93	154.75
15 Mar	E	36.92	154.65
23 Mar	E	37.46	153.30
25 Mar	E	37.60	152.68
27 Mar	E	37.36	152.48
5 Apr	E	37.20	150.75
11 Apr	E	37.75	148.26
15 Apr	E	37.58	148.41
16 Apr	E	37.55	148.44
17 Apr	E	37.45	148.57
24 Apr	E	37.56	148.23
26 Apr	E	37.71	147.87
30 Apr	E	37.63	14. .42
10 May	E	37.66	147.82
17 May	E	37.82	147.46
24 May	E	38.01	147.17
31 May	E	37.91	146.96

Figure 16 for the period 29 January through 27 February. The track of Buoy E is shown in Figure 17 covering the period of 29 January through 31 May.



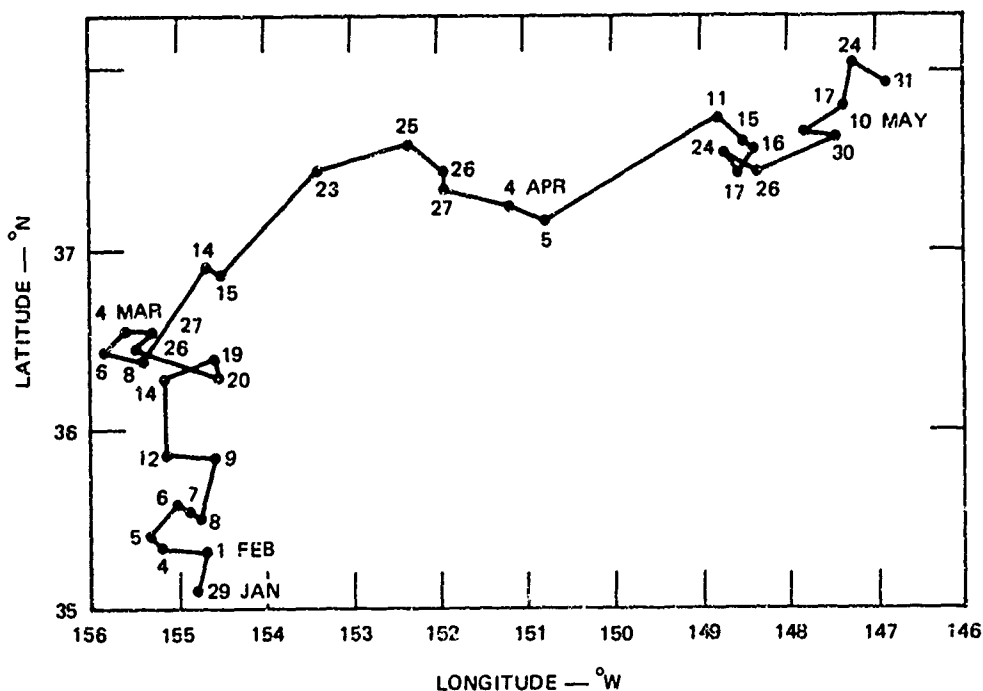
3071-1-686

FIGURE 16 TRACK OF BUOY C AS OBSERVED FROM THE LOS BANOS WARF SITE, 29 JANUARY TO 27 FEBRUARY 1974

4. Position Accuracy

a. Flip Positions

The tracking effort for the repeater on the Flip was of particular importance in evaluating tracking accuracy. Satellite fixes on the position of the flip were made during the period of the POLE experiments, and the accuracy of these fixes was estimated to be within ± 1.5 nmi. Radar positions were established on eight days between 29 January and 8 February. The radar and satellite positions are shown in Table 3 and are plotted in Figure 18. The range differences in nautical miles between the two sets of positions are shown in Table 4. The differences are expressed in terms of ΔN and ΔE in order to separate the errors into possible range and azimuth errors of the radar positions. As seen in Figure 18, the radar positions are all to the east except for



3071-1-687

FIGURE 17 TRACK OF BUOY E AS OBSERVED FROM THE LOS BANOS WARF SITE, 29 JANUARY TO 31 MAY 1974

8 February, and all to the north except for 29 January. The errors for the remaining days are generally in the same direction and similar in magnitude.

The mean error for the six days, excluding 29 January and 8 February, is $15.6/29.3^\circ$ nmi. The direction of the error is nearly along the path to the radar and implies that the error is primarily one in range. This error could arise from errors in the assumed virtual height. The radar observations of the Flip were made near 2300Z on five days (29 and 31 January, and 1, 4, and 7 February) during the POLE experiment and near 2000Z during three days (5, 6, and 8 February). As shown in Figure 18, on each of the five days when data were taken in late afternoon the range to the Flip is less than the correct value, implying that the assumed virtual height is higher than the real virtual height. On two days (6 and 8 February) when the data were taken near local noon, the range was close to the true range, indicating that the assumed

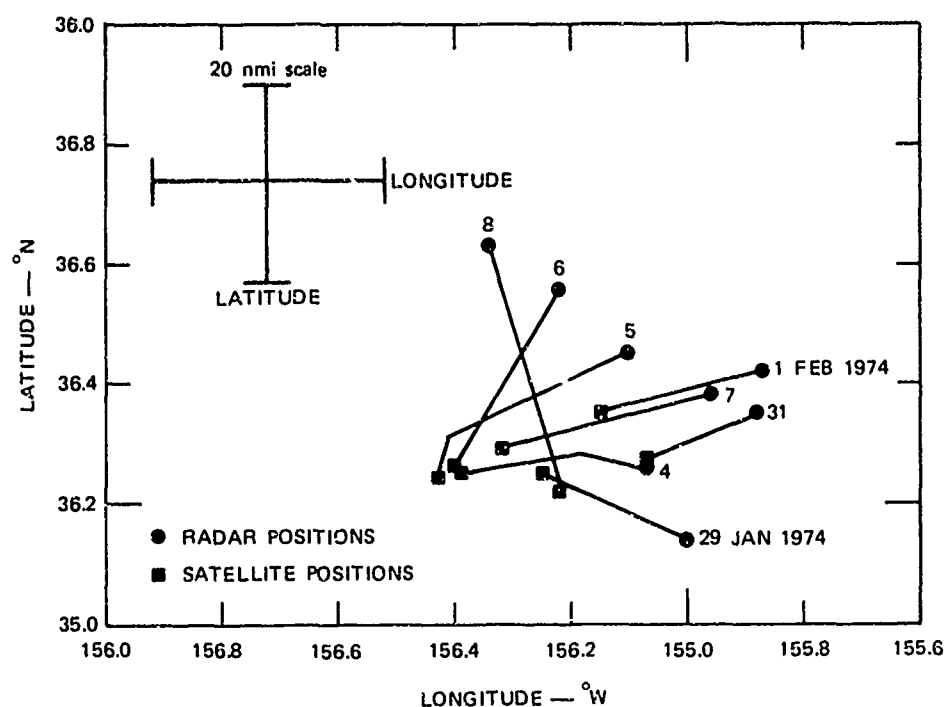
Table 3

POSITIONS OF R.V. FLIP FROM SATELLITE AND WARF DATA

Date	Satellite		WARF	
	Latitude (° N)	Longitude (° W)	Latitude (° N)	Longitude (° W)
29 Jan	35.038	155.143	34.94	155.00
31 Jan	35.072	155.072	35.15	154.88
1 Feb	35.152	155.150	35.22	154.87
4 Feb	35.053	155.387	35.06	155.07
5 Feb	35.037	155.427	35.25	155.10
6 Feb	35.057	155.403	35.36	155.22
7 Feb	35.087	155.320	35.18	154.96
8 Feb	35.020	155.222	35.43	155.34

height (which was approximately 310 km for all tests) more nearly matched the real height. It is thus evident that improved virtual-height measurements would significantly reduce position errors, and such measurements have already been implemented at WARF. Initial tests of this implementation are described in Appendix E.

Figure 18 and Table 4 also show that the azimuthal error on 6 and 8 February was significantly greater than on the other dates. The mean δN for these days was 18.5 nmi, while for the other five days the mean error was 4.2 nmi. The mean radar azimuth of the Flip for 6 February was -6.7° and for 8 February it was -6.9° . On 7 February it was -6.2° . The observed azimuth thus appears to be related to the local time of observation, and possibly to a change in ionospheric tilts.



3071-1-688

FIGURE 18 RADAR AND SATELLITE POSITIONS OF FLIP, 29 JANUARY TO 8 FEBRUARY 1974

Table 4

RELATIVE POSITIONS OF R V. FLIP FROM SATELLITE AND WARF DATA

Date	δN	δE	δR	Bearing (deg)
29 Jan	-6.50	12.20	13.82	118
31 Jan	4.70	9.41	10.52	26
1 Feb	4.10	13.74	14.34	17
4 Feb	.40	15.55	15.56	2
5 Feb	12.80	16.05	20.53	39
6 Feb	18.20	9.00	20.30	64
7 Feb	5.60	17.67	18.54	18
8 Feb	24.60	-5.81	25.27	347
Average Values	9.61	12.43	15.71	38

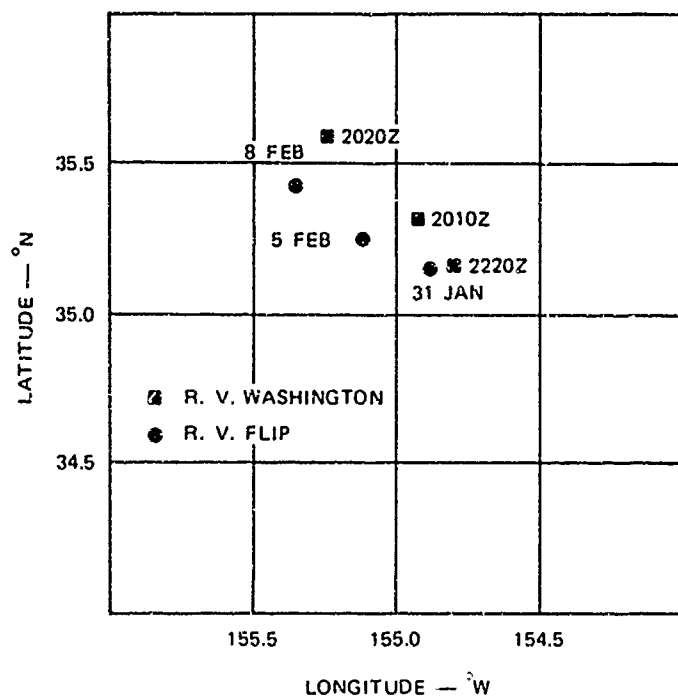
b. R.V. Washington Positions

Positions were also recorded for the R.V. Washington during the POLE experiment. It was intended that these positions relative to the R.V. Flip would provide additional data on the accuracy of the WARF system. Measurements made on both targets at nearly the same time should give relative positions within the resolution limits of the radar, since virtual-height errors would cancel out. A limited number of detections were made in which both repeaters were operating at the same time, but the apparent positions were spread due to antenna sidelobe reception of the strong repeater signals. Not enough data were recorded at these times to permit exclusion of such errors. Also, no log data were available on the actual relative positions of the ships, so no accuracy estimates could be made. The observed mean positions for the R.V. Washington are shown in Table 5 for four days on which detections were made. On three of these days, 31 January, and 5 and 8 February, position data on the Flip were also available, and the positions of the two ships are plotted in Figure 19. On 9 February, detections were made of both the Flip and the Washington, but the apparent positions were highly spread and were therefore not used.

Table 5

POSITIONS OF R.V. WASHINGTON FROM WARF DATA

Date	Time (GMT)	Latitude (° N)	Longitude (° W)
28 Jan	2315	35.16	154.86
31 Jan	2220	35.16	154.78
5 Feb	2010	35.30	154.95
8 Feb	2020	35.59	155.22



3071-1-689

FIGURE 19 RELATIVE POSITIONS OF R.V. WASHINGTON AND R.V. FLIP ON THREE DAYS OF SIMULTANEOUS DETECTIONS

c. Buoy Positions

We had proposed that the radar be operated for a 3-to-4-hour period for buoy repeater detection in order to ensure the best possible absolute and relative position accuracies. We likewise had hoped that the Flip repeater would stay on for the same period of time to provide an additional position reference. Since we can only estimate an average virtual ionospheric height during the experiment--either with computer raytracing or vertical-incidence soundings over WARF--data are needed over a period of an hour or more during which a suitable average can smooth out short-term ionospheric height variation. After initial location of one or more buoys, at least an hour of data was recorded on the buoy positions. Our specially designed operator console for buoy tracking gave us the capability for switching between two preset repeater radar positions. This switching was done constantly throughout the

tracking period, except when only Buoy E was operating. The five-receiver processor was optimized to detect one buoy at a time, giving the capability for accurate position estimates and precise VCO frequency measurement. The processor switching between buoys over a long period, with subsequent time averaging, provides a more accurate estimate of relative position than if two buoys had been detected simultaneously. Apparent position errors caused by localized short-term ionospheric-height variations are different at different radar coordinates; however the longer-term average will smooth these variations at each buoy location. It also follows from our past experience that the long-term averaged position estimates should yield absolute position accuracies with the specified ± 10 nmi error.

F. Propagation Conditions

Several ionospheric propagation phenomena may occur in the operation of an OTH radar that affect detection sensitivity and target location accuracy. The effects of these phenomena vary with the season of the year, hours of operation, target range, the frequency of operation, and the particular OTH radar application. Propagation problems that were encountered in the NORPAX experiment could be traced to (1) the longer-than-anticipated range of the POLE location, and (2) insufficient frequency range and on-time of the repeaters.

1. Illumination of Target Area

The basic requirement for any operation is that the target area be adequately illuminated by the radar. The best illumination is achieved by first observing the distribution of backscatter energy versus range and frequency as displayed on ionograms, then by choosing the most suitable operating frequency. The sea-clutter spectrum display then

gives a precise measure of the signal strengths over the path. The sub-clutter visibility and the shape of the sea-clutter spectrum permits the operator to evaluate the usefulness of the operating frequency.

Examples of the backscatter ionograms are shown in Figures 20 and 21, for 1 February and 23 May, respectively. Figure 20 shows acceptable illumination of the target area on 1 February; (Buoy E was at 21.4 ms). By comparison, the 23 May record in Figure 21 shows heavy direct ionospheric scatter and blanketing E-layer propagation--such that no illumination was possible to the range of Buoy E at 18 ms during the day on that date.

The diurnal variation in propagation conditions is such that strong signals in the target area were possible typically between about 1600Z and 2400Z in January-March. During the POLE experiment in early February the conditions were especially good for buoy detection; no difficulties were experienced in illuminating the target area, except on occasional magnetically disturbed days.

The long-range, single-hop propagation degradation in Figure 21 began in April and was generally caused by losses in signal strength due to refraction, or possibly total reflection, by the ionospheric E and sporadic-E layers. These losses were such that operation after 2300Z, possibly to 0400Z, would have resulted in much better detection capability. In general, the propagation beyond 1000 nmi in the summer, typically May through August, is poor during the day, but good during the hours from late afternoon through approximately 0600Z. By contrast, during the late fall, winter, and early spring months, the long ranges are covered well during the day, but rather poorly (except at very low frequencies) between sunset and sunrise. Because the duty cycle was constrained to a total of 6 hours per day, and because we wanted to average all the buoy hits over about 3 to 4 hours, we chose to make the

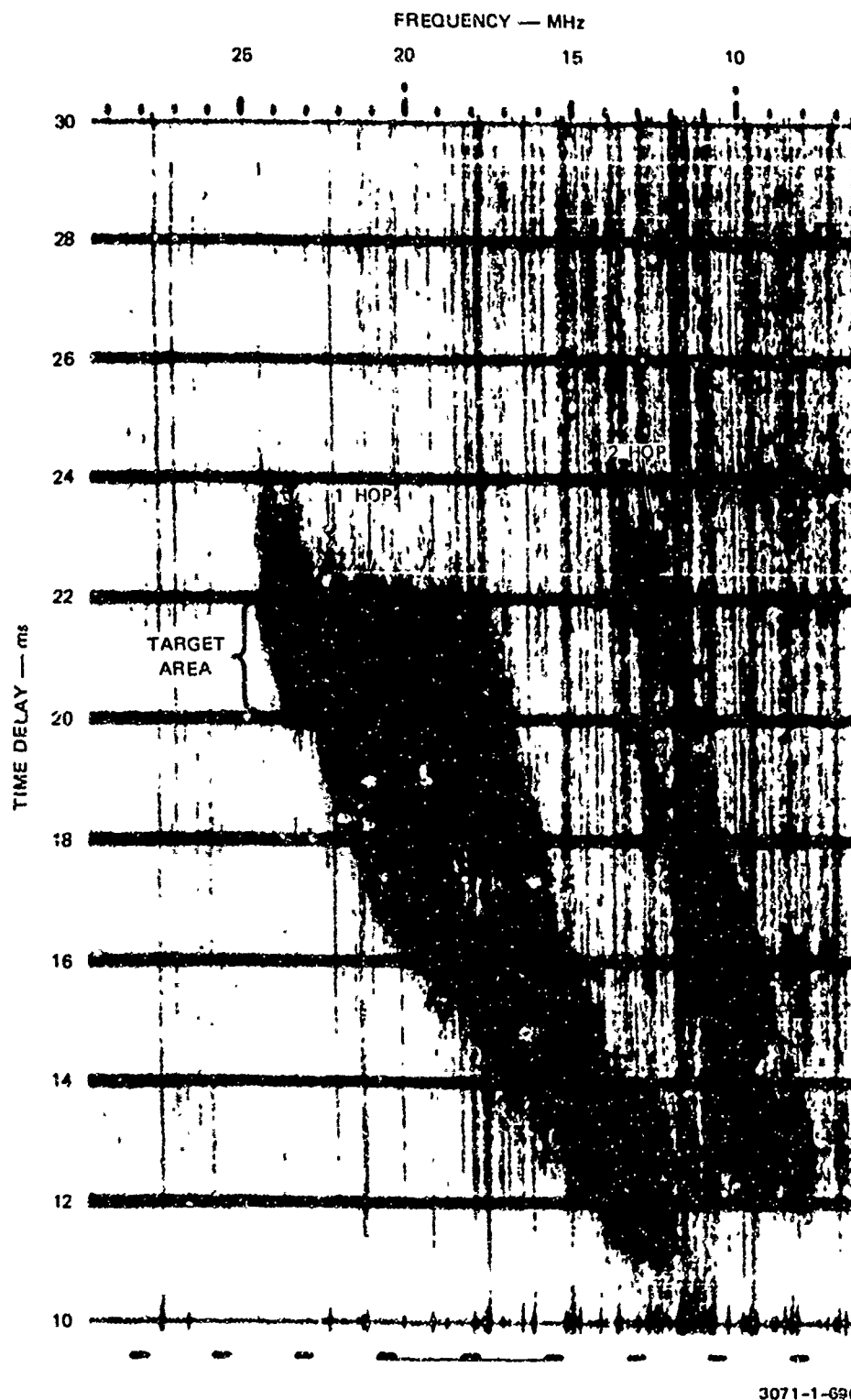
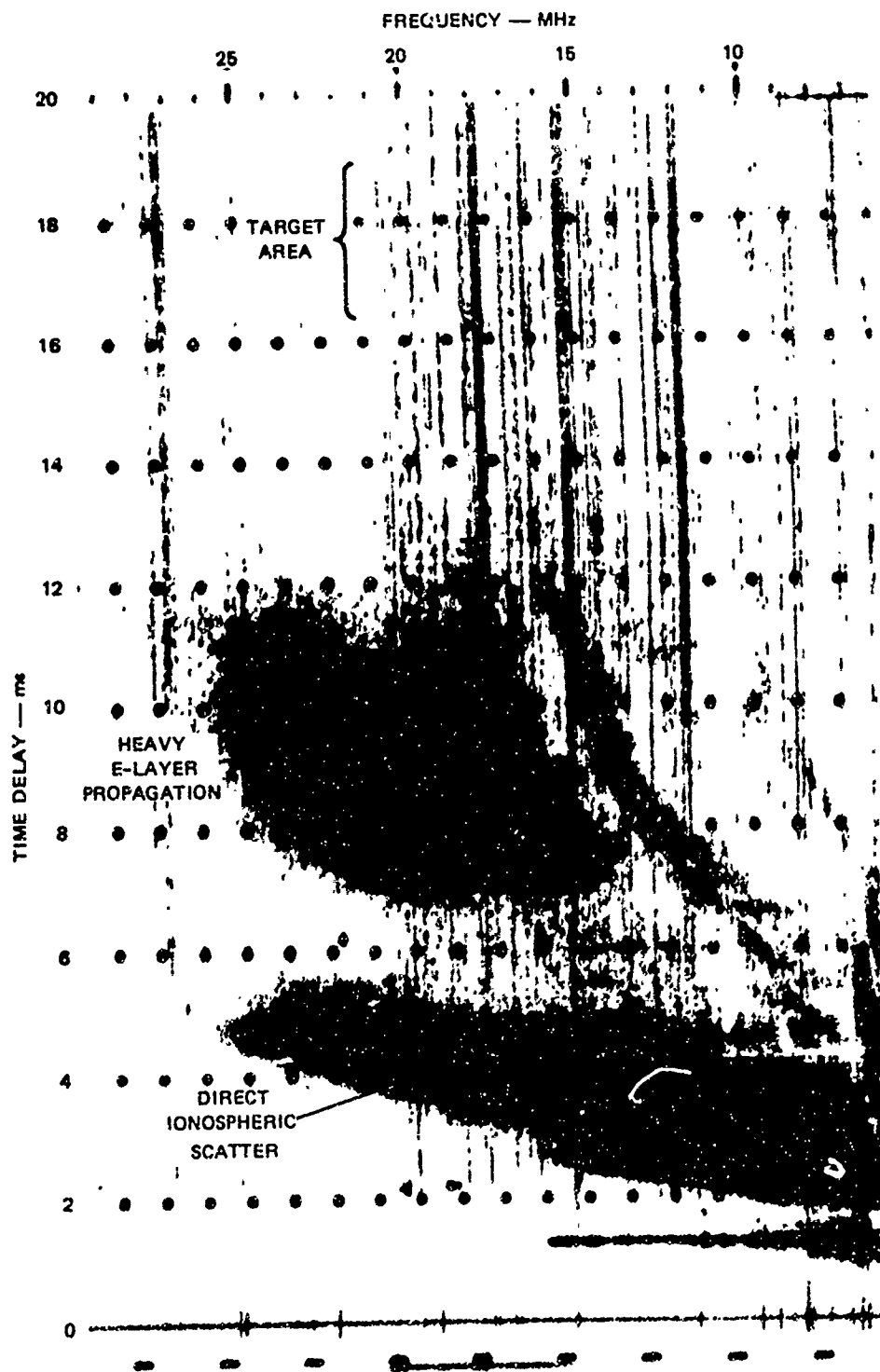


FIGURE 20 BACKSCATTER IONOGRAM OF TARGET AREA ON 1 FEBRUARY 1974



3071-1-691

FIGURE 21 BACKSCATTER IONOGRAM SHOWING HEAVY E-LAYER BLANKETING AND DIRECT SCATTER, 23 MAY 1974

6 hours continuous. This also simplified the buoy clock design. Since the buoys were turned off at 2300Z, it was not possible to use the night-time propagation conditions in tracking Buoy E, and no detections were made after 31 May.

2. Repeater Frequency Limit

The buoy launch point was at the extreme range usable for the single-hop propagation mode, even under the best of conditions. The buoy design called for a repeater frequency range of 15 to 25 MHz, which would have been ideal for 1-hop propagation at the originally planned launch position of 35° N, 150° W--some 250 nmi closer. Also, it was expected that the buoys would probably drift eastward (as Buoys C and E in truth did), leading to an even better propagation situation.

On many days, better illumination could have been achieved by the use of 2-hop F-layer propagation. Unfortunately, the frequency of operation for such a mode was almost always below 15 MHz--the lower limit of the buoy repeater. The low frequency limit was due to buoy antenna degradation caused by physical limitation on antenna length. For both long-range and very-short-range experiments (less than 1500 km) an improved antenna design is needed, and can be achieved.

3. Multiple Propagation Modes

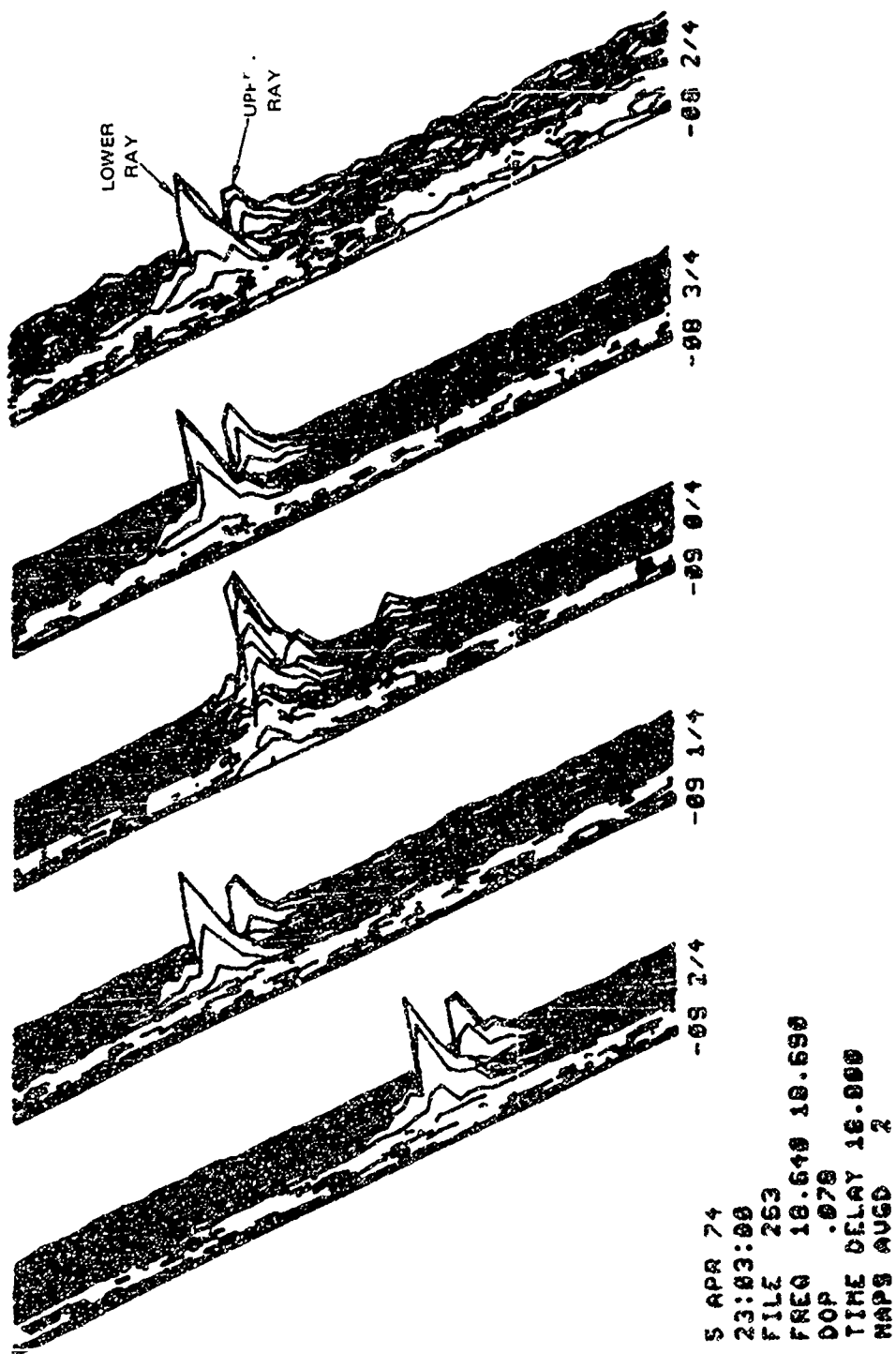
A third problem, but one of relatively little significance to the detection of discrete targets well removed from the clutter, arises from the appearance of multiple propagation modes. These modes are caused by propagation to the target and back by more than one path, where each path has a different time delay and correspondingly different apparent target ranges. This problem was very evident at the long ranges to the POLE location.

Propagation is typically by means of the lower-ray F-layer mode. However, at frequencies near the MUF the upper ray will have a time delay slightly greater than the lower ray and two or more modes may occur simultaneously within the range window of the radar. The difficulty may be compounded by the presence of other strongly reflecting layers, particularly E_s , giving rise to so-called M-modes.⁵ The presence of these multimode echoes can obviously cause errors in target location unless the exact mode can be identified. The operator can usually detect the presence of multimodes in the structure of the sea-clutter spectrum as evidenced by multiple peaks. Often, a change of frequency (especially if the operating frequency is near the MUF) will eliminate the multipath condition. It is often advantageous to generate a 3D display of the five-receiver spectral output in order to observe all range cells independently. As shown in Figure 22, multimodes are clearly displayed as discrete targets having the same Doppler but different ranges. The shortest time delay will occur for the lower-ray one-hop mode, from which positions are computed most accurately.

G. Recommendations for Future Operations

Although successful tracking of two buoys was achieved during this phase of the NORPAX effort, the fate of four others is uncertain. However, based on the knowledge obtained from these tests, an OTH radar buoy-tracking program could be implemented to give a high probability of nearly year-round detection at ranges of 800 to 5000 km. The program should have the following capabilities not available in the test just concluded:

- (1) The operating frequency range should be extended to cover 5 to 25 MHz, primarily to permit the use of night operations where the MUF is typically lower than the 15-MHz limit of the previous buoys.



3071-1-692

FIGURE 22 3D DISPLAY OF A BUOY-E DETECTION WITH MULTIMODES

These frequency limits would also permit the use of 2- and 3-hop propagation for the longer ranges. The primary changes required would be in buoy antenna design.

- (2) The repeater cross section should be increased to 70 dBsm at all frequencies to provide improved SNR, especially at the longer ranges. The amplifier output would need to be 10 to 20 watts.
- (3) The on-time of the repeater could be remotely controlled to minimize battery drain when the radar was not operating and to permit an optimum choice of operating times based on seasonal propagation conditions. With increased repeater power output, the control of operating time would offset the additional battery drain. Alternatively, a split cycle in daily operation, such as during the hours 1800 to 2200Z and 0100 to 0500Z would at least give greater detection assurance.
- (4) Additional receivers and more antenna beams would be employed to improve azimuth accuracy and provide wider coverage during a search for the target. The computer processor would be optimized for real-time tracking data.
- (5) Higher radar power could be used to improve long-range detection capability or to permit wider azimuthal coverage without sacrificing sensitivity.
- (6) Vertical soundings of ionospheric height should be implemented to improve target position accuracy.
- (7) An operational check of the system should be made with all buoys in the water for at least two weeks prior to their release.
- (8) Improved buoy identification procedures should be implemented in order to preclude false detections in a multiple-buoy environment.
- (9) The radar operation should incorporate at the beginning the following important rules:
First, never assume that anyone knows a priori where the buoys will drift, or at what speed;

Second, follow the buoys very closely (daily) for several days immediately after launch; Third, begin every day's operation with a lower resolution scan (wide-area search mode) to determine the general location of each buoy, which would be followed by the high-resolution hits aimed at more accurate positioning.

If, on any day, a buoy was not initially detected, it would be mandatory that the operator devote more time to finding it, at the expense of all but a few hits on detected buoys.

IV SEA BACKSCATTER MEASUREMENTS

Three types of data were recorded for use in a study of the correlation of the HF sea-backscatter Doppler spectrum with oceanic winds and sea state. These data included: (1) Dedicated continuous data samples near the R.V. Flip, (2) wide-area real-time surveillance of a large portion of the WARF coverage area, and (3) isolated real-time recordings near the Flip. These data sets were to be used to evaluate and refine the accuracy for measuring oceanic parameters by HF radar; the wide-area scans were also to be used to map ocean winds over a large area. Data reduction for the first and last set is essentially complete. Although it is our opinion that more could be done with the continuous samples near the Flip using high Doppler resolution. Data reduction for the wide-area surveillance will be completed in 1975. All of the reduced data are being shared among our colleagues at Scripps and Stanford.

The following sections summarize the experiments and preliminary reduction for the three sets of data.

A. Continuous Sampling for High Doppler Resolution

1. Experiment Description

During the period of the POLE experiment, 28 January to 14 February, data were recorded to permit subsequent analysis for the spectral components in energy backscattered from the ocean surface. On 12 days of this period during which tracking of buoy repeaters was the principal effort, data were recorded on digital tape using an integration time of 15 minutes. Three 15-minute samples were recorded on each of these days with the target centered in the vicinity of the Flip or near 35° N, 155° W.

The normal integration time for other records made during these experiments was 12.8 s. With a greatly increased integration time, much higher resolution of spectral components was possible in post-analysis.

Observers on R.V. Flip and R.V. Washington made simultaneous local measurements of ocean surface conditions and wind direction and speed during the POLE experiment period. The data thus obtained are being compared with the HF data recorded by the WARF OTH radar to determine the degree of correlation.

This high-resolution backscatter effort utilized the full WARF system but only a single antenna beam and a single receiver. The SFCW waveform was used with a 50-kHz bandwidth. The receiver was operated with a low-pass bandwidth of 870 Hz. The audio tone was sampled at a rate of 2560 Hz, and a total of 2250 records per file were recorded on digital tape.

Where possible, the records were taken during periods when the HF repeater on the Flip was in operation. Such records were made on six days. Data were taken near 0000Z on 11 days and near 1800Z on 1 day. A complete log of the data obtained is given in Table 6. Those files with an (†) under the column heading "Flip" indicate that the Flip repeater was clearly visible on those samples.

2. High-Resolution Data Processing

The digitized SFCW backscatter sweeps from each recording day were Fourier-analyzed 3-D output formats of amplitude versus time delay (range) and Doppler shift. This off-line processing is essentially identical to the real-time processing described earlier. The output from the off-line processor is displayed in: (1) the 3-D format, (2) the spectral average of all range lines, and (3) the SNR plot of the strongest return at each Doppler divided by the average (Item 2) less the three strongest returns at said Doppler.

Table 6

DATA LOG FOR HIGH-RESOLUTION BACKSCATTER
IN THE VICINITY OF R.V. FLIP

Date	File No.	Time (GMT)		Frequency (Mhz)	Time Delay (ms)	Az (degree)	Flip	Tape Number
		Start	Stop					
28 Jan	1	2338	2353	20.91-20.96	21.54	-6.25	†	419
	2	2353	0008	20.91-20.96	21.54	-6.25	--	
	3	0018	0033	20.30-20.35	21.54	-6.25	--	
29 Jan	1	2335	2350	23.70-23.75	21.5	-6.25	--	465
	2*	2355	0010	21.80-21.85	22.4	-6.25	†	
	3*	0010	0025	21.80-21.85	22.4	-6.25	--	
31 Jan	1	2331	2346	18.80-18.85	21.48	-6.25	†	470
	2	2346	0001	18.80-18.85	21.48	-6.25	†	
	3	0004	0019	18.30-18.35	21.48	-6.25	--	
1 Feb	1	2337	2352	19.31-19.36	21.50	-6.25	†	471
	2	2352	0007	19.31-19.36	21.50	-6.25	†	
	3	0007	0022	19.31-19.36	21.50	-6.25	--	
4 Feb	1	2345	0000	19.12-19.17	21.65	-6.25	--	479
	2	0000	0015	19.12-19.17	21.65	-6.25	--	
	3	0021	0036	17.66-17.71	21.65	-6.25	--	
5 Feb	1	1744	1759	22.72-22.77	21.65	-6.25	--	357
	2	1759	1814	22.72-22.77	21.65	-6.25	†	
	3	1829	1844	20.84-20.89	21.65	-6.25	†	
6 Feb	1	2336	2351	19.83-19.88	21.50	-7.00	--	480
	2	2351	0006	19.83-19.88	21.50	-7.00	--	
	3	0010	0025	17.45-17.50	21.50	-7.00	--	
7 Feb	1	2332	2347	22.81-22.86	21.40	-7.00	--	483
	2	2353	0008	22.81-22.86	21.40	-7.00	†	
	3	0008	0023	22.81-22.86	21.40	-7.00	--	
8 Feb	1	2326	2341	23.05-23.10	21.70	-7.00	--	485
	2	2349	0004	20.91-20.96	21.70	-7.00	--	
	3	0008	0023	19.60-19.65	21.70	-7.00	--	
9 Feb	1	2346	0001	23.80-23.85	21.86	-8.00	--	490
	2	0011	0026	18.65-18.70	21.86	-8.00	--	
	3	0027	0042	18.65-18.70	21.86	-8.00	--	
12 Feb	1	2334	2349	22.80-22.85	21.65	-8.00	--	494
	2	2358	0013	19.90-19.95	21.65	-8.00	--	
	3	0013	0028	19.90-19.95	21.65	-8.00	--	
13 Feb	1	2346	2341	19.31-19.36	21.60	-7.00	--	498
	2	2349	0004	20.60-20.65	21.60	-7.00	--	
	3	0004	0019	20.60-20.65	21.60	-7.00	--	

* Two-hop propagation.

† Flip repeater on.

The main objective of the high-resolution processing was to obtain sea-backscatter spectra processed to the highest possible Doppler resolution, so that wind and sea-state information could be detected by means of second-order backscatter components. In order to determine the relative degree of Doppler resolution permitted by the ionospheric paths, it was almost imperative to process data that included reference echoes from the Flip repeater. The geographical positions of the recordings were also determinable by this means. The procedure, therefore, was to sample each day's recording at a time when the Flip repeater was actually seen on the FAX recordings taken while digitizing, or at a time when the Flip repeater may have been on (but was not detectable). This data-sample time was chosen with the added restrictions that the radar illumination be adequate and that the Flip repeater signal be as unperturbed (as possible) by multiple ionospheric paths. This procedure took some care, because the propagation quality actually varied significantly throughout each 15-minute recording. The samples at these apparent "best" times were processed to coherent integration times of 25.6 s and 51.2 s, equal to twice and four times the on-line integration times, respectively.

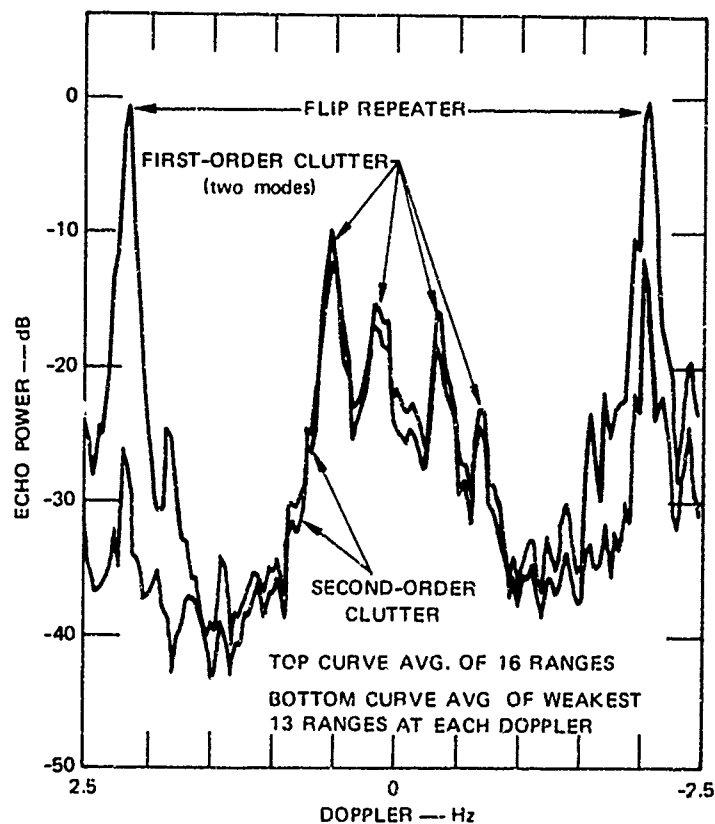
In addition to the best-time samples, we processed a larger amount of the recordings on the first file of 31 January and on all three 15-minute files of 5 February.

There were nine off-line spectra on 31 January, 28 on 5 February, and two each from the remaining 10 days. There were a total of 57 spectra, displayed in three forms for each one. A copy of these data, together with experiment logs and comments on each output, were shared with R. Stewart at Scripps for cooperative analysis.

3. Results

The off-line processing showed that many of the spectra were contaminated by ionospheric multipath. A typical example appears in

Figure 23. These data were taken from File 1 of 31 January (Table 6) and were processed coherently for 25.6 s. Note that the sea clutter has four peaks, instead of two, corresponding to the reception of sea backscatter via two independent paths. each having different ionospheric



3071-1-693

FIGURE 23 OFF-LINE SEA-CLUTTER SPECTRUM SHOWING EFFECTS OF MULTIMODE PROPAGATION

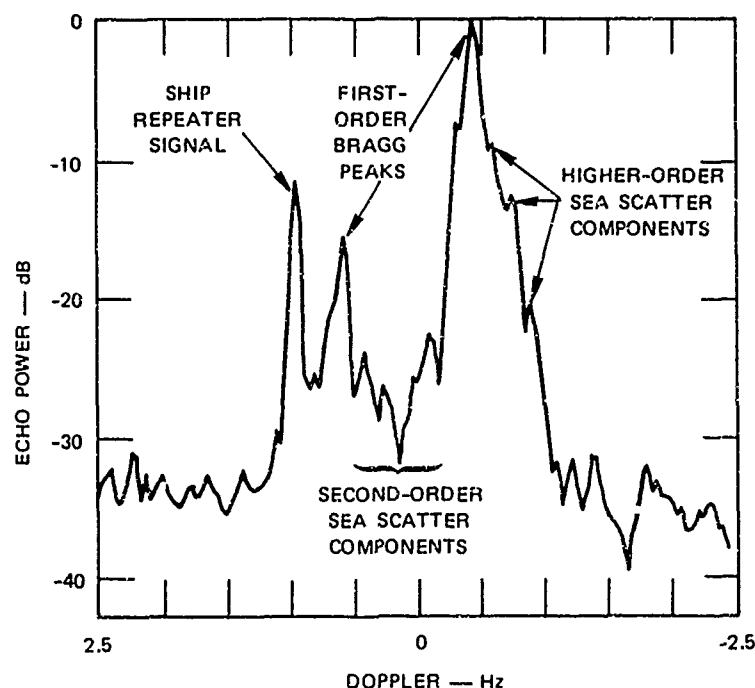
Doppler shift. Such a result will rarely affect the calculation of wind direction from the first-order spectra, but the second-order scatter is mostly covered up. Note, however, that at least two second-order returns are visible on Figure 23, and it is believed that wind-speed/sea-state information is contained in these "sidebands." No effort has yet been made to correlate such second-order returns that were occasionally visible on the off-line spectra. It is felt that further experiments are warranted at shorter ranges, where good propagation can be maintained.

As discussed in earlier sections of this report, the range to the POLE area was at the extreme limit of single-hop propagation. Frequencies available for two-hop propagation were below the 15-MHz cutoff frequency of the repeaters. Since the lower ray was attenuated by virtue of its low elevation angle, the upper-ray strength--which is normally very low by comparison--occasionally even exceeded the strength of the lower ray. These two modes normally have unequal ionospherically-induced Doppler shifts, hence the overlapped clutter spectra. The other problem, that of limited Doppler resolution caused by an unstable ionosphere, appears also to be most severe at the extreme limit of one-hop propagation. It is at this limit that we observed the illumination at a particular radio frequency to be most highly variable.

There is no doubt that the ionosphere will support single unperturbed paths, providing that the range and radio frequency are correct. Figure 24 is an example of such a recording. These data were taken on 30 March 1971 at a 2700-km range under good ionospheric conditions. The radio frequency was 25.75 MHz, with a swept bandwidth of 200 kHz. Sixteen range lines, resolved to 750 m each (5 μ s resolution) were averaged incoherently. These data also bear a ship repeater signal. Note the clean, well resolved nature of the repeater, and the many higher-order sea-scatter components. Such results are ideal for the derivation of wind direction and speed from sea scatter, and it is hoped that more such data will be recorded in the future.

B. Wide-Area Mapping of the Ocean Surface

The second type of sea backscatter data recorded during and after the POLE experiment provided maps of the ocean surface over areas from 1,800,000 to more than 2,700,000 km². The main objective of the effort was to determine the accuracy with which surface-wind conditions over very large areas can be inferred from measurements on energy backscattered from



3071-1-694

FIGURE 24 OFF-LINE SEA-CLUTTER SPECTRUM UNDER GOOD IONOSPHERIC CONDITIONS. Wind speed is found using second-order sea scatter, with high resolution processing in space and time. Wind direction is found using ratio of first-order Bragg peaks and an estimate of wind speed from second-order scatter.

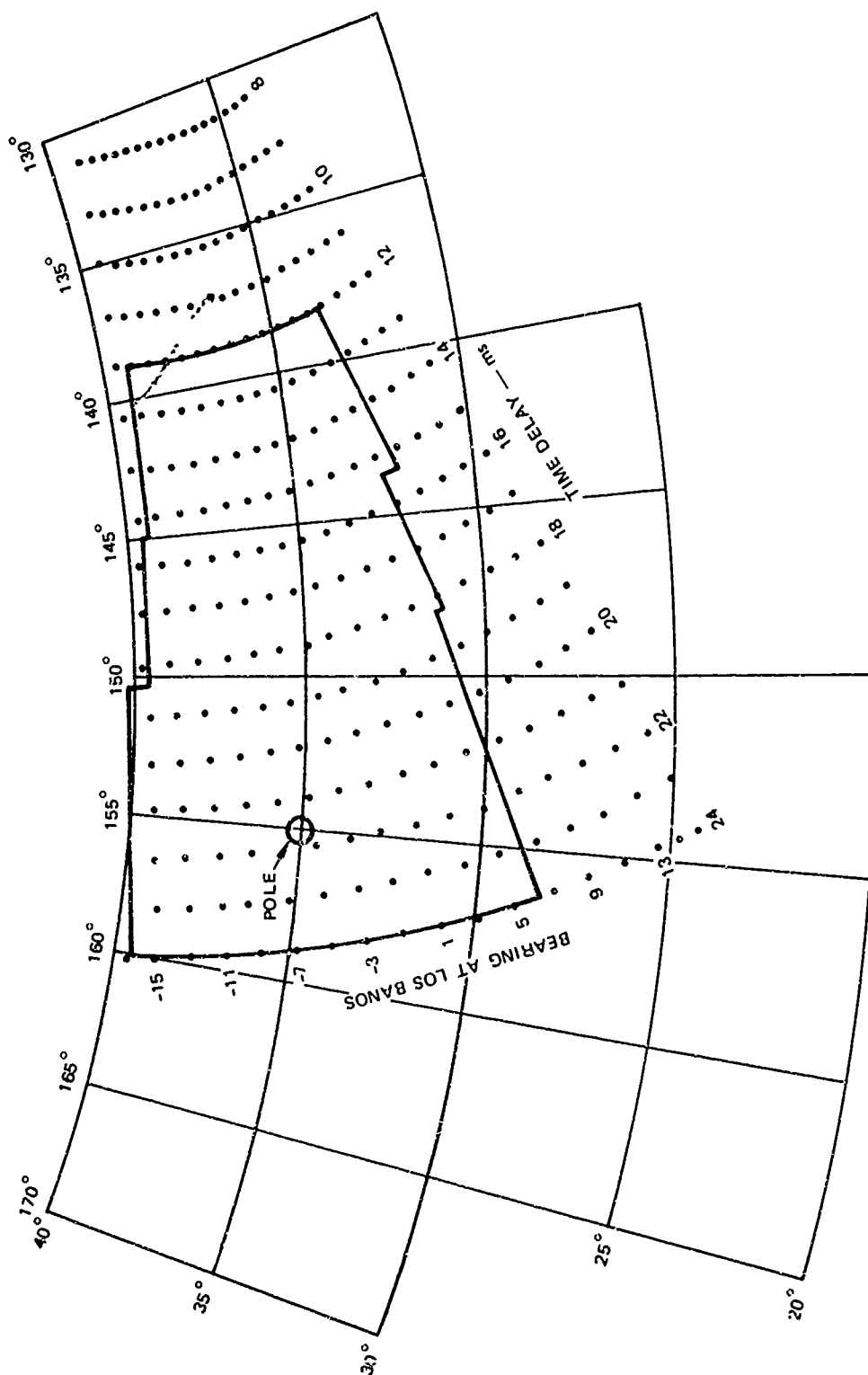
the ocean surface. A preliminary test of this data application was illustrated by Ahearn et al.⁵ The wind fields observed by the WARF radar were to be compared with weather data measured in-situ and perhaps with maps prepared from satellite data and weather stations. Another objective of the program was to study Doppler shifts observed on the same scattering cell for several different days and to determine if ionospheric Doppler shifts would average out leaving only the Doppler due to ocean currents.

The data were recorded using five antenna beams spaced at $1/4^\circ$ increments and a range window of 60 km. The azimuthal width of the area being mapped at any one time ranged from approximately 45 km to 90 km as a function of the distance from the radar to the target area. The data rate used was one sample per minute, using a double incoherent average, with about 250 maps per day.

1. POLE Experiment

During the POLE experiment, maps were recorded on four days-- 31 January, and 3, 11, and 13 February--with primary emphasis during the remainder of this period being given to tracking HF repeaters in buoys. The scanning pattern was chosen to cover an area centered roughly in azimuth on the POLE area near 35° N, 155° W. Mapping extended from the northern limit of the WARF antenna coverage at about 40° N over a total azimuthal scan at the radar of 22° . The maximum range was chosen as 24 ms or about 3600 km since one-hop propagation normally fails beyond that range. The minimum range of 12 ms or about 1800 km was set by the number of samples that could be recorded in about six hours of operation.

A total of 21 range cells were mapped, each 400 μ s, or 60 km in range. The cells were spaced at 600- μ s or 90-km intervals. The azimuthal coverage was divided into 12 cells at 2° intervals. The azimuthal coverage for each data sample was nominally 1.5° using five antenna beams. The azimuthal width of each sample varied with the distance to the area being mapped from about 45 km at an 1800 km range to 90 km at 3600 km range. A total of 252 samples were recorded over the area shown in Figure 25. The geographic coordinates at the corners of this map are given in Table 7. The total area mapped covered approximately 1,800,000 km^2 . At each time-delay increment the WARF array at the Los Banos receiving site was stepped by the computer processor by 2° each minute at the end of each sample. The transmitter array at Lost Hills, with a broader beam, was stepped every two minutes by a programmer synchronized with the receiving-site clock, thus ensuring that the area being mapped was illuminated by the transmitter. At the end of each azimuthal scan, the radar range gate was advanced by 600 μ s and successive scans normally continued without any loss of time. Periodically, as range increased, it was necessary to change the operating frequency to provide optimum propagation to the area being mapped. Also it was found that propagation at times was good at the northern end of the



3071-1-695

FIGURE 25 MAP COVERAGE AREA, NORPAX-POLE EXPERIMENT, 30 JANUARY TO 13 FEBRUARY 1974

Table 7

COORDINATES OF MAP CORNERS FOR WIDE-AREA MAPPING
OF THE PACIFIC OCEAN

	POLE Experiment 30 January to 13 February 1974		Expanded Coverage 4 March to 30 April 1974	
	Latitude (° N)	Longitude (° W)	Latitude (° N)	Longitude (° W)
NE	39.41	139.18	39.49	139.00
NW	39.06	160.07	38.54	160.10
SE	33.72	138.54	31.81	137.60
SW	28.29	156.34	24.26	154.11

scan but that it failed at the southern end. In such cases a new frequency was selected and the scan was repeated. At other times propagation was not adequate at certain ranges but was satisfactory at other ranges. Data were therefore recorded where good propagation was possible, and the remaining areas were covered as conditions improved. Thus the data were not necessarily in consecutive order by range cells.

The data were Fourier-analyzed and displayed on a computer terminal in the 5-azimuth format similar to that used in the ship repeater tracking except that no detections were made. Typical records are shown in Figures 26 through 28. Details of the data processing and display are given in Appendix C.

Each of the sea-scatter spectra typically shows two sharply defined clutter peaks. The relative amplitude of the two peaks is a function of wind direction on the area being sampled, and a series of such samples covering a wide area can provide a map of weather conditions. The processor

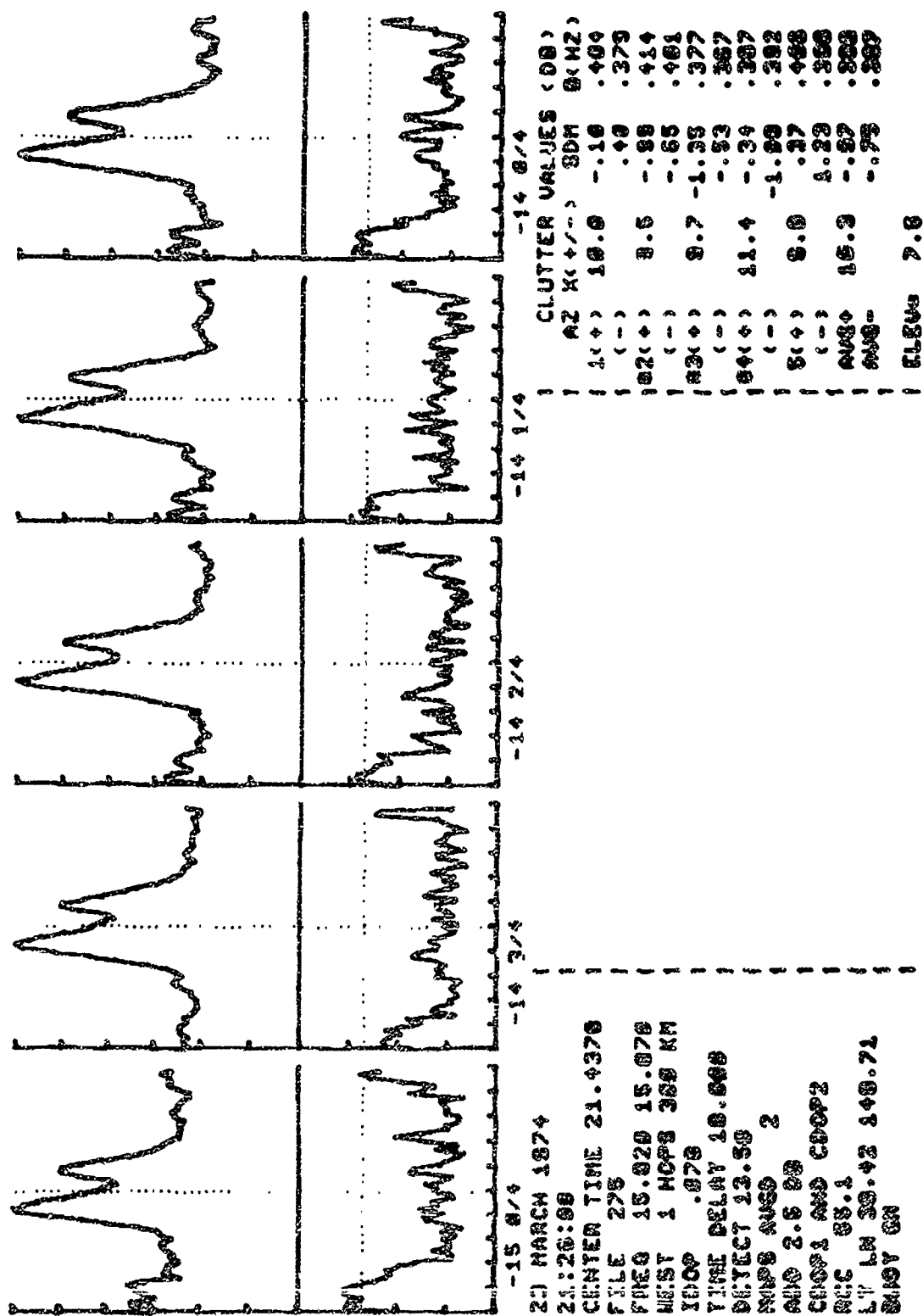


FIGURE 28 SEA BACKSCATTER DATA FOR WINDS BLOWING TOWARD THE RADAR

computes the ratio of the two peaks for each plot and lists it for each of the five azimuths under X(+/-) in the CLUTTER VALUES (dB) table. This is the ratio of the peak positive-Doppler sea-clutter component to the peak negative-Doppler component in any of the 21 range cells. A positive ratio indicates a wind direction toward the radar. Since the rms plots at the top of the record omit the three largest cells, the clutter values shown in the table may not agree exactly with a ratio scaled from the plots. Agreement should be close, but the tabulated values are most accurate.

Also shown under CLUTTER VALUES is the standard deviation from the mean (SDM) for the sea-clutter amplitudes in all 21 range cells, for the Doppler cells of the positive and negative clutter peaks. The 10-dB bandwidth, B(Hz), is also shown for each clutter peak, the value being calculated from the rms value of all 21 range lines in each Doppler cell. In the event that no 10-dB point exists, a series of symbols (\$\$\$\$\$) or digits (66667) is listed.

An average (AVG) of the values for the center three azimuths (with *) is computed and listed as shown.

2. Expanded Mapping Effort

Following the conclusion of the POLE experiment, operation of the WARF system under NORPAX was reduced to two or three days per week, with exclusive effort being devoted to buoy tracking until 4 March. After that date, wide-area mapping resumed on an expanded scale. The azimuthal scan was increased to 30° and the total area mapped to approximately 2,700,000 km². The total number of maps per day was reduced to 208, each consisting of 13 range cells at 1-ms or 150-km intervals and 16 azimuth cells at 2° increments. The reduced number of maps resulted from the allotment of a short period each day for continued tracking of buoys. At times only three antenna beams were used for mapping, with two beams

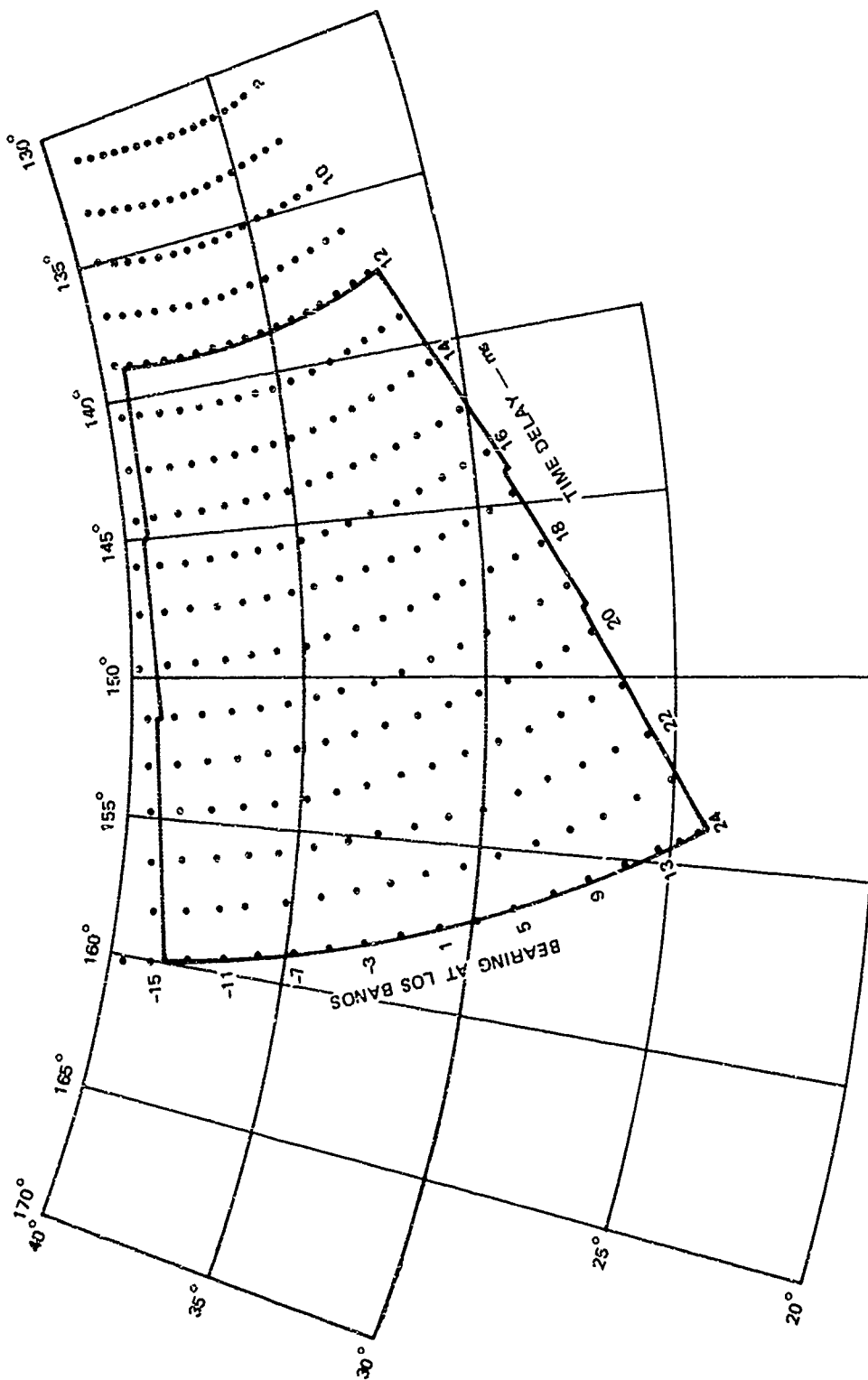
connected to buoy receivers to provide additional detection opportunities (as described in Appendix C). The area covered by the scans from 4 March is shown in Figure 29. The geographic coordinates of the corners of this map were given in Table 7.

On 23 March, a major storm was forecast for the area west of 150° W. Data were recorded on this date over an area between 18 and 24 ms time delay and azimuths from -15.75° to $+6.25^{\circ}$. The primary purpose was to provide sea backscatter records under stormy conditions for comparison with wind and sea-state conditions reported by ships in the storm area. Approximately 190 samples taken during this period were shared with Stanford and Scripps.

In addition to maps of the area described above, other records were made with a fixed azimuth and increasing time delay between 13 and 18 ms to show changes in wind direction with a change in range. Examples of these data were shown in Figures 26 through 28. The condition where cross-winds (90° relative to the radar bearing) existed is shown in Figure 27 at a time delay of 16.25 ms.

Near the end of April, propagation conditions at the longer ranges during daylight hours had deteriorated to the point at which full coverage of the area was not possible. In addition, sea conditions had become virtually calm, so that the backscatter data was less useful in any event. The mapping effort was therefore discontinued after 30 April. Tracking of Buoy E continued through 31 May.

Maps for a total of 21 days were recorded between 28 January and 30 April, providing more than 4000 samples of a systematically recorded backscatter data in 19 volumes. The data in the form of xerox copies of the computer hard-copy printouts were delivered to the Center for Radar Astronomy at Stanford University during the course of the experiment for the purpose of cooperative analysis.



3071-1-699

FIGURE 29 MAP COVERAGE AREA, NORPAX, BEGINNING 4 MARCH 1974

Each volume contains a "clutter" log generated from data stored in the disc memory for each day's operation. A sample of a portion of such a log is shown in Figure 30. It lists important parameters for each file. The ratio of the sea-clutter peaks, $X(+/-)$, shown is an average of the center three azimuths only. These are marked with asterisks, as shown in Figures 26 through 28, for example. The clutter ratio is used to calculate a wind angle shown in the log. This angle is relative to the radar bearing. Although the clutter log lists all data obtained on a given date, not all files were useful because of propagation conditions; only the records furnished with the log were considered valid.

A large quantity of the data taken during the March storm was used to predict ocean wind speed and should be published soon.⁹

C. Isolated Recordings Near R.V. Flip and R.V. Washington

Data on sea backscatter were acquired during the POLE experiment during the periods when the repeaters on the Flip and the Washington were monitored during buoy tracking. The records for these periods, similar to the examples in Figures 13 and 14, contained five receiver channels monitoring sea clutter as well as recording detections of repeaters aboard the ships. The records covered the same dates shown in Table 6 and include approximately 450 samples. These data have been fully analyzed, and the results are to be published (Ref. 9).

LOWER FILE 42
 UPPER FILE 310
 DO YOU WANT CLUTTER DATA? (Y OR N) Y
 RADIAL WIND: MAXIMUM X(+/-) 000 10.00
 FORMULA 1-2.3-OR 4? 1
 20 MAR 74

FILE	TIME	42	TD	LAY	LOM	ANG	X(+/-)	SDM(+)	SDM(-)	0(+)	0(-)
42	18:15:00	-15.75	22.000	39.44	156.56	34	15.33	-0.51	-0.94	000000	000000
43	18:16:00	-13.75	22.000	30.51	156.52	50	11.68	-1.02	-1.60	000000	000000
44	18:17:00	-15.75	22.000	39.44	156.55	20	16.14	.13	-1.20	000000	000000
45	18:18:00	-13.75	22.000	36.51	156.52	32	10.56	-0.52	-1.09	000000	000000
46	18:19:00	-11.75	22.000	37.57	156.36	31	15.77	-0.80	-0.97	000000	000000
47	18:20:00	-9.75	22.000	36.56	156.16	40	14.10	-1.54	-1.85	000000	000000
48	18:21:00	-15.75	22.000	39.44	156.66	9	17.00	-1.24	-1.14	000000	000000
49	18:22:00	-13.75	22.000	30.51	156.52	20	14.99	-1.42	-1.75	000000	000000
50	18:23:00	-11.75	22.000	37.57	156.36	41	14.06	-2.73	-1.56	000000	000000
51	18:24:00	-9.75	22.000	36.56	156.16	46	12.08	-1.80	-0.46	000000	000000
52	18:25:00	-7.75	22.000	35.72	155.93	126	-10.33	-1.82	-0.62	000000	000000
53	18:26:00	-5.75	22.000	34.00	155.67	34	16.20	.17	-0.07	000000	000000
54	18:27:00	-3.75	22.000	33.09	155.30	42	13.72	-2.19	-0.94	000000	000000
55	18:28:00	-1.75	22.000	32.00	155.00	117	-7.66	-1.11	-1.30	000000	000000
56	18:29:00	.25	22.000	32.00	154.74	120	-12.30	-1.36	-1.70	000000	000000
57	18:30:00	2.25	22.000	31.18	154.30	22	16.08	-1.99	-1.44	000000	000000
58	18:31:00	4.25	22.000	30.31	153.80	30	15.90	-2.09	-1.00	000000	000000
59	18:32:00	6.25	22.000	29.43	153.50	34	15.26	-0.50	-0.09	000000	000000
60	18:33:00	-15.75	23.000	30.26	150.37	33	15.51	-0.69	-1.01	000000	000000
61	18:34:00	-13.75	23.000	30.20	150.21	43	13.62	-0.26	-1.42	000000	000000
62	18:35:00	-11.75	23.000	37.32	150.01	40	14.10	-2.99	-2.23	000000	000000
63	18:36:00	-9.75	23.000	36.30	157.70	35	15.03	.10	-1.10	000000	000000
64	18:37:00	-7.75	23.000	35.46	157.52	40	12.33	-0.41	.65	000000	000000
65	18:38:00	-5.75	23.000	34.46	157.24	40	11.92	.20	-1.01	000000	000000
66	18:39:00	-3.75	23.000	33.50	156.80	43	13.63	-1.71	-1.60	000000	000000
67	18:40:00	-1.75	23.000	32.50	156.50	37	14.72	-1.16	-0.23	000000	000000
68	18:41:00	.25	23.000	31.52	156.22	30	16.03	-0.93	-1.07	000000	000000
69	18:42:00	2.25	23.000	30.79	155.80	27	10.20	-2.10	-0.24	000000	000000
70	18:43:00	4.25	23.000	29.70	155.41	20	10.47	-0.05	-1.00	000000	000000

3071 : 700

FIGURE 30 LOG OF SEA CLUTTER PARAMETERS AS RECORDED BY THE WARF RADAR

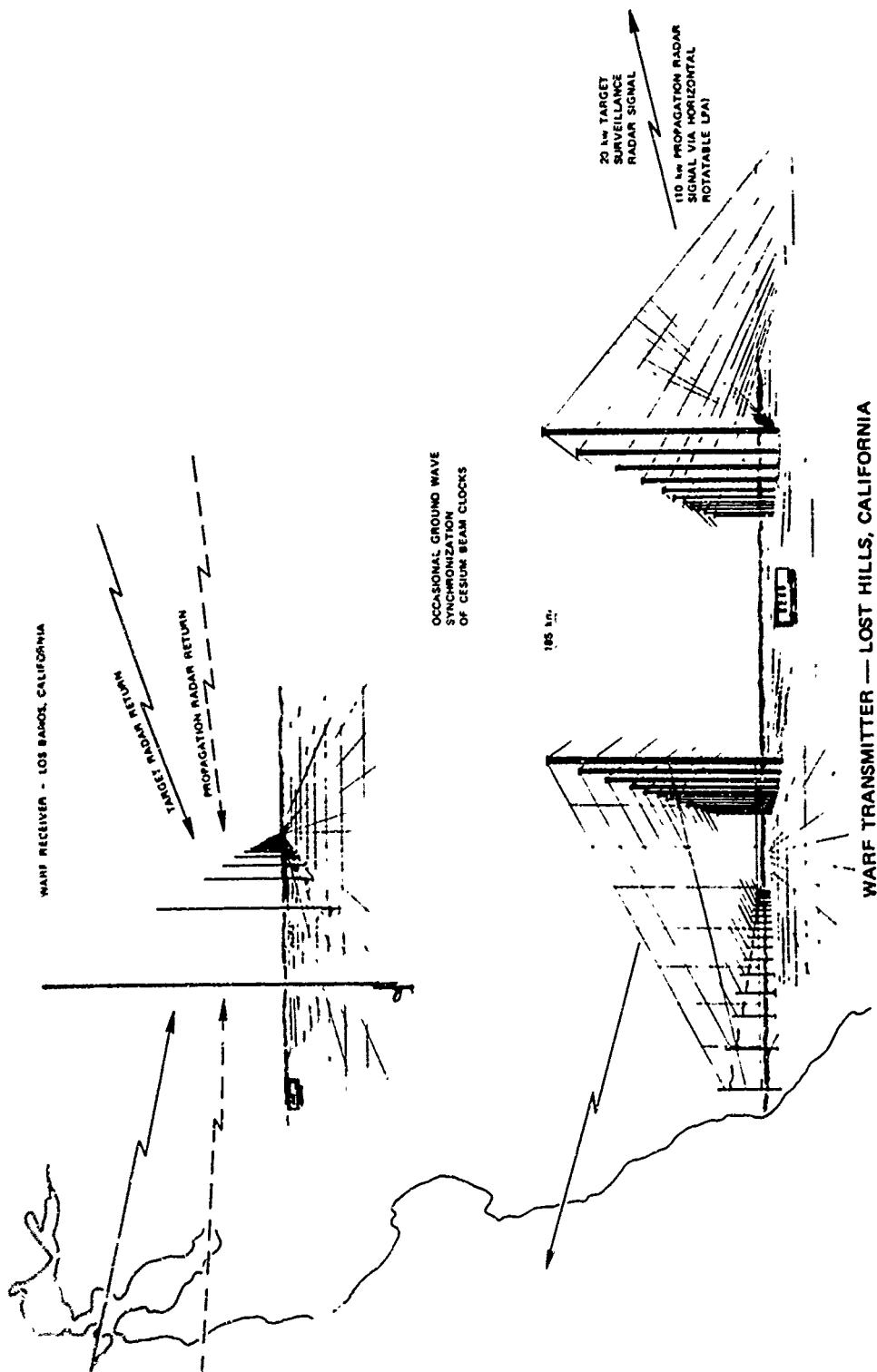
Appendix A

WARF OVERVIEW

WARF has the capability of collecting, analyzing, and displaying HF radio signals backscattered from over-the-horizon ranges to more than 3600 km. The receiving and data-processing site is located near Los Banos, California. The principal feature of the receiving system is an antenna array 2.55 km in length providing an azimuthal beamwidth of $1/2^\circ$ at 15 MHz steerable over $\pm 16^\circ$ from an east or west boresight. The array consists of 256 vertical monopoles whose outputs are combined and time-delay-steered to provide narrowbeam outputs at the main data-processing van. The array has a nominal gain of 27 dBi.

The transmitting facility is located near Lost Hills, California, 185 km SE of the receiving site. It has two 18-element vertically polarized antenna arrays, one directed on a 90° boresight and one on 270° . Either antenna may be steered $\pm 30^\circ$ about its boresight, providing target illumination with a beamwidth of approximately 6° at 15 MHz. Two linear amplifiers provide up to 20 kW CW power to either array. Operation with the west array covers 6 to 30 MHz and with the east array, 9 to 26 MHz. The arrays have a nominal gain of 20 dBi at 15 MHz. In addition, a rotatable horizontally polarized log-periodic antenna and a 10-kW amplifier are available for backscatter soundings over a wide frequency range for propagation evaluation and frequency management. Figure A-1 is a drawing of the basic bistatic radar system. Photographs of the three antenna arrays are shown in Figures A-2, A-3, and A-4. The coverage provided by these antennas is shown in Figure A-5.

*Pages 73 and 74
are blank*



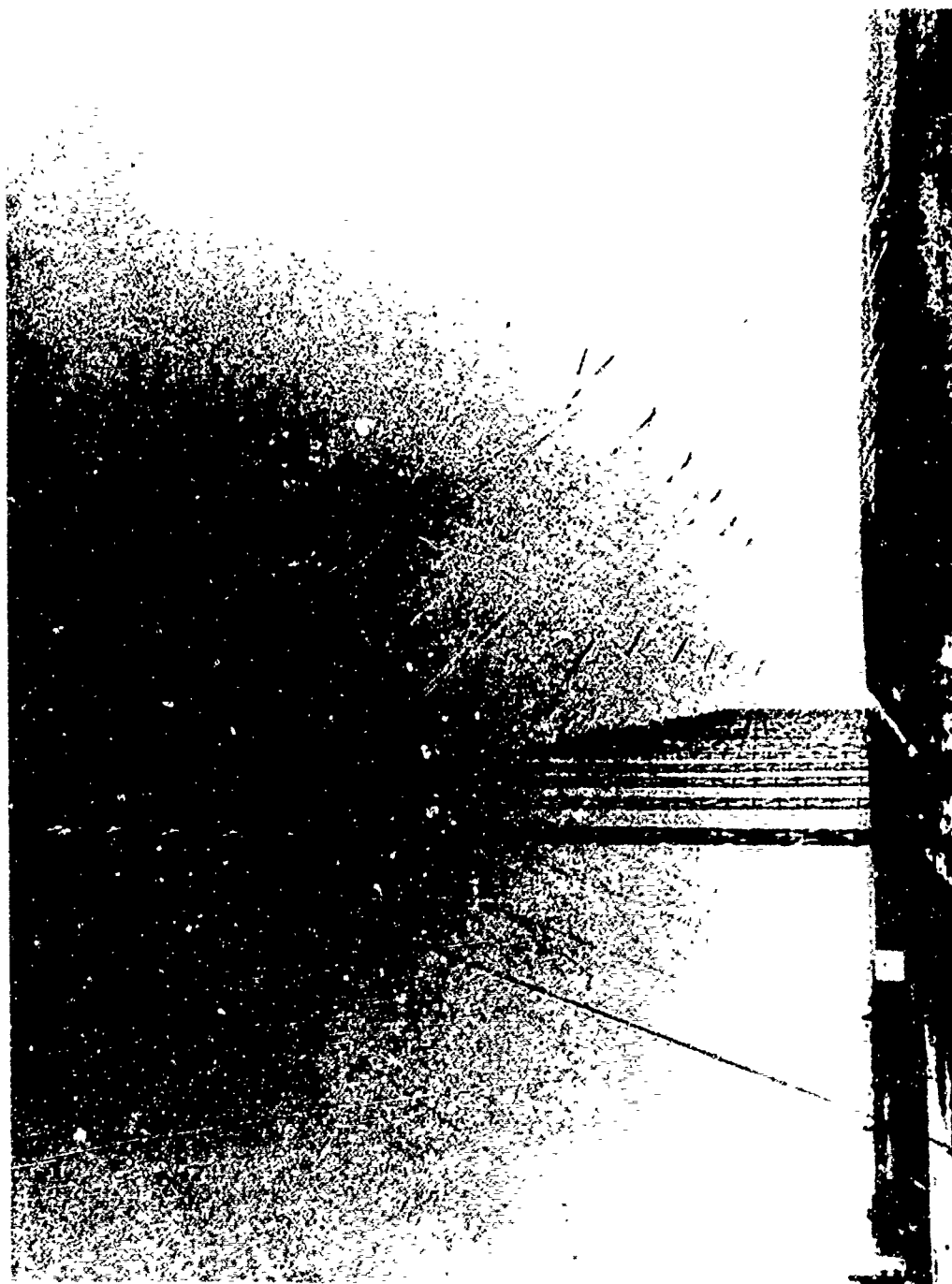
3071-1-701

FIGURE A-1 THE WARF RADAR SYSTEM



3071-1-702

FIGURE A-2 RECEIVING ARRAY AT LOS BANOS WARF SITE



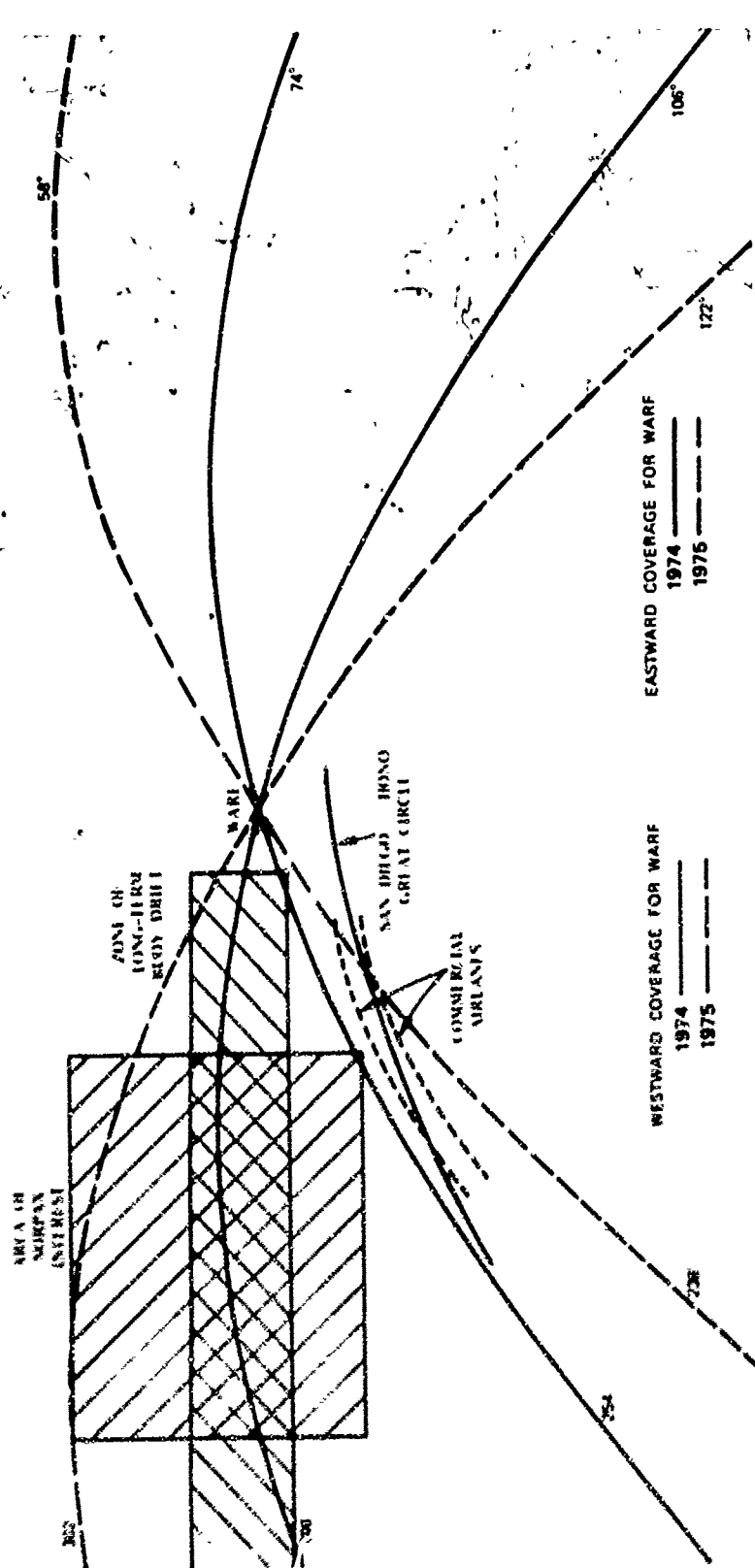
3071-1-703

FIGURE A-3 THE WARF 18-ELEMENT EASTWARD-LOOKING TRANSMITTING ARRAY LOCATED NEAR LOST HILLS, CALIFORNIA



3071 1 704

FIGURE A-4 THE 18-ELEMENT WESTWARD-LOOKING TRANSMITTING ARRAY
LOCATED NEAR LOST HILLS, CALIFORNIA



3071-1-706

FIGURE A-5 PRESENT AND PROPOSED COVERAGE OF WARE

The receiving system provides a total of seven steered antenna beams directed to 0° , $\pm 1/4^\circ$, $\pm 1/2^\circ$, and $\pm 1^\circ$ with respect to the selected steer position. These multiple beams provide broad azimuthal coverage for search and track operations and permit more accurate determination of target and sea-scatter variations with azimuth by comparison of the outputs of adjacent beams.

The waveform used by the radar is swept-frequency CW (SFCW). The transmitted frequency is linearly varied over a typical bandwidth of 50 kHz at a rate of 250 kHz/s. The waveform is thus repetitive at a 5-Hz rate. The receiver is also swept in the same manner, with both waveforms being synchronized to within 10 μ s by means of cesium clock standards.

Such a waveform is particularly useful in the HF spectrum where wide bandwidths normally associated with high range resolution (>1 MHz) are not available. The use of a sweeping frequency and a narrowband receiver also minimizes interference from other transmissions. The signal back-scattered from the target area is delayed by the round-trip propagation time, and when it is mixed with a comparably delayed SFCW signal at the receiver an audio tone results that is proportional to target (or target area) range. The receiver output is computer-processed using the fast Fourier transform (FFT) to obtain three-dimensional storage of the back-scatter amplitude versus range and Doppler shift. The spectral results are then displayed on a computer terminal with a storage CRT. The display may be hard-copied to provide a permanent record of each data sample.

The processor measures the sea-clutter-spectrum parameters and the range to each discrete target whose SNR exceeds a preselected threshold level, and lists all such targets with their SNR, azimuth, range, Doppler, radial velocity, and radar cross section. From the relative SNR values versus azimuth the operator may steer the antenna to center the beam on the strongest target. He may also move the range interval being displayed

to place the target near the center of the area under surveillance. This area was typically 60 km in range and 50 km in azimuth for buoy tracking.

In order to select an operating frequency that will provide illumination of the selected target area, it is necessary to provide backscatter ionograms over a wide frequency range at the target ranges of interest. Such a backscatter sounder was operated typically over a frequency range of 6 to 30 MHz and over a time delay range of 0 to 20 ms or 10 to 30 ms, corresponding to target ranges of 0 to 3000 km and 1500 to 4500 km. Facsimile records of the backscattered signal permitted the selection of an optimum frequency for the target area. In order to minimize multimode effects and hence multiple target and sea-clutter returns, the operating frequency was chosen to be 2 to 4 MHz below the MUF for the target range. Typical ionograms obtained during the experiments are shown in Section II-D-1. The frequency selected also should be relatively free of interference from other radio transmissions to avoid spurious detections or suppression of a weak target signal. A swept surveillance receiver was used with the backscatter soundings to locate a 50-kHz band with the least interference. Any 100-kHz portion of the HF spectrum could be displayed on a storage CRT and the operating band chosen. In some cases where no 50-kHz band was available, operation with a 20-kHz BW was used for buoy tracking. Since the swept BW also determines the length of the range gate, the narrow BW was also occasionally used in order to provide a wider range gate and reduce the search time for a target.

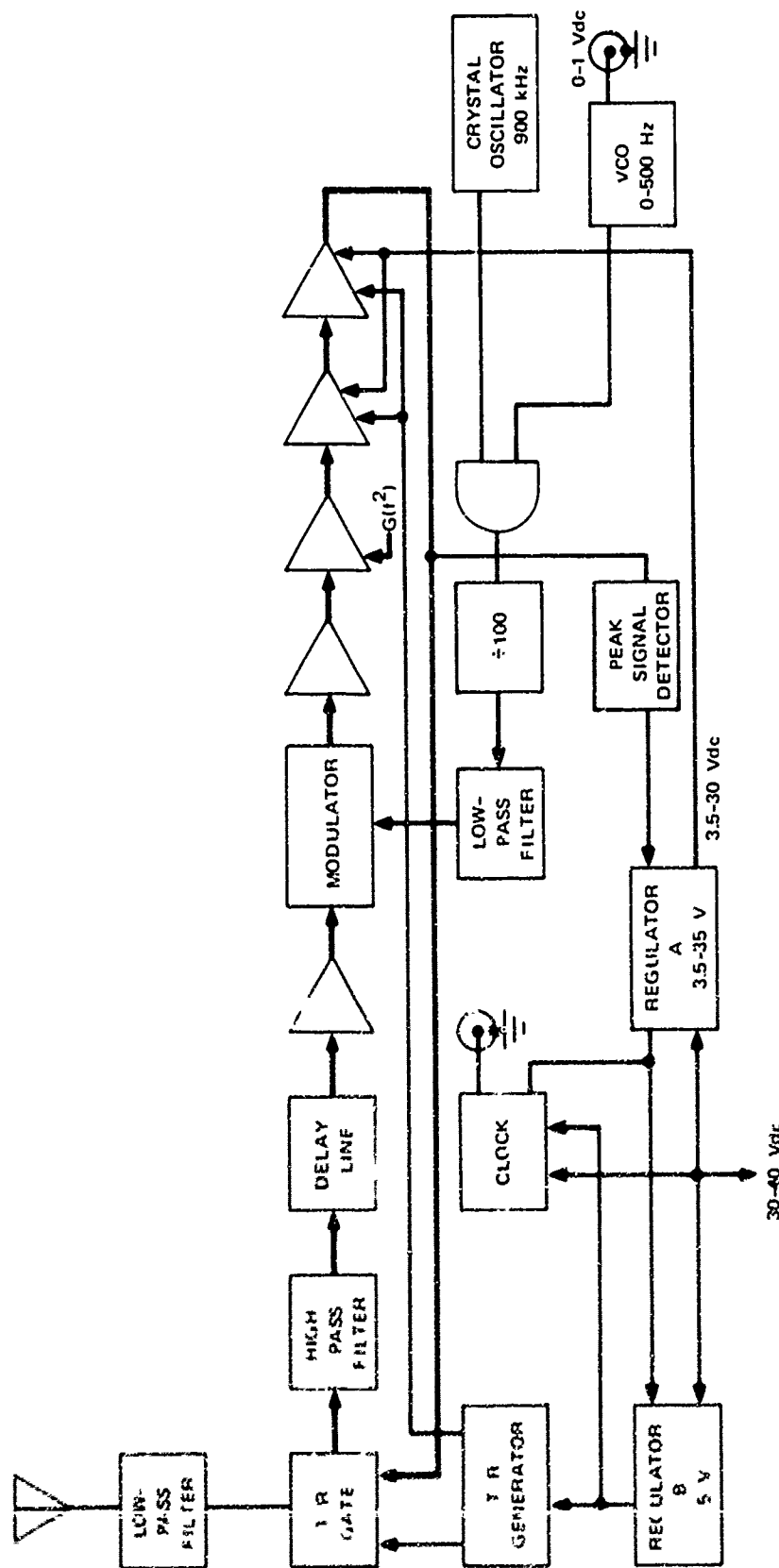
To provide still greater coverage when searching for a target, an independent receiving system was often employed using a single receiver with a wide bandwidth, a real-time digital spectrum analyzer, and a facsimile display. Such a system typically displayed 480 km of range and 4° or 200 km in azimuth. Although only rough range and azimuth information could be measured from the display, it provided a rapid and fairly sensitive means of detecting a target and obtaining approximate coordinates.

Appendix B

REPEATER ELECTRONICS

1. Buoy Repeaters

A simplified block diagram of the buoy-repeater electronic package equipment is shown in Figure B-1. The incoming signal is connected to a TR switch through a low-pass filter with a cutoff of about 25 MHz. In the receive mode a high-pass filter at 12 MHz minimizes interference from much of the HF broadcast band. The signal is then stored in a glass delay line for 25 μ s, and is then amplified and fed to a balanced modulator. Modulation at frequencies shown in Table 1 derived from a quartz oscillator provides a double-sideband suppressed-carrier signal to a power amplifier. The TR switch then connects the antenna to the transmitter output and the delayed, modulated signal is radiated for about 20 μ s. A period of about 5 μ s is provided between the transmit and receive cycles to allow transients to decay and avoid oscillation. The TR switching thus occurs at a rate of about 20 kHz, and additional sidebands are generated at that frequency. However, they are well removed from the desired sidebands (near 9 kHz) and are outside the passband of the first IF amplifier in the WARF receivers. The maximum power output is about 1 watt. The gain of the repeater is set at about 40 dB with a $1/f^2$ roll-off to maintain approximately constant cross section. The effective radar cross section is approximately 50 dBsm, which is comparable to the average radar cross section of the ocean surface within the range/azimuth window of the WARF system. Repeater echoes should then have SNRs comparable to the sub-clutter visibility (i.e., typically 20 to 70 dB, depending on range, between 800 and 4500 km) as observed on a receiver channel monitoring sea clutter.



3071 .1 706

FIGURE B-1 BLOCK DIAGRAM OF NORPAX BUOY REPEATER

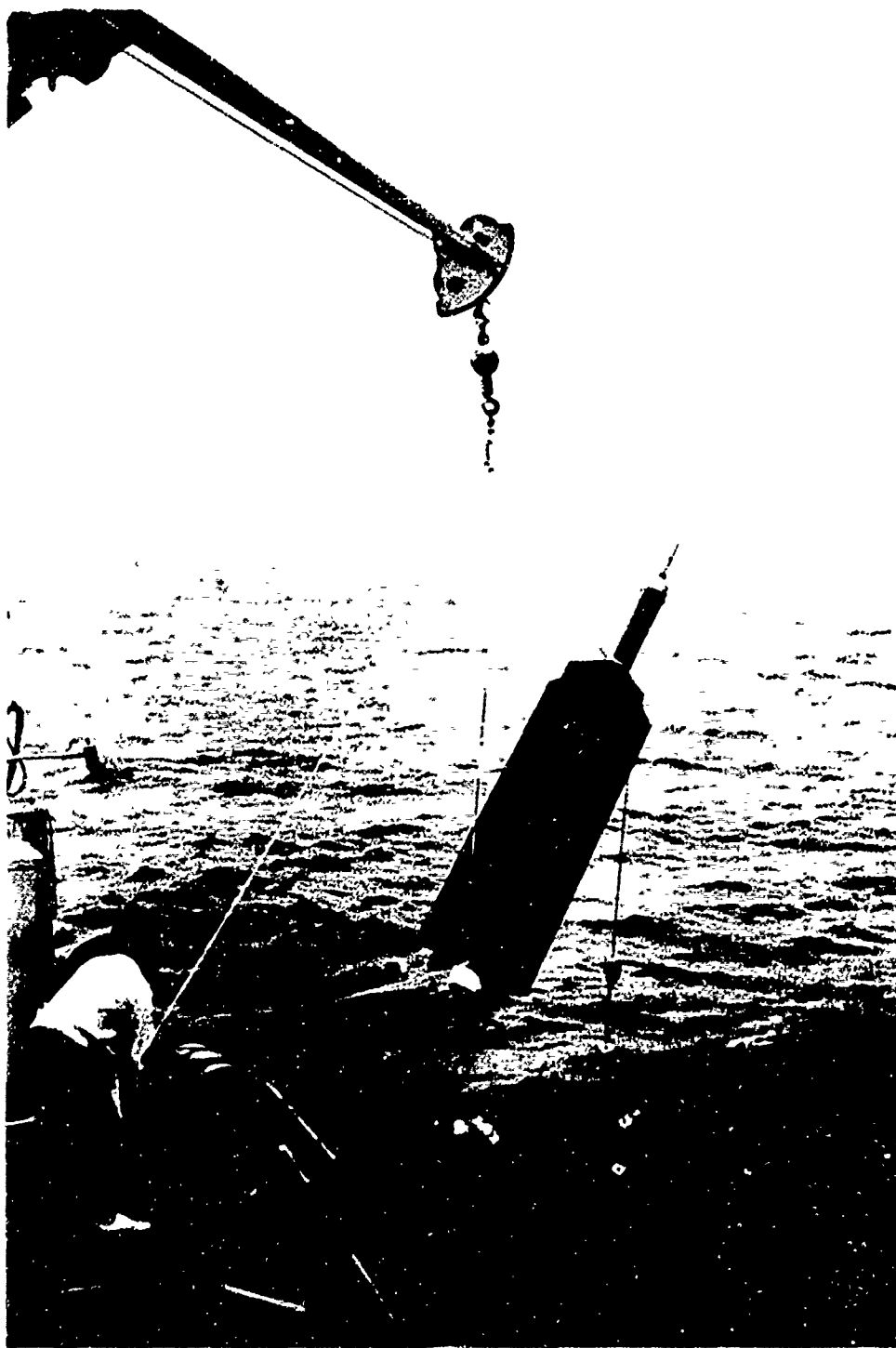
The amplifier has a unique power supply whose output voltage is continuously adjusted to prevent clipping on the peak signal. When low-level signals are present, the voltage is correspondingly low and unnecessary battery drain is avoided.

The operating period of the buoys was controlled by a fail-safe precision clock. The start of the period was established when the equipment was energized at 1700Z prior to launch. If the clock oscillator failed or if for any reason the clock switch failed to operate during any 24-hour period, an override system would have turned the repeater on continuously.

The repeaters were designed and built by the Barry Research Corporation. The electronics package was housed in a tube 44 inches in length by 1-1/2 inches in diameter. The Scripps Institution of Oceanography provided the buoys, antennas, and battery supplies and installed the repeaters in the buoys. The buoy repeaters used a single fiberglass-encased antenna 15 ft in length that was designed to operate at a lower-frequency limit of 15 MHz. A photograph of one such buoy is shown in Figure B-2.

2. Ship Repeaters

Two research vessels, the R.V. Washington and R.V. Flip, conducted tests during the POLE experiment. HF repeaters installed on these ships were designed and built by SRI and have been used in numerous experiments where a fixed target was required as a radar reference.¹⁰ A delay line of 53 μ s was used and the switching rate was near 9 kHz. These repeaters were operated with low-frequency modulation, 43 Hz on the R.V. Washington and 23 Hz on the R.V. Flip. They were manually operated for very limited periods of time during tests coordinated by HF radio communication, usually after buoy tracking was completed. These repeaters had a maximum gain in excess of 90 dB and power output of 10 watts. They could thus be a serious source of interference to tests being run in the POLE area. However, it was particularly important to obtain position data on the Flip using OTH



3071-1-707

FIGURE B-2 PHOTOGRAPH OF A NORPAX BUOY BEING LAUNCHED
FROM THE R.V. WASHINGTON

sensors in order to compare it with position data obtained by satellite navigation and thereby evaluate the accuracy of the WARF system. Tests with the Flip were typically conducted for one hour or less per day.

Appendix C

RECEIVING AND DATA-PROCESSING SYSTEMS

1. Buoy-Tracking Receivers

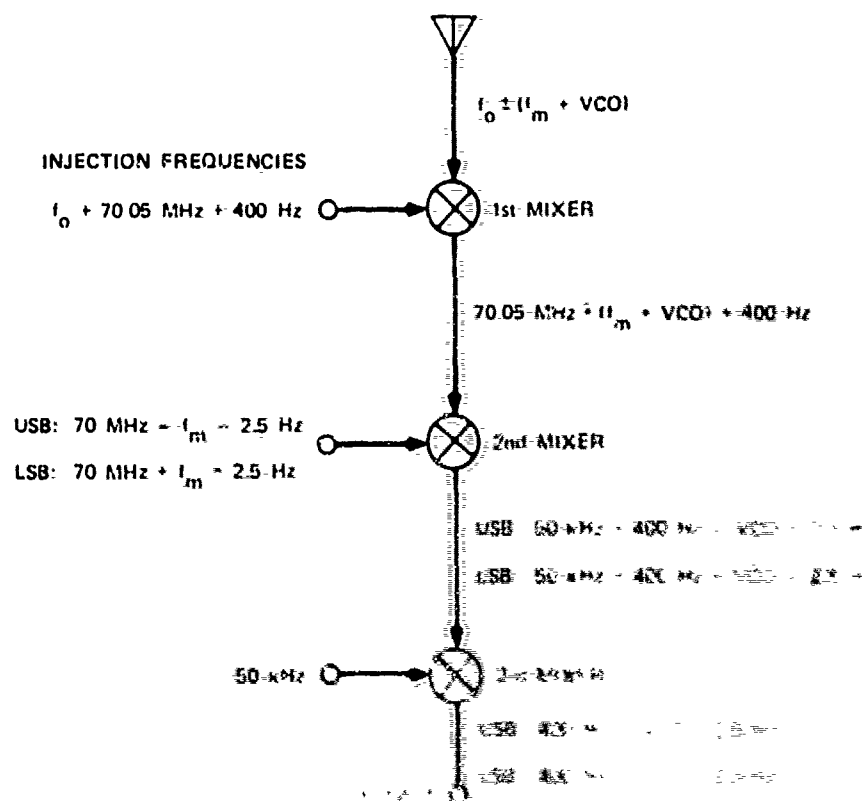
The HF receivers used for these tests were the same that are employed in all WARF applications. They are fully synthesized, with all frequencies being derived from a cesium-beam frequency standard. The output is a coherent audio tone, typically at 400 ± 50 Hz. The SFCW input to the receiver is offset by $+20.05$ Mz + 400 Hz from the transmitted signal and is up-converted in two stages to minimize image frequencies. The first IF amplifier passes both the upper and lower sidebands of the buoy signal. The second-mixer input is derived from an operator-selected signal near 35 MHz that determines the buoy and the particular sideband to be monitored. The modulation frequencies for each of the buoys and the corresponding local-oscillator injection frequencies are shown in Table C-1.

Table C-1

NORPAX BUOY FREQUENCIES AND LOCAL-OSCILLATOR INJECTION FREQUENCIES

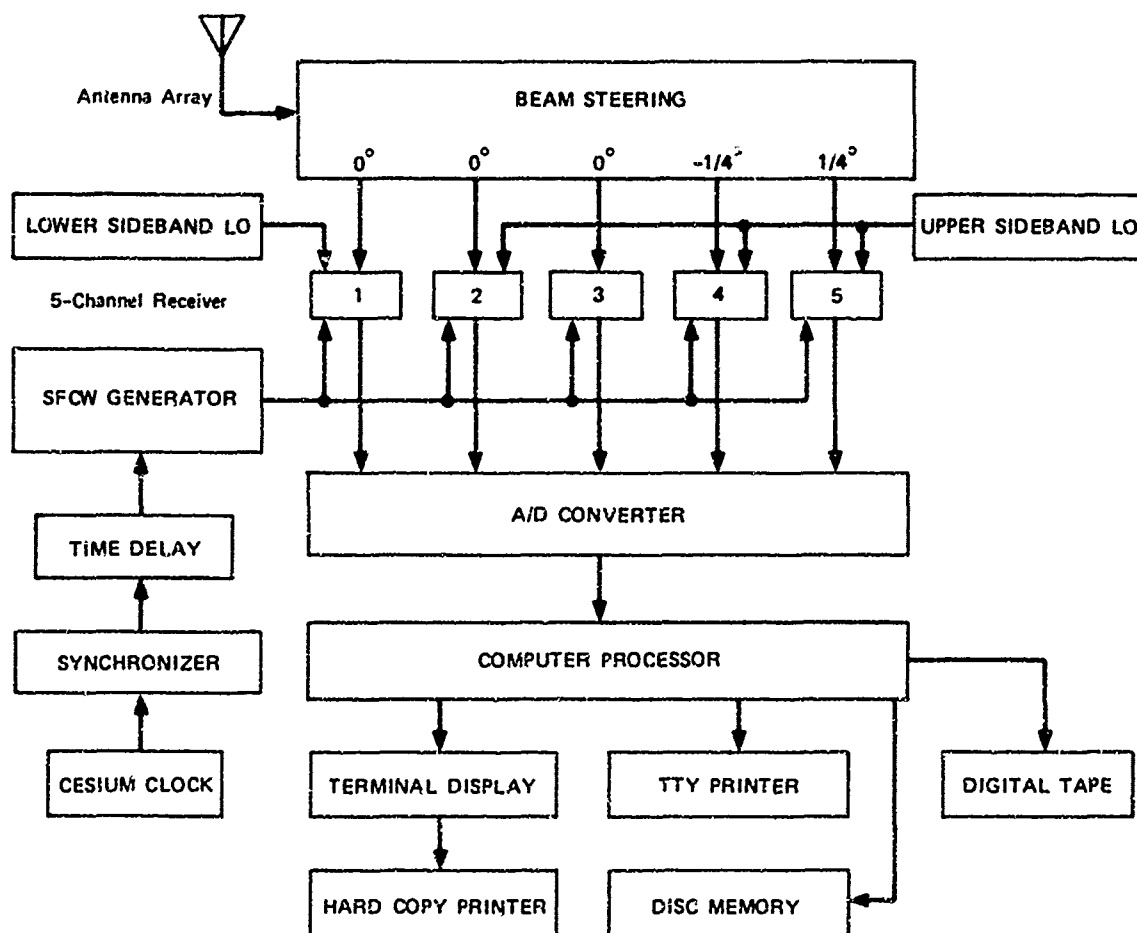
Buoy ID	Buoy Modulation Frequency (Hz)	Receiver Upper-Sideband Local Oscillator (Hz)	Receiver Lower-Sideband Local Oscillator (Hz)
A	9000.00	14,995,498.75	15,004,501.25
B	9120.50	14,995,438.50	15,004,561.50
C	9241.00	14,995,378.25	15,004,621.75
D	9361.50	14,995,318.00	15,004,681.00
E	9482.00	14,995,257.75	15,004,741.25
F	9602.50	14,995,197.50	15,004,801.50
G	9723.00	14,995,137.25	15,004,861.75
H	9843.50	14,995,077.00	15,004,921.00
I	9964.00	14,995,016.75	15,004,981.25
J	10084.50	14,994,956.50	15,005,041.50
K	10205.00	14,994,896.25	15,005,101.75
L	10325.50	14,994,836.00	15,005,161.00
M	10446.00	14,994,775.75	15,005,221.25
N	10566.50	14,994,715.50	15,005,281.50
O	10687.00	14,994,655.25	15,005,341.75
P	10807.50	14,994,595.00	15,005,401.00
Q	10928.00	14,994,534.75	15,005,461.25
R	11048.50	14,994,474.50	15,005,521.50
S	11169.00	14,994,414.25	15,005,581.75
T	11289.50	14,994,354.00	15,005,641.00
U	11410.00	14,994,293.75	15,005,701.25
V	11530.50	14,994,233.50	15,005,761.50
W	11651.00	14,994,173.25	15,005,821.75
X	11771.50	14,994,113.00	15,005,881.00
Y	11892.00	14,994,052.75	15,005,941.25
Z	12012.50	14,993,992.50	15,006,001.50

For the sea-clutter channel, the input is exactly 35 MHz. Both of these signals are doubled in the receiver to provide an input near 70 MHz to the second mixer. A third mixer translates the signal to an audio tone. A simplified frequency-conversion diagram is shown in Figure C-1.



2. Buoy Data Processing

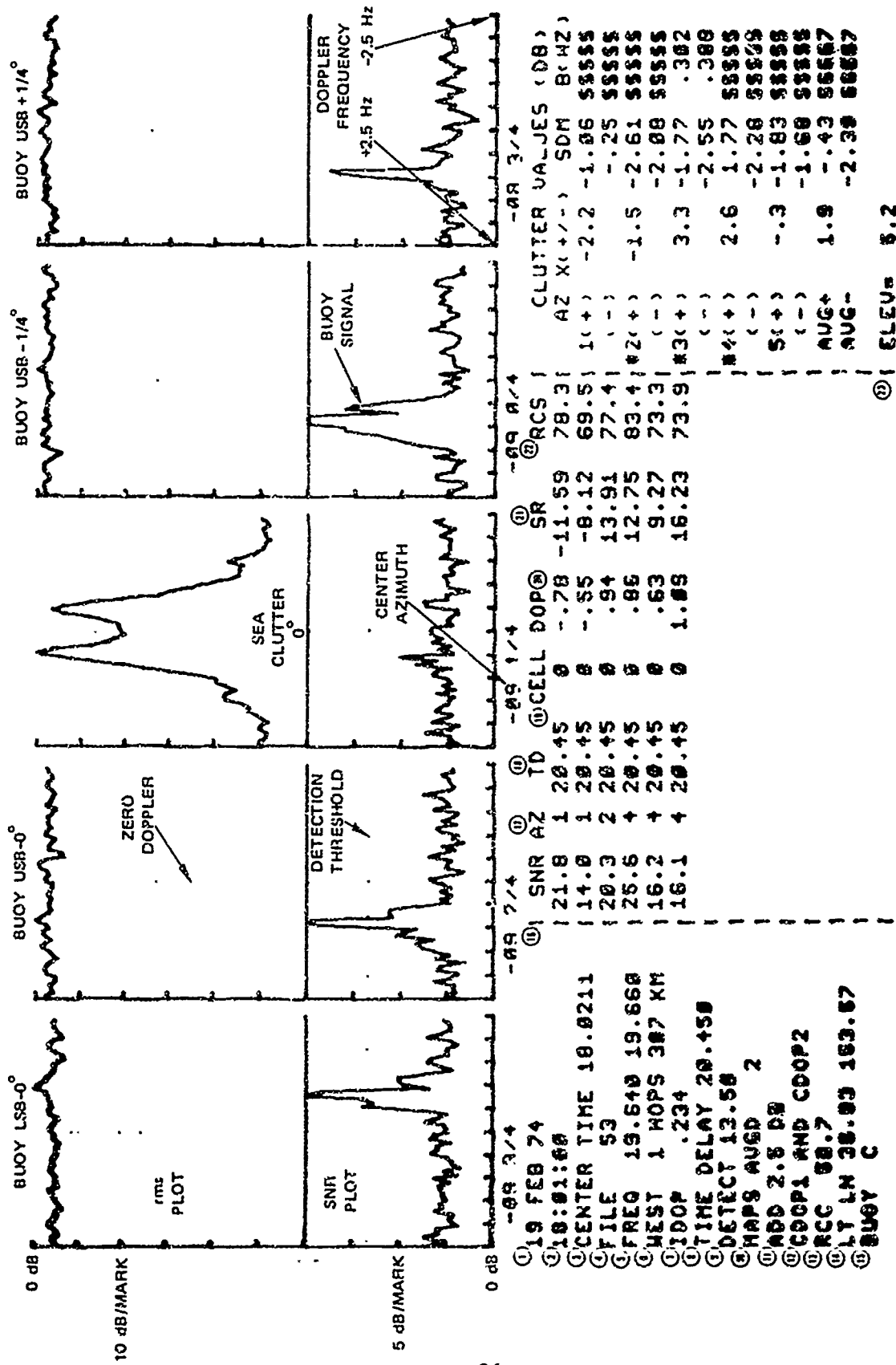
An overall block diagram of the receiving and data-processing system for buoy detection is shown in Figure C-2. Data from the five receivers are computer-processed and displayed on a CRT terminal at the operator console. This data are also recorded by a hard-copy printer as a permanent record of each data file.



3071-1-709

FIGURE C-2 NORPAX BUOY-TRACKING RECEIVING AND DATA-PROCESSING SYSTEM

An example of the processor output is shown in Figure C-3. The upper plot shows rms signal level for each of the five receiver channels versus Doppler over a 5-Hz Doppler range. The rms value in each of 64 Doppler



3071-1-710

FIGURE C-3 SAMPLE PROCESSOR RECORD SHOWING BUOY DETECTION IN RANGE CELL 0

cells is computed for 18 of the 21 range lines, after the three largest range lines are omitted. This procedure permits the calculation of a noise or clutter level in Doppler cells where discrete targets, such as a buoy, are present without having the target bias the noise floor. Where the return signal is range-spread, as with sea clutter or an interfering RF signal, the rms calculation is only slightly reduced by omitting the three largest range cells. The plot covers a 60-dB range, although the processing dynamic range exceeds this amount. It is normalized to the largest rms signal in any Doppler cell of each plot. The center plot is the sea-clutter channel and it provides a good measure of the propagation conditions. It typically shows two sharply defined sea-clutter peaks corresponding to the first-order HF Bragg-scattering reflections from sea waves traveling toward (positive Doppler) and away (negative Doppler) from the radar. Positive Dopplers appear to the left of the center line, and negative Dopplers to the right. The relative amplitude of the two peaks is a function of wind direction and is particularly significant in studies of sea backscatter for weather monitoring. Such studies were a part of the wide-area ocean mapping conducted as a part of the SRI participation in NORPAX. The shape of the sea-clutter return is also a function of propagation conditions. If more than one mode is present, more than two peaks may occur. Under these conditions target range may be ambiguous, and the radar frequency is therefore changed if possible to avoid this "multipath" ambiguity. Finally, the midpoint of the two peaks is used as a zero-Doppler reference from which other Doppler frequencies are computed. A vertical line is drawn at this point. Normally the zero-Doppler line is placed at the center of the plot and the Doppler-frequency scale is 2.5 Hz or 0.5 Hz per scale division. Ionospherically induced Doppler shifts and those caused by ocean currents are thereby subtracted out so that they do not affect the measurement of repeater Doppler frequencies. A switch option permits shifting the displays by an amount

equal to the ionospheric Doppler (IDOP). The computer still plots target Doppler with reference to the zero-Doppler line, but the display is shifted to show total Doppler (ionospheric plus target).

With buoy tracking, the rms plots for all but the center channel show no sea clutter because the receivers are offset about 9 kHz to monitor modulation sidebands. The rms plots for buoys will normally show only noise, since buoy returns are discrete in range (typically 3 range lines or less) and they would be omitted from the plot. If significant peaks occur in the rms plots of the buoy channels they are due to interfering signals or range-spread buoy returns. (If the buoy signal is exceptionally strong it will sometimes appear in the rms plot because it will cover more than 3 range lines.) These plots are therefore a further aid in determining the best operating frequency for the radar, since they reveal interference if present.

The lower plot in Figure C-3 shows the SNR for each Doppler cell and is the ratio in dB of the peak signal in any of the 21 range lines (e.g., the largest of the three lines discarded from the rms plot) to the rms value for that Doppler cell as computed for the upper plot. This plot emphasizes discrete targets (such as a buoy) and removes clutter and interfering signals (where the peak and rms signals are nearly equal). The display is clipped at 20 dB although the peak SNR and the Doppler frequency at the peak are measured and preserved in the table of detections.

Signals in the SNR plot that exceed the detection threshold level (set by the computer) and are stronger than neighboring detections at the same time delay and Doppler are listed in the table in the center of the record. All detections are stored in the computer memory and may be listed in edited format any time during operation (typically at the end of a test). The detection file is also dumped onto a digital tape for additional processing.

Beneath the SNR plots are shown the azimuth with respect to antenna boresight for each of the five receivers. The actual bearings for the NORPAX data differ from those shown in the records because the receiver configuration was modified as described earlier.

The data tabulated in the lower part of the record in Figure C-3 are explained in the following list (item numbers correspond to circled numbers in the figure):

- (1) GMT date: Changed by the operator at 0000Z.
- (2) File time: GMT time at the start of the data sample.
- (3) CENTER TIME: GMT time at the center of the total data-sampling period.
- (4) FILE: Consecutive numbering of data samples.
- (5) FREQ: Frequency in MHz for the radar SFCW limits.
- (6) WEST or EAST: Direction of transmission, followed by number of ionospheric reflections to the target area, and estimated (or programmed) virtual height in km.
- (7) IDOP: Calculated Doppler frequency due to ionospheric motion, corresponding to the midpoint between the two first-order Bragg spectral peaks. This measure also includes Doppler caused by ocean currents.
- (8) TIME DELAY: A time delay at the center of the range interval as set by the operator.
- (9) DETECT: The detection threshold in dB.
- (10) MAPS AVGD: The number of range/Doppler maps averaged. May be set to any integer.
- (11) ADD 2.5 dB or SUB 2.5 dB: An operator option to modify the detection threshold set by the computer.
- (12) CDOP1 and CDOP2: A switch option to allow detections to be listed within 1 Doppler cell of the CDOP1 and CDOP2 cells. Otherwise such detections are omitted. CDOP1 and CDOP2 are the Dopplers of the two first-order Bragg peaks in the sea clutter in the center azimuth.
- (13) RCC: The estimated radar cross section in dBsm of the ocean area within the range/azimuth window of the radar; computed assuming an average sea cross-section per unit area of 5×10^{-3} .

- (14) LT LN: The latitude and longitude of a point at the center azimuth and center time delay.
- (15) BUOY C: Buoy identification number as selected by the operator.
- (16) SNR: The signal level of a discrete signal detection.
- (17) AZ: The azimuth of a detection numbered 1 to 5, from left to right.
- (18) TD: The time delay for a detection.
- (19) CELL: The range cell of a detection, numbered between +10 and -10 from the center of the range interval or Range Cell 0.
- (20) DOP: The Doppler frequency at the peak of the signal detected, measured with respect to the zero Doppler reference line.
- (21) SR: The equivalent radial speed in knots for a target with the given Doppler.
- (22) RCS: The estimated target radar cross section.
- (23) ELEV: The calculated elevation angle at the receiver for the given virtual height, time delay, and propagation mode (1-hop or 2-hop).

The clutter values on the lower right are applicable to the sea backscatter measurements and are described in Section IV.

Each data sample requires 12.8 s of sample time plus about 2 s for processing. Averaging several such coherent samples will enhance the detection sensitivity and position accuracy but will lower the data rate. It was found that a "two-map" average was usually a suitable compromise. Total sample and process time for a two-map average, including plotting and listing all the data, requires about 51 s. It was thus convenient to take one data file per minute and allow time to change parameters between files as necessary.

In addition to the computer processor output on the terminal display already described, the data are recorded on digital tape and some of the data are printed on a TTY. The digital tape record may be reprocessed

off-line using a different detection threshold and a different assumed ionospheric propagation condition, if desired. The detection data generated are dumped on tape and they too, reprocessed. If records of single files have been lost or damaged they may be reproduced.

The TTY record is primarily a log of important operating parameters for each file. It may also be used to print out data on all detections. However, it requires additional time during real-time data processing, and during buoy tracking it was used only for a log. A sample record is shown in Figure C-4. Listed are the date, operating frequency, number of hops, boresight direction, file number, file time, detection threshold, center azimuth, center time delay, virtual height, and center latitude and longitude. Data on detections are omitted from the range cell, Doppler, and speed columns in this mode. However, a series of asterisks indicates that detections were made and stored in disc memory for subsequent listing on the display terminal. If no detections exist in a file, a series of dashes is printed. If the operator elects to list detections on the TTY, all columns show the parameters of each detection. The dB column records actual SNR, and the azimuth, time delay, and latitude/longitude are given instead of center values for each target. A sample of this type record is shown in Figure C-5.

This record classifies detections as D, E, or S types after the AZIMUTH listing. If duplicate detections (same range and Doppler) exist in two or more adjacent azimuths, the strongest of the detections is listed as D (duplicate). The detections paired with this detection carry no designation. A detection appearing in Azimuths 2, 3, or 4 and not paired with another detection is classified as S (single). A detection in Azimuths 1 or 5 not paired with another detection is classified E (edge). Only D, E, and S detections are listed on the computer display but all detections appear in the disc memory and, if desired, on the TTY record.

NEW PARAMETERS

19 FEB 74

FREQ 19.64 19.66

MOPS 1

EAST 1, WEST 0 2

FILE	TIME	DB	AZIM	T	CELL	DOP	SPEED	HT	LAT	LONG
1	17:03:52	11.0	-07 0/4	21.50	*****			310	35.54	155.04
2	17:04:47	11.0	-07 0/4	21.50	*****			310	35.54	155.04
3	17:06:00	11.0	-07 0/4	21.50	-----			310	35.54	155.04
4	17:07:00	11.0	-07 0/4	21.50	*****			310	35.54	155.04
5	17:08:00	11.0	-07 0/4	21.50	*****			310	35.54	155.04
6	17:09:00	11.0	-07 0/4	21.50	-----			310	35.54	155.04
7	17:10:00	11.0	-07 0/4	21.50	*****			310	35.54	155.04
8	17:11:00	11.0	-07 0/4	21.50	*****			310	35.54	155.04
9	17:12:00	11.0	-07 0/4	21.50	*****			310	35.54	155.04
10	17:13:00	11.0	-07 0/4	21.50	*****			310	35.54	155.04
11	17:14:00	11.0	-07 0/4	21.50	*****			310	35.54	155.04
12	17:15:00	11.0	-07 0/4	21.50	*****			310	35.54	155.04
13	17:16:00	11.0	-07 0/4	21.50	*****			310	35.54	155.04
14	17:17:00	11.0	-07 0/4	21.50	*****			310	35.54	155.04
15	17:18:00	11.0	-08 3/4	21.50	*****			310	36.33	155.24
16	17:19:00	11.0	-08 1/4	21.50	*****			310	36.10	155.19
17	17:20:00	11.0	-08 3/4	21.10	*****			309	36.44	154.59
18	17:21:00	13.5	-08 3/4	21.10	*****			309	36.44	154.59
19	17:23:00	13.5	-09 2/4	21.10	-----			309	36.78	154.66
20	17:25:00	13.5	-08 3/4	21.10	-----			309	36.44	154.59
21	17:26:00	13.5	-08 0/4	21.10	-----			309	36.11	154.51
22	17:27:00	13.5	-08 0/4	21.40	-----			310	36.02	155.00
23	17:28:00	13.5	-08 2/4	20.10	-----			306	36.60	152.93
24	17:29:00	13.5	-08 0/4	20.10	*****			306	36.39	152.89
25	17:30:00	13.5	-09 1/4	20.10	*****			306	36.92	153.00
26	17:31:00	13.5	-09 1/4	20.10	*****			306	36.92	153.00
27	17:32:00	11.0	-09 3/4	20.40	*****			307	37.06	153.54
28	17:33:00	11.0	-09 3/4	20.40	-----			307	37.06	153.54
29	17:34:00	11.0	-09 1/4	20.40	-----			307	36.85	153.49
30	17:35:00	11.0	-09 1/4	20.40	*****			307	36.85	153.49
31	17:36:00	11.0	-09 1/4	20.40	*****			307	36.85	153.49
32	17:37:00	11.0	-09 1/4	20.40	*****			307	36.85	153.49
33	17:38:00	11.0	-09 1/4	20.40	*****			307	36.85	153.49
34	17:39:00	11.0	-09 2/4	20.45	*****			307	36.94	153.60
35	17:40:00	11.0	-09 1/4	20.45	*****			307	36.83	153.57
36	17:41:00	11.0	-09 1/4	20.45	*****			307	36.83	153.57
37	17:42:00	11.0	-09 1/4	20.45	*****			307	36.83	153.57
38	17:44:00	11.0	-09 1/4	20.45	*****			307	36.83	153.57
39	17:46:00	11.0	-08 3/4	21.10	*****			309	36.44	154.59
40	17:47:00	11.0	-08 3/4	21.10	*****			309	36.44	154.59

3071-1-711

FIGURE C-4 SAMPLE TTY LOG OF OPERATING PARAMETERS FOR NORPAX DATA FILE

NEW PARAMETERS

1 FEB 1974

FREQ 17.55 17.60

WHOPS 2

EAST 1, WEST 0 0

104 19:12:24	17.7	-06	3/4E	21.50	5	-1.09	-18.15	280	35.84	153.58
	18.9	-06	2/4S	21.50	5	1.09	18.15	280	35.73	153.55
	15.5	-06	0/4	21.50	5	1.09	18.15	280	35.50	153.49
	21.0	-05	3/4D	21.50	5	1.09	18.15	280	35.39	153.46
	12.0	-05	3/4E	21.50	5	.70	11.67	280	35.39	153.46
105 19:13:17	14.2	-06	2/4S	22.38	-6	.00	.00	281	35.43	155.00
	13.5	-06	0/4	22.36	-7	.00	.00	281	35.21	154.90
	20.8	-05	3/4D	22.38	-6	.00	.00	281	35.08	154.90
	12.6	-05	3/4E	22.38	-6	-.23	-3.89	281	35.08	154.90
	11.7	-05	3/4E	22.32	-9	-1.09	-18.15	281	35.10	154.80
106 19:14:10	25.5	-06	2/4S	22.42	-9	-.16	-2.59	281	35.42	155.06
	12.4	-06	2/4S	22.50	-5	-1.41	-23.33	281	35.39	155.20
	*11.2	-06	1/4S	22.64	2	1.25	20.74	281	35.22	155.40
	16.8	-05	0/4	22.40	-10	-.16	-2.59	281	35.19	154.97
	27.3	-05	3/4D	22.42	-9	-.16	-2.59	281	35.07	154.97
	16.2	-05	3/4E	22.50	-5	-1.41	-23.33	281	35.04	155.10
	14.3	-05	3/4E	22.42	-9	-.47	-7.78	281	35.07	154.97
107 19:15:03	16.1	-06	3/4E	22.50	-5	.86	14.26	281	35.51	155.23
	15.0	-06	3/4E	22.76	8	-.70	-11.67	281	35.42	155.66
	30.1	-06	2/4S	22.40	-10	-.08	-1.30	281	35.43	155.03
	15.9	-06	2/4S	22.48	-6	-1.33	-22.04	281	35.40	155.16
	15.3	-06	2/4S	22.76	8	.16	2.59	281	35.30	155.63
	15.2	-06	2/4S	22.40	-10	-.39	-6.40	281	35.43	155.03
	14.7	-06	2/4S	22.40	-10	.31	5.18	281	35.43	155.03
	26.9	-06	0/4	22.40	-10	-.08	-1.30	281	35.19	154.97
	20.8	-05	3/4D	22.40	-10	-.08	-1.30	281	35.08	154.93
	16.4	-05	3/4E	22.50	-5	-1.25	-20.74	281	35.04	155.10
	15.4	-05	3/4E	22.76	8	.16	2.59	281	34.94	155.53
108 19:15:55	16.5	-06	3/4E	22.00	-10	-.94	-15.55	281	35.68	154.40
	20.6	-06	2/4S	22.38	9	-.08	-1.30	281	35.43	155.01
	18.1	-06	2/4S	22.04	-8	1.41	23.33	281	35.55	154.44
	21.2	-06	0/4	22.40	10	.00	.00	281	35.19	154.90
	17.7	-06	0/4S	22.04	-8	1.41	23.33	281	35.32	154.38
	20.6	-05	3/4D	22.38	9	-.08	-1.30	281	35.08	154.91
	15.4	-05	3/4E	22.02	-9	1.25	20.74	281	35.21	154.31
109 19:17:15	20.2	-06	3/4E	21.88	-6	-1.09	-18.15	280	35.72	154.20
	17.2	-06	3/4E	21.96	-2	-.63	-10.37	280	35.69	154.34
	14.4	-06	3/4E	21.88	-5	-1.41	-23.33	280	35.72	154.20
	21.5	-06	2/4S	21.88	-6	1.09	18.15	280	35.60	154.17
	17.4	-06	2/4S	21.88	-6	.86	14.26	280	35.60	154.17
	15.8	-06	2/4S	22.02	1	1.41	23.33	280	35.56	154.41
	22.3	-06	0/4D	21.88	-6	1.09	18.15	280	35.37	154.11

3071-1-712

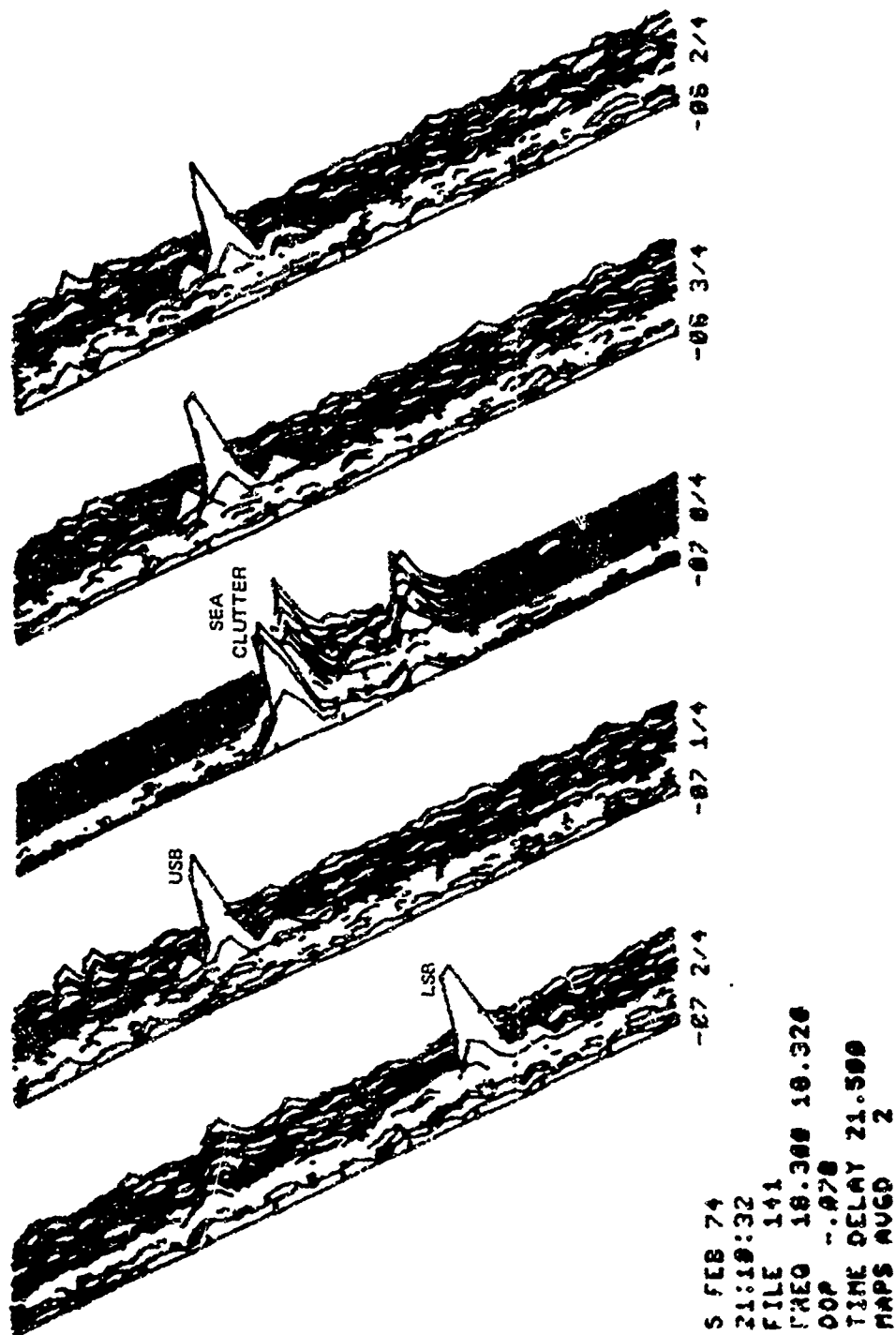
FIGURE C-5 SAMPLE TTY LOG SHOWING ALL DATA ON DETECTIONS

Two primary records were made during the buoy-tracking effort--a hard-copy print of every data file from the computer terminal display and the detection log stored in disc memory. The hard copies not only provide the operator with a real-time permanent record of operating conditions and target data, but they are invaluable in post-experiment analysis to determine the presence of spurious targets that the computer processor may not recognize. The clutter display is an especially useful record of propagation conditions.

In addition to the detection records shown in the main text, the operator may elect to display a three-dimensional plot of all range cells of any data file in order to examine in more detail the nature of the target return. The display shows amplitude, range, and Doppler for each of the five receiver channels. Each range cell is plotted individually with a linear voltage scale. For very small signals, a scale factor of $\times 10$ may be selected causing large signals to clip. For buoy tracking, the display was particularly useful in showing the discrete nature of the target and the presence of multiple target echoes. In tracking conventional repeaters such as those used on the R.V. Flip and R.V. Washington, it was useful to display the relative positions in range and Doppler of both sidebands, especially if two repeaters were at similar ranges and likely to present identification problems. Displays of buoy and Flip repeaters in 3D format are shown in Figures C-6 and C-7, respectively.

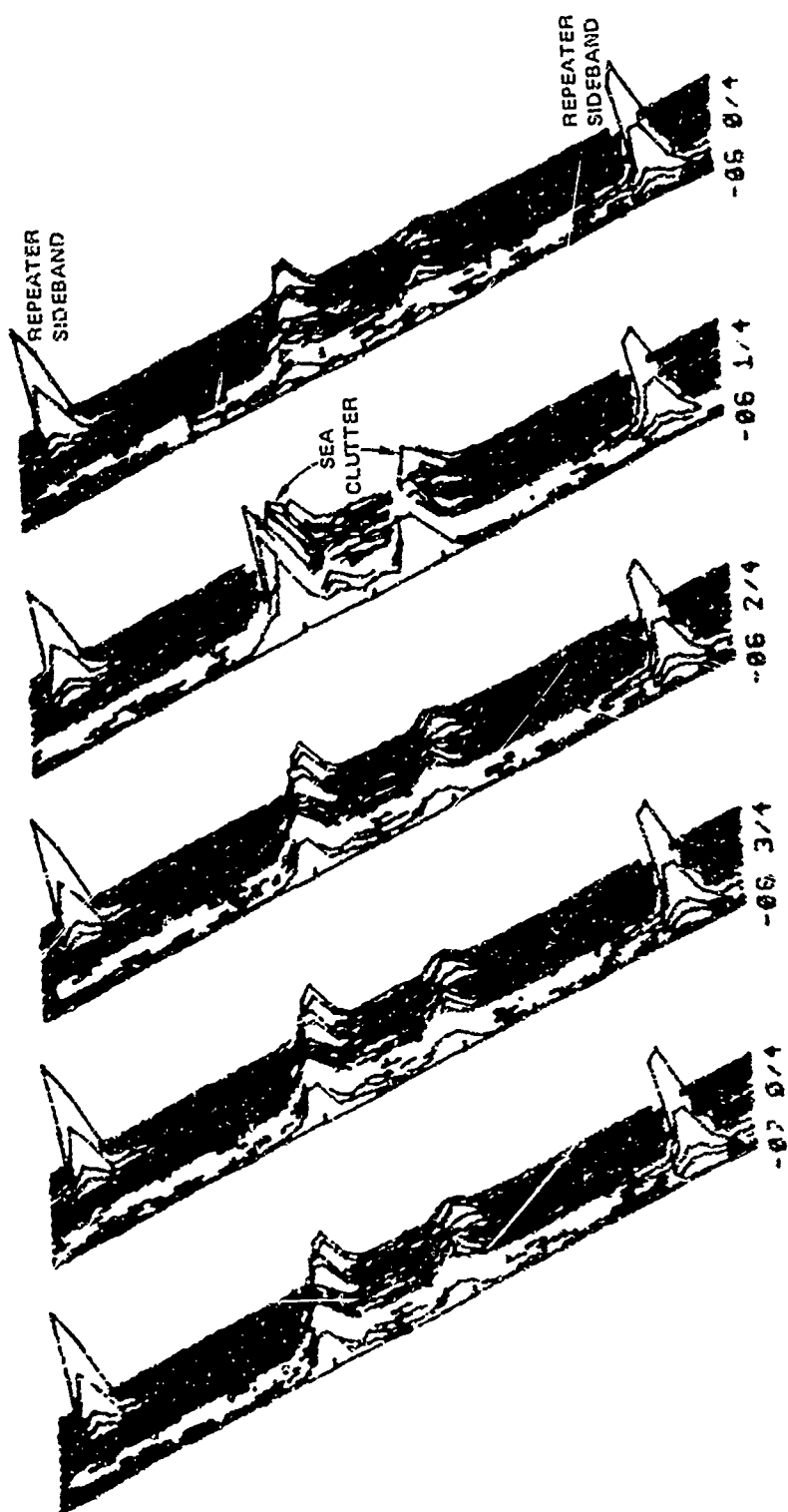
3. Sea Backscatter Recording

The receiving system for the wide-area backscatter data is largely the same as described above for buoy tracking. All receivers, however, operate with a common local-oscillator injection frequency to provide sea-clutter signals in each receiver. Antenna connections are also different from buoy tracking, with five beams being used at 0° , $\pm 1/4^\circ$, and $\pm 1/2^\circ$ from the steered azimuth of the array.



30/1-1-713

FIGURE C-6 BUOY DETECTION RECORD IN 3D FORMAT



5 FEB 74
19:57:46
FILE 66
FREQ 18.528 18.570
DOP -2.500
TIME DELAY 21.630
MAPS AUGD 2

3071-1-714

FIGURE C 7 FLIP REPEATER DETECTION IN 3D FORMAT

The coherent outputs of the five receivers were audio tones at 400 : 50 Hz. These tones were digitized and computer-processed to provide the spectral characteristics of the sea clutter. The processing was identical to that used for buoy tracking as described previously. Examples of the processor output have been shown in the main text (Figures 26 through 28). The format is similar to that for buoy tracking except that detection data for discrete targets (such as buoys) are omitted from the display. The antenna bearings shown in these records are correct. The identification BUOY GN at the bottom of each record indicates that the receivers were operated to record sea clutter in all five channels.

During part of the mapping program, two receivers were operated to receive buoy signals and the three center channels were devoted to mapping. Records of this type show a buoy identification (B through F) and the plots in Channels 1 and 5 show no sea clutter. These records also include detection data in the lower center of the record. For sea-scatter purposes these additional data may be ignored.

Appendix D

OFF-LINE PROCESSING FOR BUOY AND SHIP POSITIONS

All detections of buoy and ship repeaters were stored in a disc memory during tracking and then transferred to digital tape at the end of each operation. This tape was used with a comprehensive off-line processor to provide data and plots on buoy and ship positions. During processing of this tape, files may be deleted that do not contain useful data or that possibly contain spurious data, such as local calibration signals. The processor then examines each detection listed to determine if an LSB in Azimuth 1 and a USB in Azimuth 2 are present within ± 1 range cell and whether the signs of their Doppler frequencies are opposite-- e.g., with a VCO greater than 2.5, the LSB Doppler frequency is negative and the USB frequency is positive. The two sidebands are normally symmetrical about the zero-Doppler line, which is an operator's first clue to a probable detection. If both sidebands are from the same buoy, the range cells will correspond or differ by ± 1 cell at most. The processor then assigns the correct azimuth to the detection (Azimuth 1 and Azimuth 2 are 0° , Azimuth 4 is $-1/4^\circ$, and Azimuth 5 is $+1/4^\circ$ with respect to Azimuth 3). Detections in Azimuth 3 are ignored since no buoy detections can occur in that receiver. The USB azimuth (Azimuth 2, 4, or 5) having the largest SNR is then selected as the correct target bearing, and the time delay for that detection is computed, subtracting 25 μ s for the delay line in the buoy repeater.

Based on the azimuth, the time delay, the virtual height, and the locations of the transmitter and receiver, the latitude and longitude of the target are computed. Finally the frequency of the VCO is computed as:

$$VCO = \frac{5 - f_{D,L} + f_{D,U}}{2}$$

where $f_{D,L}$ and $f_{D,U}$ are the Doppler frequencies of the LSB and USB, respectively.

Since repeaters on the ships Flip and Washington operate with both sidebands present in the same receiver channel, a different identification process is required. Modulation frequencies of 43 Hz on the Washington and 23 Hz on the Flip were used. These are entered by the operator as initial processor parameters. These sidebands would appear ± 9 range cells from the range cell of the Washington and ± 5 range cells from the range cell of the Flip, and each would have a nominal Doppler of 2 Hz. If both sidebands are present at the correct spacing, the processor selects the strongest signal, assigns the correct azimuth, and computes the time delay to the ship (midpoint between the two sidebands) with a 50- μ s correction for the repeater delay line. The ship is identified, based on sideband spacing, and its coordinates are then computed.

The initial chronological listing process for a typical day's record requires less than one minute of processor time. The operator may then examine the list and delete any files that have obviously incorrect coordinates or VCO. A new list is then generated arranged in order of buoy identification. If no detections are found for any buoy, it is so stated. This list also includes the SNR of the buoy detection and the RCS for the ship repeater.

For each target a separate plot of latitude and longitude versus time is generated, with both scales adjusted to fit the range of coordinates and time as needed. A least-squares line is fitted to both plots, and the mean latitude and longitude are calculated, plus standard deviation from the mean and the least-squares line. From these plots the operator is given a final opportunity to delete points that are far

removed from the mean. A plot is also generated for each buoy showing the VCO versus time. It should be a straight line, and any point with a significant deviation should be deleted.

Finally, the processor will give a position for each buoy or ship at times input by the operator. The position may be requested referenced to the least-squares line or extrapolated from the nearest actual times. The mean position may also be requested, in which case the time is irrelevant, since all points are used.

It was found that the drift rate during any six-hour period was typically too low for the least-squares line to be significant. In a number of records this line was found to have a slope due chiefly to variations in ionospheric virtual height during the day. This was particularly evident if a group of detections were made at time periods separated by several hours. Procedures to help correct for these height variations in future tests are described in Appendix E.

After the coordinates of all buoys and ships are listed, the relative range and bearing between any selected reference and all others are listed.

The complete post-processing requires typically less than 10 minutes, much of which is time required by the operator to decide which files should be deleted and the times for listing coordinates. Typical post-experiment processing records are shown in Figures D-1 through D-7. A list of all detections made on 29 January is shown in Figure D-1. The list includes Buoy D, but these detections were later shown to be false. The longitude and latitude for all Buoy E detections on that date are shown in Figure D-2 with a least-squares line for the 10 detections. A list of the average coordinates for all buoys and Flip is given in Figure D-3, and the relative positions of all buoys with respect to Flip are given in Figure D-4.

20) 3600 1874	FILE	C	TIME	ID	PAGE	↑	NY	LAT	LONG	UCO	SMR	REC
NY) 0000 DETECTIONS HERE FOUND FOR ID 1												
100	20:50:20	2	-5.50	21.470	310.3	34.872	154.823	3.7100	23.0000			
172	20:54:41	2	-5.75	21.460	310.6	34.881	154.823	3.7100	20.2000			
173	20:54:55	2	-5.75	21.460	310.6	34.881	154.823	3.7100	18.3000			
137	22:00:51	2	-6.00	21.440	310.0	35.334	154.804	3.6710	25.0700			
138	22:09:44	2	-6.25	21.440	310.0	35.222	154.804	3.7100	24.1200			
139	22:10:37	2	-6.00	21.440	310.0	35.110	154.822	3.7100	22.2500			
106	18:07:49	3	-6.00	21.380	309.7	35.120	154.732	3.5100	32.0000			
107	18:08:41	3	-6.00	21.380	309.7	35.120	154.732	3.5935	25.1000			
108	18:09:30	3	-6.25	21.380	309.7	35.240	154.763	3.5540	33.2400			
109	18:11:27	3	-6.25	21.420	310.3	35.220	154.823	3.5540	22.1300			
110	18:13:11	3	-6.25	21.420	310.4	35.205	154.935	3.5545	20.2400			
111	18:15:41	3	-6.00	21.430	310.4	35.113	154.807	3.5540	23.0000			
110	18:23:05	4	-6.00	20.970	309.7	35.202	154.800	3.5930	21.7300			
121	18:26:00	4	-6.00	20.940	309.1	35.274	154.820	3.5930	20.5000			
122	18:28:42	4	-6.00	20.940	309.1	35.274	154.820	3.4750	20.4300			
146	18:52:50	4	-6.25	20.910	309.1	35.301	154.825	3.5540	21.7700			
147	18:55:35	4	-6.25	20.930	309.0	35.307	154.844	3.5540	21.5000			
64	17:25:16	5	-6.00	21.300	310.0	35.130	154.724	3.5530	20.6200			
65	17:27:51	5	-6.00	21.300	310.3	35.130	154.720	3.6320	14.0700			
70	17:40:25	5	-6.00	21.420	310.3	35.110	154.702	3.5930	10.0700			
71	17:41:10	5	-6.25	21.420	310.3	35.220	154.823	3.6320	13.0000			
81	17:43:00	5	-6.00	21.440	310.3	35.100	154.824	3.6320	16.3000			

3071 1-715

FIGURE D-1 BUOR AND SHIP DETECTION LOG AND POSITION DATA FROM POST-PROCESSOR, 29 JANUARY 1974

20 JAN 1974	PAGE	5	HT	LAT	LONG	UCO	BMK	RCB
FILE C TIME	AZ	TD						
02 17:58:35	-8.00	21.400	310.3	35.000	154.000	3.7100	14.0400	
04 17:58:27	-8.00	21.400	310.3	35.000	154.000	3.8320	18.0200	
05 17:57:18	-6.25	21.400	310.3	35.200	154.020	3.8320	11.2300	
112 18:16:53	-8.00	21.430	310.4	35.113	154.007	3.8320	22.2700	
148 22:17:49	-6.25	21.419	310.6	35.229	154.020	4.0620	15.0000	
02 17:44:48	-6.00	21.440	310.3	35.109	154.024	3.8715	16.4000	
03 17:46:23	-6.50	21.500	310.3	35.314	154.903	3.7105	19.1600	
04 17:47:57	-6.00	21.400	310.3	35.123	154.760	3.6710	19.4400	
147 22:20:26	-6.00	21.419	310.6	35.117	154.700	3.7495	19.0000	

NO GOOD DETECTIONS OF USS WASH

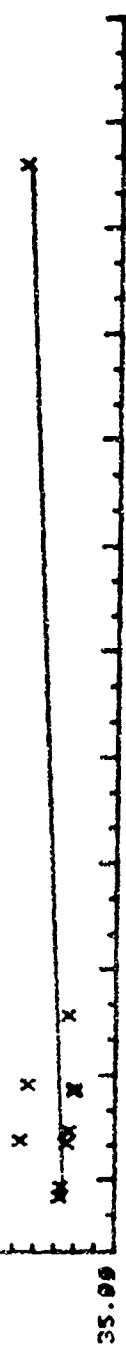
348 22:21:17	7F	-6.00	21.470	310.6	35.100	154.070	17.650
349 22:22:50	7F	-6.00	21.470	310.8	35.100	154.070	54.930
350 22:23:40	7F	-6.00	21.470	310.6	35.100	154.070	40.930
351 22:24:39	7F	-5.75	21.490	310.6	34.901	154.870	53.050
355 22:39:00	7F	-5.75	21.660	310.9	34.922	155.139	54.030
356 22:40:00	7F	-5.00	21.670	310.9	34.900	155.056	53.370
357 22:43:00	7F	-5.75	21.720	311.2	34.902	155.234	55.300
359 22:46:40	7F	-5.75	21.610	311.2	34.027	155.026	53.930
371 22:40:45	7F	-5.75	21.590	311.1	34.947	155.026	53.050

HOW MANY FILES TO BE DELETED? 0

3071-1 716

FIGURE D-1 (Concluded)

29 JAN 1974 PAGE 9
 LATITUDE VS TIME FOR BUOY 5 MEAN=38.148 STDN=.081 STDL=.046
 36.00



LONGITUDE VS TIME FOR BUOY 5 MEAN=154.82 STDN=.062 STDL=.061
 153.00



FIGURE D-2 LATITUDE AND LONGITUDE PLOT FOR BUOY E, 29 JANUARY 1974

29 JAN 1974 PAGE 13
 HOW MANY FILES TO BE DELETED 0
 TO USE SAME TIME FOR ALL BUOYS AND SHIPS TYPE 1, ELSE 0: 5

PLEASE INPUT HOURS, MINUTES, SECONDS FOR BUOY 2: 22:18:00
 ACTUAL (TYPE 0), AVERAGE (-1), OR LEAST SQUARES (1)? -1
 PLEASE INPUT HOURS, MINUTES, SECONDS FOR BUOY 3: 18:18:00
 ACTUAL (TYPE 0), AVERAGE (-1), OR LEAST SQUARES (1)? -1
 PLEASE INPUT HOURS, MINUTES, SECONDS FOR BUOY 4: 18:25:00
 ACTUAL (TYPE 0), AVERAGE (-1), OR LEAST SQUARES (1)? -1
 PLEASE INPUT HOURS, MINUTES, SECONDS FOR BUOY 5: 17:48:00
 ACTUAL (TYPE 0), AVERAGE (-1), OR LEAST SQUARES (1)? -1
 PLEASE INPUT HOURS, MINUTES, SECONDS FOR BUOY 6: 17:45:00
 ACTUAL (TYPE 0), AVERAGE (-1), OR LEAST SQUARES (1)? -1
 PLEASE INPUT HOURS, MINUTES, SECONDS FOR FLIP 22:48:00
 ACTUAL (TYPE 0), AVERAGE (-1), OR LEAST SQUARES (1)? -1

BUOY 2 HAS LATITUDE	35.09	LONGITUDE	154.04	DEGREES
BUOY 3 HAS LATITUDE	35.17	LONGITUDE	154.00	DEGREES
BUOY 4 HAS LATITUDE	35.32	LONGITUDE	154.04	DEGREES
BUOY 5 HAS LATITUDE	35.15	LONGITUDE	154.02	DEGREES
BUOY 6 HAS LATITUDE	35.17	LONGITUDE	154.04	DEGREES
FLIP HAS LATITUDE	34.84	LONGITUDE	155.05	DEGREES

IF YOU WISH TO INPUT ANOTHER TIME TYPE 1, ELSE 0: 0

3071 1 716

FIGURE D-3 AVERAGED POSITIONS FOR BUOYS AND R V FLIP ON 29 JANUARY 1974

29 JAN 1974 PAGE 14
 INPUT BUOY ID, OR 0 FOR WASH OR 0 FOR FLIP
 FROM WHICH TO COMPUTE RANGE & BEARING OF OTHERS: 0

FROM ID 0 TO ID 2	DISTANCE=	21.0 KM	BEARING ANGLE=	42.0 DEGREES
FROM ID 0 TO ID 3	DISTANCE=	31.5 KM	BEARING ANGLE=	35.4 DEGREES
FROM ID 0 TO ID 4	DISTANCE=	37.0 KM	BEARING ANGLE=	33.8 DEGREES
FROM ID 0 TO ID 5	DISTANCE=	28.4 KM	BEARING ANGLE=	35.2 DEGREES
FROM ID 0 TO ID 6	DISTANCE=	28.4 KM	BEARING ANGLE=	29.0 DEGREES

TYPE 1 IF YOU WISH MORE RELATIVE POSITIONS, ELSE 0:

IF YOU WISH TO INPUT ANOTHER TIME TYPE 1, ELSE 0: 0
 IF YOU WISH TO RESTART THE PROGRAM PLEASE TYPE 1, ELSE 0: 1
 PLEASE REWIND TAPE OR LOAD A NEW ONE

3071 1 717

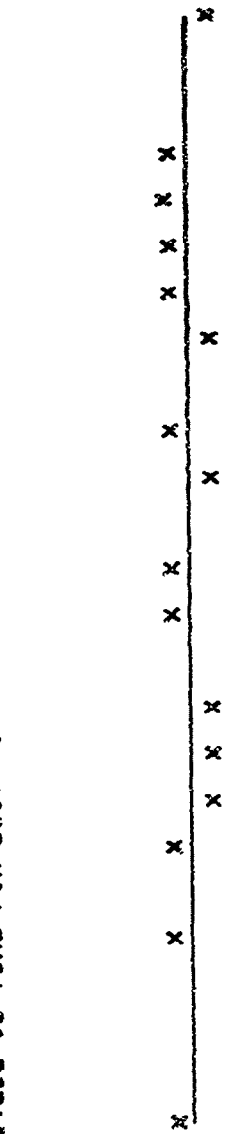
FIGURE D-4 RELATIVE POSITIONS OF BUOYS WITH RESPECT TO R V FLIP ON
 29 JANUARY 1974

11 APR 74	PAGE	2	AZ	TO	HT	LAT	LONG	UCO
FILE	TIME	ID						
172	21:05:00	21.9211	5	17.880	301.4	37.807	149.2320	3.3200
176	21:09:00	21.9370	5	17.830	288.9	37.615	149.2355	3.3200
178	22:01:00	22.0211	5	17.830	289.9	37.615	149.2355	3.3200
179	22:02:00	22.0370	5	17.830	289.9	37.615	149.242	3.3200
180	22:03:00	22.0544	5	17.830	299.9	37.615	149.242	3.3200
181	22:04:00	22.0711	5	17.830	299.9	37.615	149.242	3.3200
183	22:05:00	22.1044	5	17.830	299.9	37.615	149.255	3.3200
184	22:07:00	22.1211	5	17.830	299.9	37.615	149.255	3.3200
185	22:09:00	22.1544	5	17.830	299.9	37.615	149.241	3.3200
187	22:10:00	22.1711	5	17.829	299.7	37.615	149.254	3.3200
188	22:12:00	22.2044	5	17.829	299.7	37.615	149.241	3.3200
189	22:13:00	22.2211	5	17.829	299.7	37.615	149.254	3.3200
190	22:14:00	22.2378	5	17.829	299.7	37.615	149.254	3.3200
191	22:15:00	22.2544	5	17.829	299.7	37.624	149.169	3.3200
192	22:16:00	22.2711	5	17.779	299.7	37.624	149.169	3.3200
195	22:19:00	22.3211	5	17.829	299.7	37.615	149.254	3.3200
TO DELETE FILES TYPE -1, TO INCLUDE TYPE 1, ELSE 0								

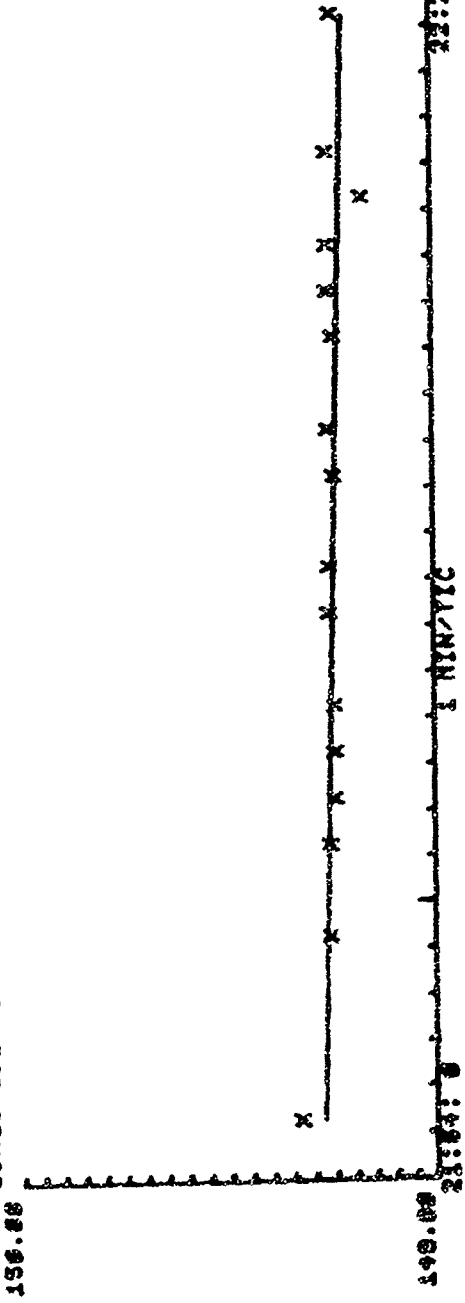
3071 1 720

FIGURE D-5 DETECTION LIST FOR BUOY E ON 11 APRIL 1974

11 APR 74 PAGE 5 LATITUDE VS TIME FOR BUOY 5 MEAN=37.678 STDN=.548 STDL=.048



37.00 LONGITUDE VS TIME FOR BUOY 5 MEAN=149.26 STDN=.029 STDL=.025



3071 1 721

FIGURE D-6 LATITUDE AND LONGITUDE PLOT FOR BUOY 5, 11 APRIL 1974

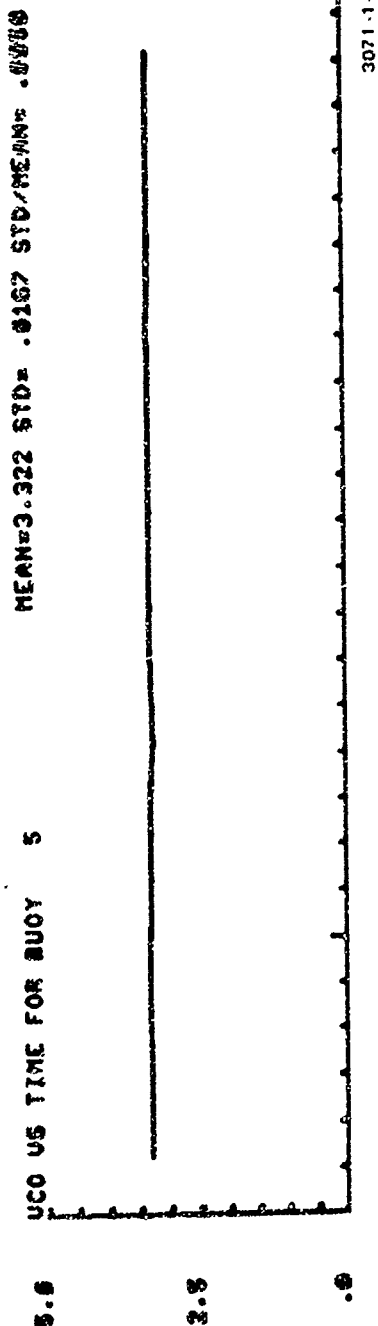


FIGURE D-7(a) VCO PLOT FOR BUOY E, 11 APRIL 1974

11 APR 74 PAGE 7
 HOW MANY FILES TO BE DELETED? 0
 TO USE SAME TIME FOR ALL BUOYS AND SHIPS TYPE 1, ELSE 0: 1
 AT WHAT TIME DO YOU WANT TO TAKE POSITIONS?
 PLEASE INPUT HOURS, MINUTES, SECONDS 22:10:00
 ACTUAL (TYPE 0), AVERAGE (-1), OR LEAST SQUARES (1)? -1
 BUOY 5 HAS LATITUDE 37.58 LONGITUDE 149.35 DEGREES
 IF YOU WISH TO INPUT ANOTHER TIME TYPE 1, ELSE 0: 0
 IF YOU WISH TO RESTART THE PROGRAM PLEASE TYPE 1, ELSE 0: 1
 PLEASE REWIND TAPE OR LOAD A NEW ONE

3071.1723

FIGURE D-7(b) AVERAGED POSITION DATA FOR BUOY E, 11 APRIL 1974

Especially good records for Buoy E were obtained on 11 April, as shown in Figures D-5 through D-7. The longitude and latitude plots of Figure D-6 show very little dispersion, while the VCO measurement in Figure D-7(a) is nearly constant.

Appendix E

VIRTUAL-HEIGHT MEASUREMENT

One requirement of any ionospheric radar used for providing highly accurate target positioning is an accurate measure of virtual height. The computer processor used for the buoy tracking estimated the virtual height based on a model ionosphere, the operators judgment as to the mode of propagation, and the range to the target. Typically, this computed height varied very little during the day. The operator could also enter a fixed height if information was available on which to base such an estimate. Since the experiment covered a period of four months, seasonal changes occurred later in the experiment for which a new height model was used. Nevertheless, the mode of propagation was sometimes difficult to evaluate.

Using the monostatic model shown in Figure E-1, the effect of virtual height on measured time delay can be expressed by:

$$\sin \alpha/2 = \frac{1}{4} \sqrt{\frac{P^2 - 4h^2}{R(R+h)}}$$

where

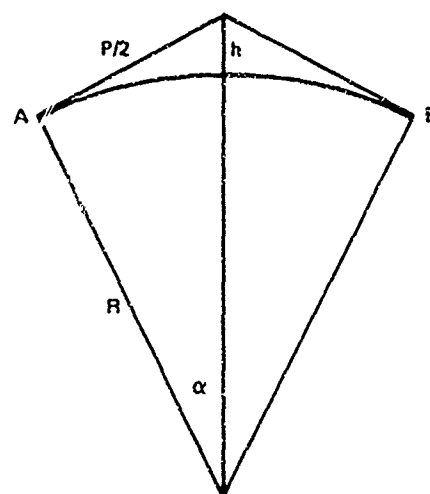
R = 6371 km, earth's radius

P = Path length, km

h = Virtual height, km

2 α : Great-circle arc from A to B.

P is measured by the radar at 150 TD km, where TD is the round-trip time delay in ms. At a ground range of 3000 km, a 10-km change in virtual



3071-1-724

FIGURE E-1 GEOMETRY FOR IONOSPHERIC PROPAGATION

height results in a 6.2-km change in measured range. Since the operator normally has no means for estimating such a change, he must accept the error. At shorter ranges such as 1200 km, the error increases to 12.3 km for a 10-km height change.

In April and May of the buoy-tracking effort, vertical soundings were implemented to provide real-time measurements of virtual height over the radar. A SFCW transmission from the Lost Hills site was received at Los Banos. Although the path was not actually vertical but at an elevation angle of 70° , it was possible to calculate the virtual height from the measured time delay. It was significant that variations of more than 10 km were observed in periods as short as 20 minutes. This observation is not uncommon, and it is the reason why at least an hour of data (preferably more) should be recorded and averaged to obtain good position accuracy.

In order to use vertical soundings at the radar to minimize OTH radar position errors, it is necessary to extrapolate the height data to the midpoint of the path to the target. Since virtual- height changes are a

function of the sun's position or local time, an estimate of the midpath height for a target west of the radar may be made based on measured heights at an earlier time. For buoy targets in the NORPAX tests, midpoint times ranged from 45 to 68 minutes earlier than the time at the radar. Vertical soundings made at these times could be used for position measurements. Although such extrapolation is also subject to error, especially where ionospheric disturbances exist, it could very well provide a closer estimate of height than can be obtained from seasonal average data. An example of vertical soundings obtained on 17 May is shown in Figure E-2.

The radar operating frequency is related to the vertical sounding frequency by:

$$f_o = k f_v \sec \phi$$

where

ϕ = Vertical angle

k = Correction factor for a curved ionosphere (typically $1 < k < 1.05$).

Since ϕ is a function of virtual height, and virtual height is a function of f_v , an iterative process must be used to satisfy this frequency relationship. With vertical-sounding data stored in the computer processor, virtual-height data could be updated automatically or on command. Although such a process was not implemented during the NORPAX program, virtual heights scaled from ionogram records were used in tracking operations during May.

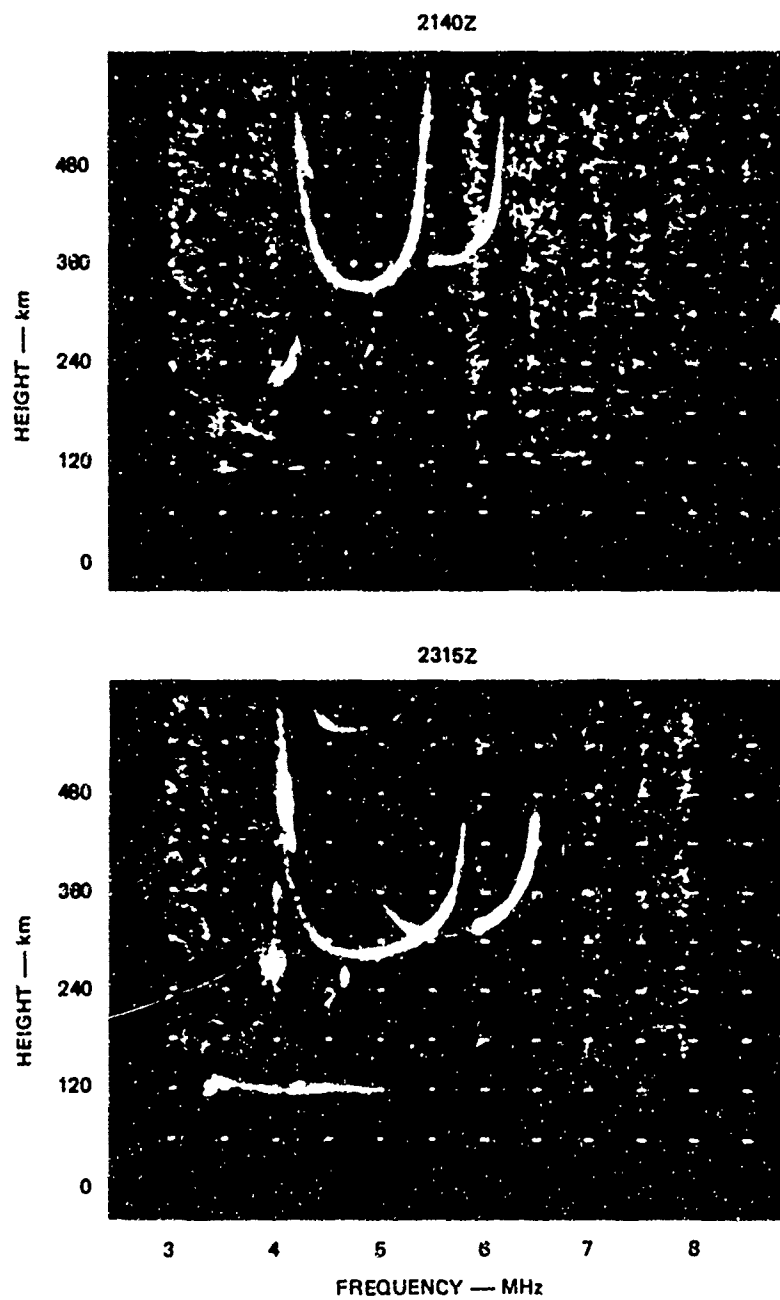


FIGURE E-2 VERTICAL IONOGRAMS ON 17 MAY 1974 SHOWING CHANGE OF MORE THAN 50 km IN VIRTUAL HEIGHT

REFERENCES

1. SRI Ionospheric Dynamics Laboratory, Wide Aperture Research Facility, Special Facility Brochure, Contract N00014-70-C-0413, Stanford Research Institute, Menlo Park, California (June 1974).
2. L. E. Sweeney, Jr., "Spatial Properties of Ionospheric Radio Propagation as Determined With Half-Degree Azimuthal Resolution," Report SEL-70-034 (TR No. 155), Stanford Electronics Laboratories, Stanford, California (June 1970).
3. J. R. Barnum, "The Effect of Polarization Rotation on the Amplitude of Ionospherically Propagated Sea Backscatter," Report SEL-70-036 (TR No. 157), Stanford Electronics Laboratories, Stanford, California (June 1970).
4. T. W. Washburn, "Discrete Echoes in Ionospherically Propagated Ground Backscatter," Technical Report 5, Contract N00014-70-C-0413, SRI Project 8727, Stanford Research Institute, Menlo Park, California (August 1971).
5. J. R. Barnum, "Mixed Mode Oblique Ionograms: A Computer Ray-Tracing Interpretation," Report SEL-68-095 (TR No. 148), Stanford Electronics Laboratories, Stanford, California (December 1968).
6. D. E. Barrick et al., "Sea Backscatter at HF: Interpretation and Utilization of the Echo," Proc. IEEE, Vol. 62, No. 6, pp. 673-680 (June 1974).
7. G. L. Tyler et al., "Wave Directional Spectra from Synthetic Aperture Observation of Radio Scatter," accepted for publication by Deep-Sea Research.
8. J. L. Ahearn et al., "Tests of Remote Skywave Measurement of Ocean Surface Conditions," Proc. IEEE, Vol. 62, No. 6, pp. 681-686 (June 1974).
9. R. H. Stewart and J. R. Barnum, "Radio Measurements of Oceanic Winds at Long Ranges: An Evaluation," submitted to Radio Science.

10. A. C. Phillips, "A Single-Antenna Repeater for HF Radio Propagation Studies," Report SEL-69-064 (TR No. 154), Stanford Electronics Laboratories, Stanford, California (October 1969).